

Leaf phenology: from physiology to global change

Dissertation
zur Erlangung des Doktorgrades
der Naturwissenschaften

vorgelegt beim Fachbereich 11 Geowissenschaften / Geographie
der Johann Wolfgang Goethe-Universität
in Frankfurt am Main

von
Robert Buitenwerf
aus Bedum

Frankfurt 2015
D30

vom Fachbereich 11 Geowissenschaften / Geographie der
Johann Wolfgang Goethe-Universität als Dissertation angenommen.

Dekan: Prof. Dr. Ulrich Achatz

Gutachter: Prof. Dr. Thomas Hickler

Gutachter: Prof. Dr. Steven I. Higgins

Datum der Disputation: 2 April 2015

Contents

Abstract	9
1 Introduction	11
2 Three decades of multi-dimensional change in global leaf phenology	27
3 Convergence in the physiological niche of evergreen and deciduous vegetation	43
4 Effects of leaf phenology and leaf habit on the carbon budget of African savanna trees	71
5 Synthesis	103
Summary	115
Zusammenfassung	123
Bibliography	130

Acknowledgements	149
A Three decades of multi-dimensional change in global leaf phenology	153
B Convergence in the physiological niche of evergreen and deciduous vegetation	163
C Effects of leaf phenology and leaf habit on the carbon budget of African savanna trees	167
D Soil water retention curves for the major soil types of the Kruger National Park	173
E Curriculum Vitae	191

List of Figures

1.1	The distribution of evergreen and deciduous trees.	20
2.1	Calculated phenological metrics.	32
2.2	Phenological change between 1981 and 2012 in SD units.	38
2.3	Syndromes of phenological change.	39
3.1	Evergreenness and phenome classification.	54
3.2	Physiological niche dimensions of phenomes from different realms	57
3.3	Projecting phenomes into non-native realms based on their physiological niche.	60
3.4	Overlap in the projected distributions of three phenomes from four biogeo- graphic realms.	63
4.1	Canopy greenness and leaf lifespan for nine species.	88
4.2	Temporal separation of phenological events.	89
4.3	The relationship between species, phenological variables and physiological variables	91

4.4 Relationship between ecological dominance and annual carbon gain. 95

A.1 The location of individual phenomes 155

A.2 Change in vegetation activity between the studied time windows 157

A.3 Per phenome change in vegetation activity between the studied time windows 159

A.4 Work-flow diagram 161

B.1 Overlap in phenome projections from different realms. 165

C.1 Observed and predicted photosynthetic rates from ACi and AQ curves . . . 169

C.2 Observed and optimal stomatal conductance 171

D.1 Dominant soil types of the Kruger National Park 178

D.2 The relationship between soil moisture and water potential by site 185

D.3 The relationship between soil moisture and water potential by substrate . . 186

D.4 Comparing site-specific and geology-specific curves 187

D.5 The relationship between soil moisture and water potential from 0 to -100
MPa 189

List of Tables

3.1	Performance of the TTR model as comparisons between observed and predicted phenome distributions in the native realm.	56
3.2	Niche overlap and similarity between phenomes in their native realm and analogous phenomes from different realms.	58
4.1	Measured phenological and physiological traits.	93
4.2	Annual carbon gain	95
D.1	Coordinates of the sampling sites and description of soils	179
D.2	Water retention curves parameters	183

Abstract

The timing and duration of leaf deployment strongly regulate earth-atmosphere interactions and biotic processes. Leaf dynamics therefore have major implications for life on earth, including the global energy balance, carbon and water cycles, feedbacks to climate, species extinction risk and agriculture. Evidence of shifts in the timing of leaf deployment and senescence (leaf phenology) as a result of climate change has been accumulating over the past decades, particularly in relation to spring phenology in the northern hemisphere. However, leaf phenological change in other parts of the world has received less attention. This thesis quantifies global phenological change over the past three decades using remotely sensed data. Phenological change was found to be widespread and severe, also in the southern hemisphere. While the detected change testifies of the phenological plasticity of many plant species, it is not clear if the duration of leaf deployment (leaf habit) is equally sensitive to environmental change. Since evergreen and deciduous leaf habits are often distinctly sorted along environmental gradients, ecologists have hypothesised that these patterns result from natural selection for an optimal leaf habit, under a given environmental regime. Such evolutionary convergence can be examined by testing if the physiological niche that is occupied by a particular leaf habit (evergreen or deciduous) is similar among regions with distinct evolutionary histories. Using a process-based model of plant growth and a constructed map of evergreen and deciduous vegetation, the physiological niche of leaf habits was quantified in four global biogeographic realms. Substantial niche overlap was found between the same leaf habit in different realms, sug-

gesting evolutionary convergence of the physiological niche. This implies a sensitivity of leaf habit to environmental change, as environmental variables determine the geographic space where the physiological niche allows a positive carbon balance, and therefore occurrence of the leaf habit. Since the physiological niche consists of the integrated effects of physiological traits and trade-offs, environmental dependencies and leaf habit and phenology, an understanding of the carbon economy of individual plants requires decomposing the physiological niche into its components. Using empirical data on leaf phenology, leaf habit and physiological processes from woody species in a seasonally dry African savanna, a simple carbon balance model was parametrised. Carbon gain varied considerably between species as a result of substantial variation in leaf habit, leaf phenology and physiological traits. The multiple lines of evidence in this thesis therefore suggest that, while convergent selective forces may determine the dominant leaf habit in a particular environment, interspecific variation is substantial, potentially as a consequence of historical contingencies or competitive interactions.

Chapter 1

Introduction

Background

Genesis of leaves

The advent of the first, leafless, terrestrial plants was during the early Devonian, approximately 400 million years ago. Although there are indications from the fossil record that the genetic capacity to produce leaf like structures was already present, it took another 40 million years for plants with megaphyll leaves to become widespread (Kenrick & Crane, 1997; Beerling *et al.*, 2001; Beerling, 2007). This begs the question of why it took such a long time for plants with planar and veined leaves to become ecologically dominant. Recently, the ecological success of leafy plants during the late Devonian has been linked to a tenfold drop in the atmospheric CO₂ concentration during that period (Beerling, 2007). Current evidence from the fossil record and from simulation studies points to a positive feedback loop, where reduced atmospheric CO₂ concentrations stimulated the evolution of different leaf forms and the spread of leafy plants, which in turn further reduced atmospheric CO₂ concentrations (Berner, 1998; Osborne *et al.*, 2004; Beerling, 2005). In the novel, low CO₂ atmospheres, leaves were required to extend the surface area through which CO₂ could be taken up. The additional surface area that is gained by deploying leaves also lead to greater interception of solar radiation and this energy absorbing capacity of leafy plants has major implications for the global energy budget and thus the climate. Because of the carbon and energy uptake capacity of leaves, seasonal dynamics in leaf deployment have a strong modulating effect on the exchange of carbon and energy between the terrestrial surface and the atmosphere. Since both climates and the timing of leaf deployment are changing as a result of anthropogenic climate forcing (Menzel *et al.*, 2006; IPCC, 2013), there is an urgent need to understand the extent of such changes, the mechanisms that underlie change and the consequences of change on ecosystem services and biodiversity.

How leafy plants changed the world

The rise to dominance of early leafy plants radically altered geochemical and atmospheric processes on a global scale and accelerated the evolution of terrestrial animals by creating novel habitats (Kenrick & Crane, 1997; Beerling, 2007). In this section, I review the main processes by which plants modify the physical and chemical environment at nearly all spatial and temporal scales. Over millions of years the long-term carbon cycle is driven by the weathering of silicate rock. The weathering releases bicarbonates (HCO_3^-), which through soil erosion and transportation by rivers end up in the ocean where they are incorporated into the calcium carbonate shells of marine organisms. The shells accumulate on the ocean floor until subduction transports them into Earth's liquid mantle where high heat and pressure break down the chemical bonds, so that the carbon can be released into the atmosphere as CO_2 by volcanic eruptions. Because root activity by plants accelerates the weathering of rock, they have promoted the removal of CO_2 from the atmosphere since the end of the Devonian, 400 million years ago (Berner, 1997; Kenrick & Crane, 1997). On a more immediate time scale, climate forcing by plants occurs via three main processes (Bonan, 2008), where climate forcing refers to the effect that a process has on the global energy balance, i.e. by either warming or cooling the system (Myhre *et al.*, 2013).

First, by capturing CO_2 from the atmosphere and sequestering it into biomass, plants regulate atmospheric CO_2 concentrations. Removing CO_2 or other greenhouse gases from the atmosphere decreases its capacity to warm the surface by absorbing radiative heat and re-radiating it back to the surface. The capacity of plants to regulate atmospheric composition is illustrated by the seasonal fluctuations of atmospheric CO_2 concentrations in response to seasonal vegetation activity (Keeling *et al.*, 1996). The second major climate forcing directly affects the global energy budget. Energy exchange between the land surface and the atmosphere depends strongly on the reflectivity of the surface to radiation i.e. albedo. A high albedo means that a large proportion of radiative energy is reflected from the surface, while surfaces with a low albedo absorb most of the energy, which causes

warming of the surface. The albedo of tree-dominated vegetation is typically low, while grassy ecosystems or ecosystems with low ground cover have a higher albedo (Bonan, 2008). The third major process by which vegetation forces the climate is evapotranspiration. During photosynthesis stomata release water vapour into the atmosphere, which results in evaporative cooling of the surface. Since transpiration in plants takes place primarily through the leaves, the seasonal pattern of leaf deployment has a large effect on water fluxes between the surface and the atmosphere. In addition to evaporative cooling, the transpiration of water by vegetation stimulates the formation of cumulus clouds, which play a crucial role in modulating the exchange of heat, water and radiation between the surface and the atmosphere (Freedman *et al.*, 2001; Schwartz, 1996). An additional process by which vegetation forces the climate is the burning of biomass by natural fires during the dry season (Dwyer *et al.*, 2000; Bowman *et al.*, 2009). The release of CO₂ and methane and the deposition of black carbon on snow and ice positively force the climate, while aerosol emission and increases in albedo may have the opposite effect (Randerson *et al.*, 2006; Bowman *et al.*, 2009). The effect on the global energy balance therefore depends on the time since burning (Randerson *et al.*, 2006).

In summary, climate forcing by plants is not only a function of vegetation type and net primary productivity, but also of seasonal fluctuations in plant activity. The seasonality in plant activity, in turn, is largely driven by seasonality of climates.

How the abiotic world affects plants

The previous section described how the type of vegetation and its seasonal physiological activity and patterns of leaf deployment have profound effects on geochemical cycling and atmospheric composition. At the same time, the potential distributions of a plant species is constrained by their ability to achieve a positive carbon budget under the prevailing abiotic conditions. The basic requirements for plant growth are light, water, CO₂ and mineral nutrients (Lambers *et al.*, 2008). Plant growth is therefore co-limited by light in-

tensity, water availability, atmospheric CO₂ concentrations and the availability of mineral nutrients, but also by temperature, which prevents water uptake under freezing conditions and regulates the rate of biochemical processes (Lambers *et al.*, 2008; Craine, 2009).

The climate thus has a major effect on the global distribution of vegetation types (Woodward *et al.*, 2004). The capacity for climate and climatic change to affect the distribution of vegetation is well illustrated by extensive forests that covered the Arctic and Antarctic regions over much of the past 250 million years, when climates were warmer (Royer *et al.*, 2003; Spicer & Chapman, 1990). A more recent example is the evidence of abundant vegetation in the Sahara only 5500 years ago, when it was wetter than the current climate (Ritchie *et al.*, 1985; Foley *et al.*, 2003). Recent warming, caused largely by anthropogenic emissions of greenhouse gases since the start of the industrial revolution around 1760 (IPCC, 2013), has already caused shifts in the distribution ranges of plant species (Parmesan & Yohe, 2003; Parmesan, 2006; Kelly & Goulden, 2008; Chen *et al.*, 2011).

Anthropogenic emissions have caused CO₂ concentrations to rise from 280±10 ppm (parts per million) in circa 1760 to a current concentration of approximately 398 ppm (Prentice *et al.*, 2001; IPCC, 2013). This rise directly affects plant functioning, since the photosynthetic rate of plants with the C₃ photosynthetic pathway is limited by CO₂ at ambient concentrations (Farquhar *et al.*, 1980). Higher atmospheric CO₂ concentrations therefore stimulate photosynthetic rates, at least on immediate time scales. Whether the short term effects result in increased primary productivity over the longer term appears to be location- and species-specific (Long *et al.*, 2004; Ainsworth & Long, 2005). Nonetheless, some studies suggest that elevated atmospheric CO₂ is likely to have already had a major impact on Earth's vegetation, by stimulating the encroachment of woody species into grassy ecosystems (see list in Archer *et al.*, 2001; Morgan *et al.*, 2007; Wigley *et al.*, 2010; Buitenwerf *et al.*, 2012; Bond *et al.*, 2012). In addition to direct stimulation of photosynthesis by atmospheric CO₂ in C₃ plants, associated increases in water use efficiency may conserve soil moisture and thereby effectively extend the growing season in seasonally

dry ecosystems (Field *et al.*, 1995). Increased water use efficiency is expected, as water is necessarily lost through stomata when they open to take up CO₂. Since stomata are assumed to optimise the balance between carbon gain and water loss, higher CO₂ concentrations would allow a reduction in stomatal opening, which would curb water loss (Cowan & Farquhar, 1977). An alternative mechanism to reduce transpiration in response to high atmospheric CO₂ would be to reduce the number of stomata. This is exactly what has been found in studies using herbarium specimens to quantify changes in stomatal density over the past century (Woodward, 1987; Woodward *et al.*, 2004).

The preceding sections show that vegetation is a key link in the feedback loops that govern the exchange of energy and matter between the terrestrial surface, the ocean and the atmosphere. To understand how these feedbacks might be affected by climate change and increasing atmospheric CO₂, it is crucial to know what determines the distribution of vegetation types and what determines their seasonal patterns of activity and leaf deployment. These spatial and temporal aspects of vegetation dynamics will be explored in the following two sections.

Leaf phenology

Leaf phenology refers to the seasonal sequence of leaf development, expansion and senescence. Phenological observations have a rich history, particularly in Europe (Menzel, 2013a) and recent analyses of phenology time series in Europe and North America have shown significant shifts in response to climatic change (Menzel & Fabian, 1999; Schwartz & Reiter, 2000; Menzel *et al.*, 2006; Cleland *et al.*, 2007; Morin *et al.*, 2009; Menzel, 2013b). These analyses therefore indicate that the phenology of certain species is, at least to an extent, plastic. However, for many species the potential for phenological adaptation to warming climates is likely to be limited, as the initiation of bud burst is commonly co-regulated by additional cues such as photo-period and winter chilling periods (Körner & Basler, 2010). The phenological outcome of higher spring temperatures, potentially

warmer winters and invariant photo-periods is debated (Chuine *et al.*, 2010), but is certain to vary between species. Recent evidence from a large observational study on species growing in a single location suggests that species that are sensitive to photo-period and chilling period flushed leaves significantly later than species that rely solely on temperature cues (Zohner & Renner, 2014). In order to make quantitative and species-specific predictions on the effects of climate change on leaf phenology, it is therefore essential to identify the cues that initiate bud burst in different species. Detailed studies on how gene expression and signalling pathways are triggered and regulated by environmental cues will ultimately provide a mechanistic understanding of leaf phenology (Nicotra *et al.*, 2010), but this approach is not likely to provide much needed predictive ability in the short term. An alternative approach is to quantify relationships between leaf phenological traits and other, known, functional traits and taxonomy. Recent work shows that such an approach can account for a significant part of the variation in phenology, but that unexplained variation is substantial (Panchen *et al.*, 2014). This study therefore suggests that an attempt to group species into phenological types based on correlations with other traits holds promise, but might benefit from a more structured approach, in which relative advantages and disadvantages of different phenological strategies are traded off against other physiological processes that affect the carbon and nutrient economies of plants. For example, the trade-offs described in the leaf economic spectrum identifies leaf lifespan as a key axis of variation in plant functioning (Wright *et al.*, 2004). Leaf lifespan is logically related to leaf phenology, but I am not aware of any studies that integrate potential fitness effects of leaf phenology and leaf lifespan, for example by quantifying joined effects on annual carbon gain.

The global variation in leaf lifespan is approximately 1 to 100 months (Wright *et al.*, 2004). Geographic variability in the average leaf lifespan is most obviously characterised by the distribution of deciduous and evergreen vegetation. Although both evergreen and deciduous leaf habits include a range of leaf lifespans; a deciduous leaf habit implies a leaf lifespan of less than one year, while most evergreen species have leaf lifespans that exceed

one year (Kikuzawa & Lechowicz, 2011).

Biogeography of leaf habit

Despite the enormous developments in satellite remote sensing over the past three decades, a globally comprehensive map of the distribution of evergreen and deciduous vegetation is not available. Land cover mapping has relied heavily on the biome concept (Friedl *et al.*, 2002; Bartholomé & Belward, 2005; Ellis & Ramankutty, 2008), which includes a descriptor of leaf habit for some biomes, e.g. evergreen broadleaved forest, but not for others, e.g. arid shrublands. The remote sensing product that comes closest to a global map of leaf habit was developed by DeFries *et al.* (1999) and DeFries *et al.* (2000), who described the distribution of tree-dominated deciduous and evergreen vegetation. This product shows that tree-dominated evergreen vegetation is trimodally distributed along the latitudinal gradient, with peaks in the Boreal zone, the aseasonal tropics and the temperate regions of the southern hemisphere (Figure 1.1). Although this data set has been used widely to characterise the distribution patterns of evergreen and deciduous vegetation (Givnish, 2002; Woodward *et al.*, 2004; Kikuzawa & Lechowicz, 2011), it is important to recognise that it ignores grassland and shrubland, even though evergreen plants are an important component of the vegetation in most arid shrublands and deserts (Werger, 1978; Schmida, 1985; Wickens, 1998). Moreover, the data used to draw Figure 1.1 is not accurate everywhere, as it fails to identify evergreen trees in northern Australia (Bowman & Prior, 2005). Without precise knowledge of the distribution patterns of evergreen and deciduous vegetation, it is difficult to meet the challenge of relating these patterns to potential environmental drivers.

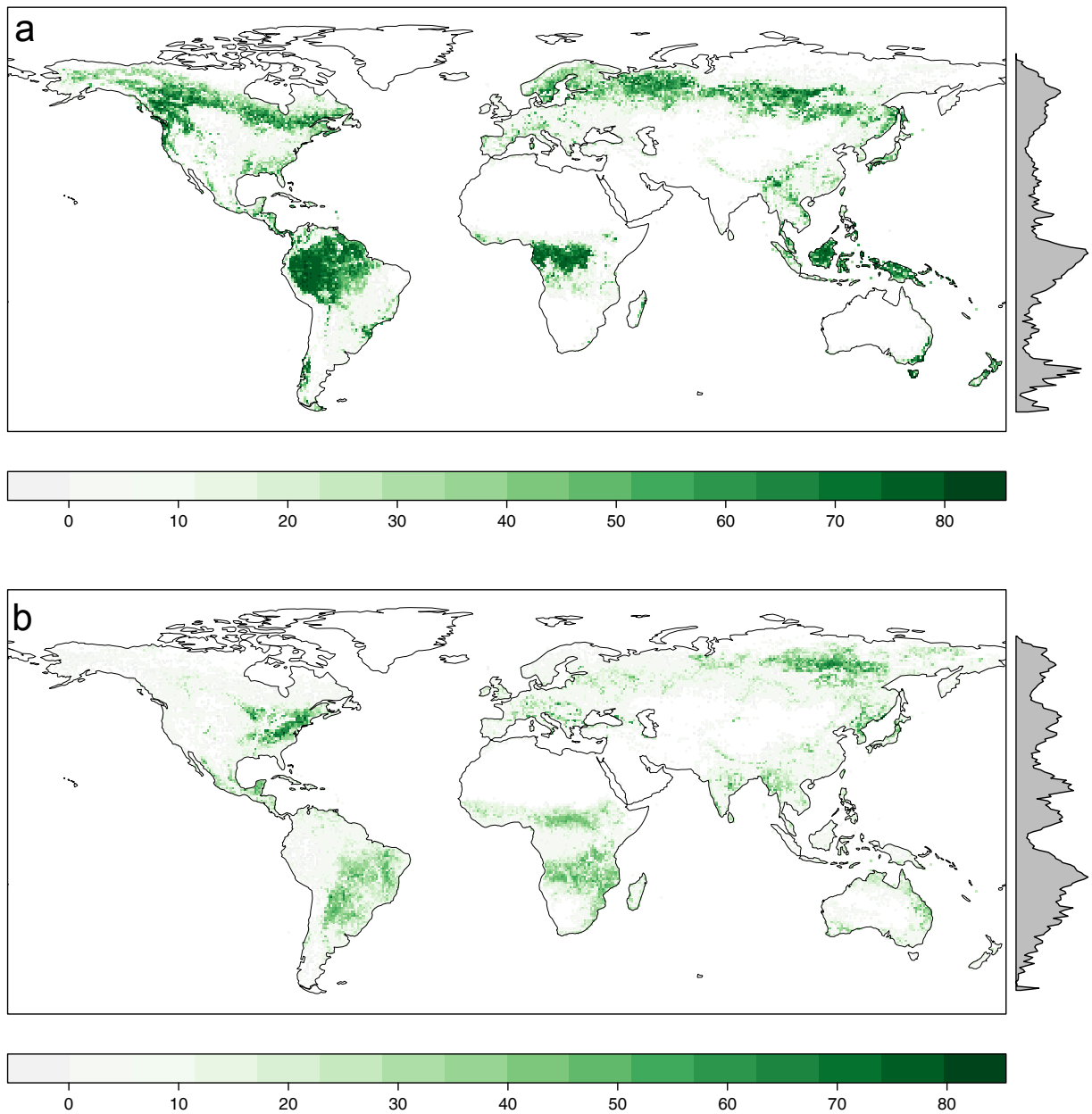


Figure 1.1: **a)** Percentage evergreen tree cover. **b)** Percentage deciduous tree cover. The right hand side panels show the average percentage of tree cover along latitude. Maps were drawn using data described in DeFries *et al.* (1999) and DeFries *et al.* (2000) and data were downloaded from <http://glcf.umd.edu/data/treecover/data.shtml>.

Understanding leaf habit and phenology

Functional and adaptive significance of leaf habit

The adaptive significance of evergreen vs. deciduous leaves has been an active area of research since the 1960s and since then at least 40 publications on the topic can be counted (Givnish, 2002; Kikuzawa & Lechowicz, 2011). The inspiration for these studies was the distinct geographic distribution of evergreen and deciduous leaf habits as described in the previous section and their aim was to explain observed patterns of leaf habit (e.g. Mooney & Dunn, 1970b; Chabot & Hicks, 1982; Kikuzawa, 1991). Givnish (2002) distinguishes between two types of models: top-down and bottom-up models, where top-down models refer to early dynamic global vegetation models (DGVMs) (Haxeltine & Prentice, 1996). Givnish (2002) criticises such models for not seeking ultimate physiological and selective bases for their parameters and instead prefers bottom-up models that use physiological principles to provide a mechanistic explanation for the distribution of leaf habits. It must be pointed out that such bottom-up mechanistic models, if they existed, could theoretically be included in DGVMs. The basic premise of the bottom-up models is the assumption that leaf habit has adaptive significance, as expressed by selection for an optimal leaf habit that maximises whole-plant carbon gain under a given environmental regime. A second, implicit assumption, is that maximising whole-plant carbon gain equates to maximising fitness. It is reasoned that a greater carbon gain should allow, for example, greater reproductive output and increased competitive ability (Givnish, 2002).

These assumptions allow the problem to be cast in a cost-benefit analysis, with the aim of estimating the leaf habit that maximises carbon gain in a given environment. On a conceptual level these models simply ask how much carbon is fixed annually by means of photosynthesis minus how much carbon is expended and lost annually through various processes. This could be written as

$$C_A \textit{ gained} = C_A \textit{ fixed} - C_A \textit{ expended} - C_A \textit{ lost}, \quad (1.1)$$

where C_A is the annual amount of carbon. The leaf lifespan with the greatest annual carbon gain (i.e. net profit in economic terms) should be favoured by selection and is expected to dominate. The difficulty with developing a realistic cost-benefit model for leaf habit lies in the cost part of the equation. The amount of expended carbon includes carbon expended in leaf construction and maintenance respiration of leaf tissue, but may also include respiration of root and stem tissue that supply the leaf with water and mineral nutrients. The amount of carbon that is lost may include losses due to herbivores, fire and other disturbances. These considerations have resulted in models with a different definition of the cost term (Chabot & Hicks, 1982; Kikuzawa, 1991; Kikuzawa & Ackerly, 1999; Givnish, 2002). Givnish (2002) argued that models that ignore whole-plant costs of photosynthesis are unrealistic and lead to false conclusions. As a solution, he proposed to include costs incurred through water and nutrient uptake in the roots. He further proposed that root costs can be estimated from the amount of water loss (transpiration) multiplied by the carbon cost of transpiration i.e. the amount of carbon that is lost in transpiring a unit of water. The carbon cost of transpiration is argued to be approximated by the marginal carbon cost of transpiration, expressed as $\frac{\delta A}{\delta E}$, where A is carbon assimilation (photosynthesis) and E is transpiration (Givnish, 1986, 2002). Givnish (2002) used his model to explore the relative advantages of evergreen and deciduous leaves under varying growing season lengths, leaf:root allocation ratios and leaf lifespans. He concludes that including root costs is essential to predict patterns of evergreen and deciduous leaf habit.

Despite the strong argument to consider root costs in carbon-balance models of optimal leaf lifespan, Givnish (2002) estimates root costs from leaf-level parameters. This is a major advantage when the model is parametrised with empirical data, as leaf-level processes are significantly easier to quantify than below ground processes. A second advantage is temporally explicit approach, which is required to assess effects of seasonal fluctuations

in physiological rates and environmental variables that affect these physiological rates. For example, carbon gain for each leaf habit could be estimated by month and would firstly depend on whether leaves were present or not and secondly on the environmental conditions during that month (Givnish, 2002). Such an approach partly considers leaf phenology, i.e. if there are no leaves carbon gain would be zero or negative, but it does not consider that the canopy might only be partly developed during certain months of the year. This suggests there is scope for improvement and the way the model is specified makes it easy to incorporate effects of leaf phenology.

Aim

The material reviewed in the preceding sections stresses how the timing and duration of leaf deployment influence a range of physical, geochemical and biotic processes that directly affect all life on Earth. It also identifies several gaps in the knowledge on how the timing and duration of leaf deployment are determined and how they are, or might be, affected by ongoing global change. Specifically, a globally comprehensive overview of phenological change is currently lacking, the geographic distribution of deciduous and evergreen plants is not fully understood and it is not clear to what extent it is driven by convergence and finally, the methods used to assess the relative advantages of evergreen or deciduous leaf habits in a given environment have not been extrapolated to include leaf phenology. I aim to answer three questions that are envisaged to make a contribution to the understanding of leaf habit and leaf phenology:

1. How has leaf phenology changed globally during the past three decades?
2. Does the geographic distribution of plants with evergreen and deciduous leaf habits suggest evolutionary convergence of the physiological niche of these leaf habits?
3. How do the combined effects of leaf phenology and leaf habit affect the carbon balance of plants?

I address these questions in separate chapters, which are introduced in more detail in the following section.

Overview

To provide a background against which to appreciate the immense impacts that the form and functioning of terrestrial plants in general, and leaves in particular, this chapter starts by describing the main effects that the appearance, evolution and ecological success of leafy plants have had on the functioning of the atmosphere and biosphere over geological time scales (millions of years). I then introduce how, on shorter time scales, the distribution of evergreen and deciduous leaf habits and seasonal patterns of leaf phenology has major effects on the exchange of energy and carbon between the terrestrial surface and the atmosphere, which has large implications for the global energy balance and local climates. I finish by reviewing existing theories and hypotheses that may help develop a better understanding of leaf habit, leaf phenology and potential changes in either.

In Chapter 2, I analyse a three-decade global time series of vegetation activity to quantify potential changes in leaf phenology. The aim of this chapter is to provide a globally comprehensive overview of leaf phenological change over the past three decades, to improve on current knowledge gained from regional studies and studies that include only one or a small number of phenological metrics. I develop novel methods to express change in relative units, which enables comparisons between ecosystems with vastly different leaf phenologies. Finally, I compare the calculated change to previously described change for some well-studied regions of the world and explore where change has previously gone undetected.

In Chapter 3, I focus on deciduous and evergreen leaf habits, which, along with leaf phenology, determine when the terrestrial surface is covered by green leaves. The aim of this chapter is to explore if the physiological properties of deciduous and evergreen plants,

i.e. the physiological niche, are convergent in biogeographically distinct regions. I start by using the normalised difference vegetation index (NDVI) to describe the geographic distribution of deciduous and evergreen leaf vegetation in four global biogeographic realms that span the tropical and austral regions of the world. Using a process-based model of plant growth, I quantify the physiological niche of plants with deciduous and evergreen leaf habits and compare the niches of vegetation with these leaf habits in different realms. I consider the implications of the calculated niche overlaps for the importance of environmental drivers on the distribution of leaf habit and whether environmental change is likely to affect the distribution of leaf habit.

In Chapter 4, I aim to consider the combined effects of leaf phenology and leaf habit on plant fitness, as measured by the annual carbon gain. I use empirical data collected in a seasonally dry African savanna to quantify leaf habit, leaf phenology and several other traits that are related to the carbon economy of a plant. I use this data to parametrise a simple carbon gain model and assess how carbon gain varies between species and to what degree carbon gain is affected by leaf habit and leaf phenology. I discuss how the results relate to theory on environmentally determined optimal leaf habits and examine the potential effect of divergent selection on leaf habit and leaf phenology.

In Chapter 5 I reflect on the main findings of each chapter and how they relate to the findings in other chapters and to the wider literature. I assess which questions that have remained unanswered in this thesis and which new questions that have arisen. I provide some suggestions for how future studies could address these questions.

Chapter 2

Three decades of multi-dimensional change in global leaf phenology

Robert Buitenwerf, Laura Rose and Steven I. Higgins¹²

¹Author declarations: RB and SIH designed the study and data analyses. RB performed the analyses with assistance from LR. RB wrote the manuscript with assistance from SIH. All authors discussed and commented on the manuscript.

²The work presented in this chapter has been accepted for publication in *Nature Climate Change*.

Introduction

Changes in the phenology of vegetation activity may accelerate or dampen rates of climate change by altering energy exchanges between the land surface and the atmosphere (Bonan, 2008; Myhre *et al.*, 2013) and can threaten species with synchronised life cycles (Thomas *et al.*, 2004; Both *et al.*, 2006; Post *et al.*, 2009). Current knowledge of long-term changes in vegetation activity is regional (Zhou *et al.*, 2001; White *et al.*, 2009; Zhu *et al.*, 2012) or restricted to highly integrated measures of change such as net primary productivity (Nemani *et al.*, 2003; Running *et al.*, 2004; Ciais *et al.*, 2005; Zhao & Running, 2010; de Jong *et al.*, 2012), which mask details that are relevant for Earth system dynamics. Such details can be revealed by measuring changes in the phenology of vegetation activity. Here we undertake a comprehensive global assessment of changes in vegetation phenology. We show that the phenology of vegetation activity changed severely (by more than 2 SD in one or more dimensions of phenological change) on 54% of the global land surface between 1981 and 2012. Our analysis confirms previously detected change in the boreal and northern temperate regions (Zhou *et al.*, 2001; White *et al.*, 2009; Zhu *et al.*, 2012). The adverse consequences of these northern phenological shifts for land-surface climate feedbacks (Bonan, 2008), ecosystems (Post *et al.*, 2009), and species (Both *et al.*, 2006) are well known. Our study reveals equally severe phenological change in the southern hemisphere, where consequences for the energy budget and the likelihood of phenological mismatches are unknown. Our analysis provides a sensitive and direct measurement of ecosystem functioning, making it useful for both monitoring change and for testing the reliability of early warning signals of change (Scheffer *et al.*, 2012).

Recent climate change has shifted species distributions (Parmesan & Yohe, 2003; Root *et al.*, 2003) and leaf phenology (Menzel *et al.*, 2006; Reyes-Fox *et al.*, 2014) around the world, leading to mismatches in previously synchronised phenological cycles (Both *et al.*, 2006; Post *et al.*, 2009). Such mismatches greatly increase the risk of extinction for affected species and ongoing climatic and phenological change is expected to further increase this

risk (Thomas *et al.*, 2004). Despite documenting and predicting effects of climate change on many organisms, these previous studies do not provide an easy way of inferring how widespread such changes are or where they are most severe. In addition to being a symptom of climate change, vegetation change also feeds back to the climatic system by forcing rates of energy exchange between the land surface and the atmosphere. Changes in the vigour and timing of vegetation activity can therefore accelerate or slow down rates of climate change (Bonan, 2008). Yet, the extent to which changes in vegetation phenology will impact the climate system by modifying albedo, transpiration, partitioning between latent and sensible heat in the atmosphere, and cloud formation has been identified as a major source of uncertainty in climate change projections (Freedman *et al.*, 2001; Myhre *et al.*, 2013).

To quantify changes in global vegetation activity, previous studies have used remotely sensed data to quantify changes in primary productivity (Nemani *et al.*, 2003; Running *et al.*, 2004; Ciais *et al.*, 2005; Zhao & Running, 2010). These studies have indicated an overall increase in NPP during the 1980s and 1990s, while evidence for a decrease during the 2000s (Zhao & Running, 2010) has been debated (Samanta *et al.*, 2011). Although estimating NPP is important for describing carbon sequestration, it is a highly integrated metric that masks important details of the nature of change. For example, it provides no information on the likelihood of phenological mismatches and limited information on consequences for the land surface energy budget. Consequently, constant NPP does not guarantee that vegetation is not responding to changing climates and increased atmospheric CO₂ in ways that affect the functioning of the Earth system. To quantify intra-annual shifts in the timing and vigour of vegetation activity, remotely sensed absorption of photosynthetically active radiation by the land surface can be used to directly infer photosynthetic activity.

We present a global analysis of change in the seasonal pattern of photosynthetically active radiation absorbed by the land surface as measured by the normalized difference vegetation

index (NDVI). We improve on previous analyses that have used NDVI to infer phenological change in two important ways. First, previous studies on long-term changes in leaf phenology have been regional (Zhou *et al.*, 2001; White *et al.*, 2005; Zhu *et al.*, 2012). We analyse the GIMMS3g data, a global record from 1981 to 2012, at 0.083° and 15 day resolution. Second, a problem that has prevented global analyses of phenology is that the information content of phenological metrics is not universal. For example, the onset of the growing season is an informative metric in deciduous forests, but less useful in evergreen forests. We use an improved method to estimate 21 ecologically interpretable metrics of the phenological cycle from the data (Figure 2.1) and evaluate the magnitude of change within 83 phenologically similar zones (hereafter called phenomes, shown in Figure A.1) to account for the fact that information content of these metrics differs between ecosystem types. These phenomes were identified using a cluster analysis of the phenological data. To obtain a spatially comparable measure of change, the change per pixel was scaled by the variance of change for the phenome to which it was assigned. Change is therefore reported in SD units, which can be interpreted as a measure of the severity of change.

Methods

Data

We used the GIMMS3g data (downloaded from ecocast.arc.nasa.gov/data/pub/gimms/3g/), which provides Advanced Very High Resolution Radiometer (AVHRR) NDVI data. The data are 15-day maximum-value composites from 1981 to 2012 at 0.083° resolution. Compositing reduces atmospheric effects (clouds, aerosols) and data have further been processed to reduce effects of navigation errors, major volcanic eruptions and orbital drift of older satellites and have been subjected to several sensor calibration steps. Finally, a rigorous analysis was carried out to resolve remaining discrepancies between data from different generations of AVHRR sensors (Pinzon & Tucker, 2014). Data quality scores

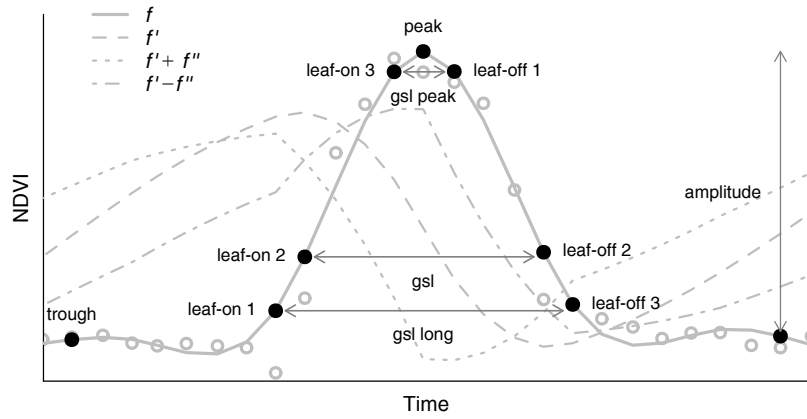


Figure 2.1: NDVI data for a single phenological year of an illustrative pixel, showing the 21 phenological metrics used in this study. Each labelled point represents a date and an associated NDVI value. The integral of the curve is also calculated. The solid line represents the fitted spline (f), the dotted lines show the first derivative (f') and functions calculated from the first and second (f'') derivatives, which were used to calculate phenological metrics.

were provided for each observation.

Defining phenological metrics

Data for each pixel were smoothed using a cubic spline function, which was weighted by data quality scores. A spline, unlike a parametric function, maintains a high fidelity to the data while retaining continuous first and second derivatives. We designed a two-step method to flexibly define the start of the time series for each pixel. First, the average Julian day of minimum NDVI (trough day) was calculated for each pixel using the 31-year time series. In the second step, the exact trough day for each phenological year was determined within a 180-day window (90 days on either side) around the 31-year mean trough day.

The period between two consecutive trough days constitutes a phenological year. For each phenological year 20 additional metrics were extracted (shown in Figure 2.1). Instead of defining the ‘start of the season’ and ‘end of season’ as a single date, we calculated three dates for start and end of season, which improved our ability to detect change. For example, in some deciduous forests, invasive understorey plants extend the growing season by retaining leaves longer than native forest trees (Fridley, 2012). Such change is difficult to describe with a single metric i.e. a large decrease in NDVI still occurs when the trees drop their leaves while the understorey plants will cause low NDVI to persist for longer. ‘Leaf-on 1’, ‘leaf-on 2’, and ‘leaf-on 3’ represent the first increase, the fastest increase, and end of increasing (i.e. the start of peak) photosynthetic activity, respectively. These dates can be interpreted as leaf emergence, rapid leaf expansion, and attainment of a full canopy. Similarly, three leaf-off dates were calculated and the number of days between leaf-on and leaf-off dates represented three measures of growing season length: ‘gsl-long’, ‘gsl’, and ‘gsl-peak’

We calculate the three leaf-on and leaf-off dates using the first and second derivatives of the spline function. For smooth functions, e.g. a sine, the maximum of the second derivative

indicates when the function starts going concave up, and could hence be used to define the start of the growing season. However, NDVI data is not always smooth and sometimes produces a spline with multiple peaks within a phenological year. Instead of sacrificing accuracy by smoothing the data further, we centred and scaled both the first and second derivatives, summed them, and calculated the days at which this sum is maximal and minimal (shown in Figure 2.1). This method selects for the maximum (or minimum) in the second derivative that is closest to the maximum (or minimum) in the first derivative and provided a robust way of defining the three leaf-on and leaf-off metrics.

This procedure yielded a 31-year time series of 21 phenological metrics for 2,075,445 pixels.

Phenological change over time

For every pixel, change for each of the 21 metrics was defined as the difference between averages of the beginning and the end of the time series, i.e. between 1981-1990 and 2003-2012. Trend analysis was avoided as there was no a priori reason to assume change should be linear or monotonic. Comparing ten-year averages buffers against effects of anomalous climatic events in a single year on the change estimate.

Comparing change spatially

As explained in the text, we scaled change of each pixel by the variance of phenologically similar regions to obtain a spatially comparable measure of change. Since existing land cover classifications based on the biome concept did not adequately summarise phenological variation, we used a model-based clustering method to identify the optimal number of phenologically similar regions (phenomes). The procedure resulted in 83 phenomes.

Summarising change

The final step in our analysis was to summarise change globally, by grouping phenomes with similar type and magnitude of change into nine syndromes (Figure 2.3a) using unsupervised hierarchical clustering. For each syndrome, average change in SD units was plotted along two axes, one representing change in NDVI, the other representing phenological change (i.e. change in dates or number of days) (Figure 2.3b). The full work flow of our analysis is summarised in Figure A.4.

Clustering pixels into phenomes

We used an unsupervised model-based clustering approach as implemented in the `mclust` package (Fraley & Raftery, 2002; Fraley *et al.*, 2012) in R (R Core Team, 2014). This two-step algorithm uses results from a hierarchical clustering step to initialize a normal mixture model, which is estimated with the expectation-maximisation (EM) algorithm. The hierarchical clustering step was performed on a random 1% subset of the data (21,000 pixels), after which all the data were clustered in the expectation-maximisation step. Previous studies have used the k-means algorithm to define phenologically similar regions (White *et al.*, 2005); however, there are several important advantages to model-based clustering. First, while the number of clusters needs to be specified a priori, the optimal number of clusters, 83 for our data, can be estimated using the Bayesian Information Criterion (BIC). Second, the algorithm estimates the probability that a pixel belongs to a cluster, i.e. membership, and thirdly, it allows for variable cluster shape, volume, and orientation whereas k-means tends to produce spherical clusters (a tendency we confirmed with preliminary analyses).

Several processing steps were required to produce the input data for the clustering algorithm from the NDVI time series. First, the mean for each of the 21 phenological

metrics was calculated for each pixel. The eight circular variables (i.e. the variables measured in Julian day) were first transformed to radians, which were then used to calculate Cartesian coordinates by taking the sine and cosine. This step yielded a matrix with 29 columns (13 NDVI variables, 8 sine of Julian day variables and 8 cosine of Julian day variables) and a row for each pixel. Since certain variables were correlated (e.g. the first and second leaf-on day), we reduced the dimensions of the data by applying a principal component analysis (PCA) to centred and scaled values and used the first three principal components (capturing 72% of total variance). From these components, a three column matrix was produced with a row for each pixel and the clustering was performed on this matrix.

Clustering 83 phenomes into 9 syndromes of change

For each phenome, the average change was calculated for each of the 21 phenological metrics, yielding a matrix with 83 rows and 21 columns. This matrix was clustered using the hierarchical clustering function in the *mclust* package (Fraley & Raftery, 2002; Fraley *et al.*, 2012) for R (R Core Team, 2014). Since this classification is merely to concisely present changes of 21 variables in 83 groups, the number of clusters was chosen to display the range in responses effectively.

Results and Discussion

We found that leaf phenology changed substantially in most regions of the world, with 95% of the land surface changing by at least 1 SD for at least one metric. Figure 2.2a shows the magnitude of change summed for all 21 metrics. Change was distinctly clustered in space, with relatively large areas where total change was homogeneous. Splitting total change into changes in the vigour of vegetation activity (NDVI) and changes in timing of the phenological cycle, reveals that regions with changes in vegetation vigour are not

necessarily associated with changes in phenological timing and vice versa (Figure 2.2b, c). For example, the conspicuous change around the Baltic and into Belarus is primarily due to temporal shifts in vegetation activity. Such changes might be associated with increased agricultural yields which have been observed in parts of this region (Ray *et al.*, 2012).

The summed changes in Figure 2.2 provide a useful summary of phenological change but do not show the complete nature of the change. To further dissect change, we therefore grouped the 21-dimensional change into nine general syndromes of change (Figure 2.3a). The direction and magnitude of change for each of these 9 syndromes of change are summarised in Figure 2.3b using plots of the average phenological cycle estimated at the start and end of our time series. We further show in Figure 2.3b how, for each syndrome of change, the average of our 21 metrics has changed in SD units. The importance of measuring change relative to the inherent variation in a phenome is illustrated clearly in syndromes 3 and 6, which show a small absolute change, but large relative changes.

In syndromes 3, 4, and 6, which occur in the Arctic and Boreal regions, growing seasons have become longer and total photosynthetic activity (NDVI integral) has increased. However, the exact phenological changes that underlie this overall greening differed between regions. In the most northern areas (syndrome 3), the growing season was not only extended, but also occurred earlier due to both earlier leaf-on and leaf-off dates. Further south (syndrome 4), earlier leaf-on dates extended the growing season, while leaf-off dates did not change. In contrast, still further south (syndrome 6), the growing season was prolonged primarily by later leaf-off dates. The variety of phenological changes we detected in these regions, all of which resulted in net greening, suggests that different mechanisms are driving change in each of these regions.

In contrast to the coherent change over large parts of the Boreal, the nature of phenological change differed dramatically over relatively short distances in other regions. This is particularly apparent in West Africa, where 5 syndromes of change span the region south of the Sahara. While increases in the peak NDVI and integral of photosynthetic activity

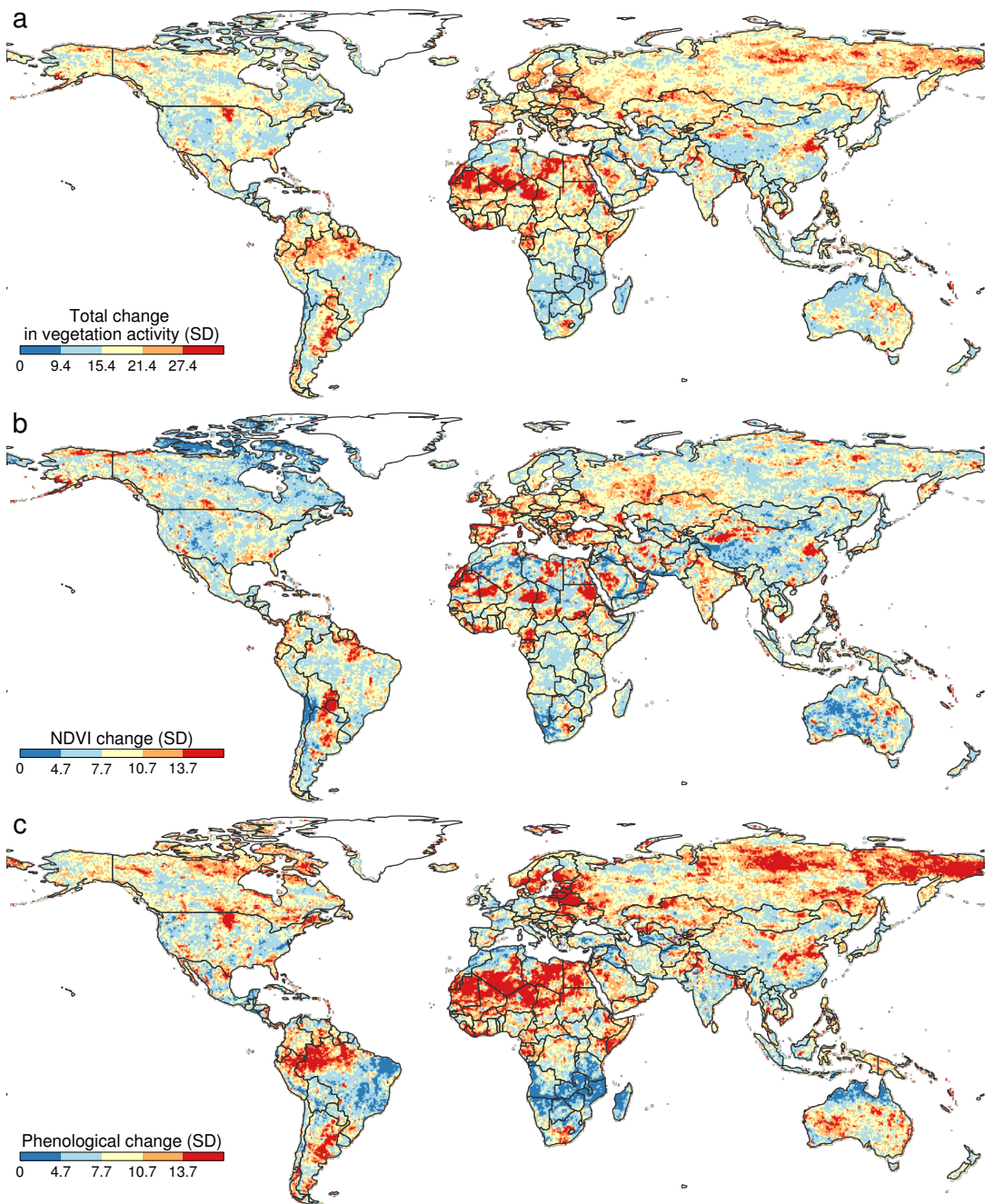


Figure 2.2: **a)** Total change in vegetation activity (the summed change of all 21 metrics). **b)** Change in the vigour of vegetation activity (the summed change of 10 metrics measured in NDVI). **c)** Change in the timing of the phenological cycle (the summed change of 11 metrics measured in days or day of year).

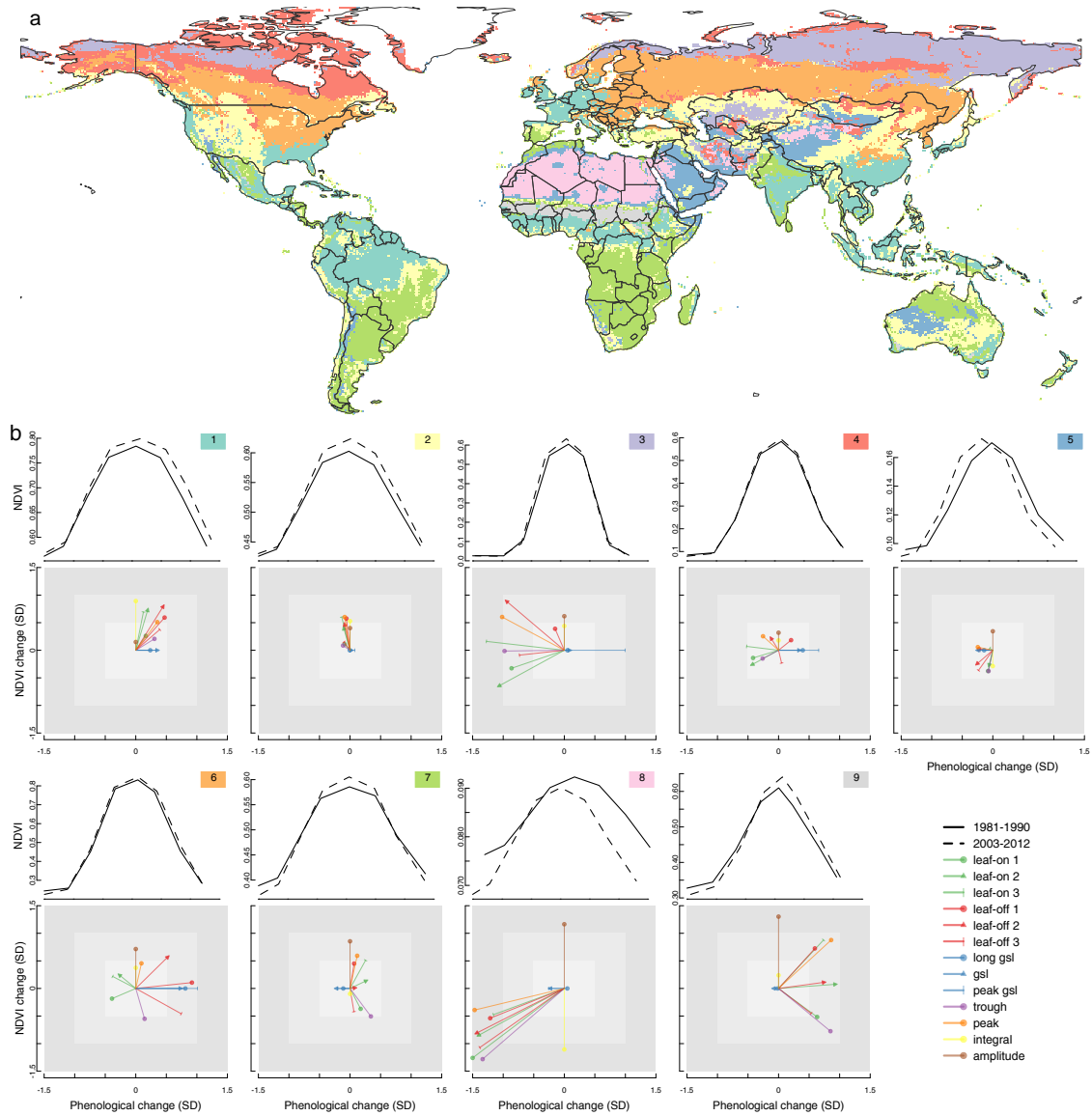


Figure 2.3: **a)** Nine global syndromes of change. **b)** For each of 9 syndromes of change, the upper panel shows the average NDVI signal of a phenological year at the start and the end of the time series. The bottom panel shows the change between the beginning and end of the time series for all metrics in SD units. The vectors parallel to the axes represent metrics that were originally measured in either NDVI or time units (days, day of year). The angled vectors represent two metrics simultaneously i.e. where an NDVI value was associated with a date.

that we detected have been previously described in studies reporting greening of the Sahel (Olsson *et al.*, 2005) (Syndromes 1 and 9), we found that an extension of the growing season contributed to greening.

In addition to recognising the distinct phenological shifts that underlie greening in the Arctic, Boreal and Sahel, we identify several areas in South America that have changed severely. The dry Chaco of Paraguay and Bolivia has experienced a drastically reduced NDVI during the dry season (Figure 2.2b, Figure A.2). In the Espinal and Pampas regions of north-eastern Argentina, the growing season has drastically shifted forward and wet season NDVI has increased. These areas are consistent with areas where linear slopes of NDVI time series changed significantly (Paruelo *et al.*, 2004).

While the described patterns of change are spatially coherent, they do not coincide with the distribution of global biomes, which have previously been used to summarise global vegetation change (de Jong *et al.*, 2012). For example, some savannas in South America, southern Africa, and Australia have experienced drastic reductions in dry season NDVI while others have not (Figure A.2). Therefore, despite having structurally similar vegetation and comparable climates, phenological change is qualitatively different in savannas of different regions, potentially as a result of differences in ecosystem functioning (Lehmann *et al.*, 2014).

An important conclusion from this study is that qualitatively different phenological changes can lead to quantitatively similar change in summary variables such as growing season length and total photosynthetic activity, a proxy for productivity. Our estimates of changes in these integrated variables are consistent with more specific studies. We detected severe change in total photosynthetic activity in e.g. Alaska, Australia, India, and the Sahel (Figure A.2), consistent with areas that experienced the greatest change in a trend analysis on NDVI time series (de Jong *et al.*, 2012). We also detected extended growing seasons in the boreal and northern temperate zones (Figure A.2), consistent with previous studies in these regions (Zhou *et al.*, 2001; Zhu *et al.*, 2012), and higher photosynthetic activity in

the Sahel (Figure 2.2a), consistent with Olsson *et al.* (2005). These agreements indicate that our methodology is sensitive, yet robust enough to be applied globally.

Our methodology also addresses disagreement between previous studies. For example, White *et al.* (2009) reported no changes in the start of the growing season in North American Arctic and taiga, while Zhou *et al.* (2001) inferred earlier leaf-on dates from the same data set. Consistent with White *et al.* (2009), our ‘leaf-on 1’ metric did not change, while our ‘leaf-on 2’ and ‘leaf-on 3’ advanced by 0-10 days throughout the North American arctic and the eastern part of the taiga, consistent with Zhou *et al.* (2001). This suggests a change in the shape of the green-up part of the phenological curve. Such differences have previously been ascribed to methodology, prompting White *et al.* (2009) to compare 10 different methods of calculating the start of the growing season and advocating an ensemble approach. Our analysis reconciles the apparent discrepancies between White *et al.* (2009) and Zhou *et al.* (2001) by revealing multiple, ecologically distinct, components to the green-up part of the phenological curve.

Our study confirms the boreal and temperate regions of the northern hemisphere as areas of rapid phenological change (Zhou *et al.*, 2001; White *et al.*, 2009; Zhu *et al.*, 2012). In northern regions, long field observational records have been used to attribute these phenological changes to warming climates (Menzel *et al.*, 2006). It has been shown that the resulting mismatches in phenological cycles disrupt trophic interactions and increase extinction risk (Both *et al.*, 2006; Post *et al.*, 2009; Thomas *et al.*, 2004), while impacts on the land surface energy budget have been assessed as significant (Bonan, 2008; Myhre *et al.*, 2013). We detected equally severe changes over large regions of Africa, South America, and Australia that have previously gone unnoticed but might have significant ecological and atmospheric consequences. In these regions, field observational records are scarce and leaf phenology is largely driven by precipitation (Higgins *et al.*, 2011). Since precipitation projections are more uncertain than temperature projections (Flato *et al.*, 2013), the potential for phenological mismatches and consequences for the land surface

energy balance in these regions are highly uncertain. Therefore, analyses of remotely sensed time series of photosynthetic activity are an important and necessary first step in identifying where vegetation might be responding to changes in climate, atmospheric CO₂, and other atmospheric forcings.

Attributing phenological responses to any of these drivers will require regional approaches since studies (Menzel *et al.*, 2006; Higgins *et al.*, 2011; Reyes-Fox *et al.*, 2014) suggest that vegetation activity is co-limited by several environmental factors and the limiting factor is likely to be region specific. For example, in African savannas where rainfall is widely assumed to limit vegetation activity, it has been shown that rainfall does not control leaf onset of all species (Higgins *et al.*, 2011). In Europe, there is a strong temperature control over leaf onset, but not leaf senescence (Menzel *et al.*, 2006). In a North American grassland, experimental evidence suggests that warming coupled with increased atmospheric CO₂ delays leaf senescence, but that increased CO₂ does not trigger earlier leaf emergence (Reyes-Fox *et al.*, 2014). Because CO₂ influences the water use efficiency of plants (Field *et al.*, 1995), we expect that increased CO₂ is most likely to extend the growing season where the beginning or end of the growing season is moisture limited. Increased photosynthetic activity over Botswana and north-east South Africa are suggestive of a CO₂ effect (Buitenwerf *et al.*, 2012), although how CO₂ interacts with climate and disturbance needs to be considered (Poulter *et al.*, 2014).

In conclusion, we show that the majority of the Earth's land surface has, between 1980 and 2012, undergone some form of change in the seasonal pattern of vegetation activity. Our analyses provide a map of where the risk of phenological mismatches is higher and a basis for modelling the radiative forcing consequences of phenological change. The direct measurements of change used here might also serve to monitor change and evaluate the performance of early warning indicators of imminent catastrophic change in ecosystem state.

Chapter 3

Convergence in the physiological niche of evergreen and deciduous vegetation

Robert Buitenwerf and Steven I. Higgins¹

¹Author declarations: RB and SIH designed the study and data analyses. RB performed the analyses. RB wrote the manuscript with assistance from SIH.

Abstract

The seasonal timing and duration of leaf deployment has major implications for earth-atmosphere interactions and biotic processes. While evidence for global change impacts on the timing of leaf deployment (leaf phenology) is accumulating, the mechanisms that determine the duration of leaf deployment (leaf habit) and its geographic distribution remain untested. Theory to explain leaf habit assumes selection for an optimal leaf habit under a given environmental regime, implying evolutionary convergence. Here we examine convergence in the physiological niche of different leaf habits. We delineate the distribution of two types of evergreen and one type of deciduous leaf habit (phenomes) across four global biogeographic realms. For each phenome in each realm, we then quantify the physiological niche using a process-based model of plant growth. The derived physiological niche dimensions of each phenome are used to project its potential distribution into other, non-native realms. Convergence is implied where the predicted phenome is consistent among projections from all realms. We find excellent agreement between observed and predicted phenomes in the native realm, suggesting that our model adequately describes the physiological niche of each phenome. Projections from each phenome into non-native realms coincided in 71% of the study area, implying widespread convergence of the physiological niches of phenomes. Where projections of all realms did not coincide the phenome type is uncertain, possibly because of historical contingencies or alternative stable states. These results imply an important role for evolutionary convergence in the biogeography of leaf habit, but also identify large regions where other forces might dominate. This is likely to have significant implications for effects of global change on the geographic distribution of leaf habit.

Introduction

The period of leaf deployment has major implications for the exchange of carbon, water and energy between the land surface and the atmosphere as leaves are the primary plant organs that absorb radiative energy, capture carbon from the atmosphere and release water vapour into the atmosphere. Changes in the timing and the duration of leaf deployment is likely to have far reaching implications at a wide range of spatial scales. For example, local runoff, regional cloud formation and weather patterns and the global energy balance may be affected (Schwartz, 1996; Freedman *et al.*, 2001; Schwartz & Crawford, 2001; Bonan, 2008), but also biotic processes such as the disruption of synchronised life cycles (Walther *et al.*, 2002; Post *et al.*, 2009; Menzel, 2013b) and agriculture (Chielewski, 2013). Significant changes in leaf phenology over the past decades (Zhou *et al.*, 2001; Menzel *et al.*, 2006; Zhu *et al.*, 2012; Buitenwerf *et al.*, 2015) suggest that leaf phenology is highly responsive to changes in climate and atmospheric CO₂ (Menzel *et al.*, 2006; Zohner & Renner, 2014; Reyes-Fox *et al.*, 2014). However, the processes that determine the timing and duration of leaf deployment remain unclear, hampering forecasts of future distributions under likely scenarios of global change.

The duration of leaf deployment depends not only on leaf phenology, the seasonal progression of leaf emergence and senescence, but also on leaf habit. The term leaf habit is used to distinguish between evergreen and deciduous habits (Kikuzawa & Lechowicz, 2011). Although the concepts of leaf phenology and leaf habit are evidently related, current evidence does not allow estimates of the extent to which they may be affected by the same ecological and evolutionary processes. Recent studies have shown that leaf phenology in many parts of the world is highly flexible (Menzel, 2013b; Buitenwerf *et al.*, 2015), but the plasticity of leaf habit remains unclear. This prevents forecasts of how global change or cascading effects of changing leaf phenology may affect the leaf habit of plants or the geographic distribution of leaf habit.

Current theory that aims to explain the distribution of leaf habit and its correlate leaf lifespan is based on the assumption that these traits have adaptive significance and that selection acts to maximise plant carbon gain and thereby fitness (Chabot & Hicks, 1982; Kikuzawa, 1991; Ackerly, 1999; Givnish, 2002). The plant strategy that maximises carbon gain is shaped by how leaf habit trades-off with physiological processes under different environmental conditions (Wright *et al.*, 2004). Hence, the combination of physiological traits and environmental variables that result in a positive carbon balance defines the physiological niche. Because environmental variables vary seasonally, this physiological niche is further characterised by the timing of when plant growth is possible and whether it is cost effective for plants to retain their leaves through unfavourable periods of the year (Kikuzawa & Lechowicz, 2011). The physiological niche is therefore intimately linked to the timing and duration of leaf deployment.

We estimate the physiological niche space using a process based model of plant growth (Higgins *et al.*, 2012b) for three leaf habit classes (phenomes) in four biogeographic realms that span tropical and austral regions. Realms denote areas within which evolutionary history and taxonomic composition is more similar than between realms (Cox, 2001), suggesting that if non-convergence in the physiological niche of leaf habit existed, it should be detectable by comparing analogous phenomes of different realms. We compare phenomes by calculating overlap in the modelled physiological niche and use the physiological niche to project geographic distributions of phenomes outside their native realm. A large overlap would suggest that vegetation with the same leaf habit uses the same physiological niche space in different realms, implying evolutionary convergence.

Methods

Delineating phenomes

The first step in our analysis was to create a map of deciduous and evergreen vegetation. Previous studies used 30 metrics derived from remotely sensed spectral time series to estimate the proportion of evergreen vegetation globally (DeFries *et al.*, 1999, 2000). Here we use a simpler approach based on two metrics derived from the GIMMS_{3g} normalised difference vegetation index (NDVI) product (Pinzon & Tucker, 2014) to estimate evergreenness. These data have a spatial resolution of 0.083° and were downloaded from ecocast.arc.nasa.gov/data/pub/gimms/3g/. NDVI time series from 1981-2012 were described using a cubic spline function, in which observations were weighted by the quality scores that are supplied for each data point. From these splines we calculated the minimum, maximum and amplitude for each year and took the mean of these annual values. Evergreenness was calculated as the ratio of NDVI amplitude (*amp*) to minimum NDVI (*min*), so that when amplitude is zero the vegetation is fully evergreen, and when amplitude is large with respect to the minimum, the vegetation is deciduous. It should be noted that this algorithm will be misleading in northern regions, where winter snow cover obscures evergreen vegetation.

Since the TTR model requires presence-absence data, pixels were assigned to one of three classes: deciduous, high leaf area index (LAI) evergreen and low LAI evergreen. The high LAI evergreen class includes evergreen forests and thickets with aseasonal climates, where conditions are continually favourable for growth. The low LAI evergreen class includes evergreen shrublands with non-seasonal climates, where growth is restricted to episodically favourable conditions. The distinction between high and low LAI evergreen was made as plants in these vegetation types are likely to have fundamentally different physiological niches (Mooney & Dunn, 1970a; Lloyd & Farquhar, 1994). We assumed that pixels with very low NDVI (maximum NDVI < 0.1) were devoid of

vegetation. These areas therefore contributed absence points, but no presence points. Lastly, to minimise effects of heavily modified surfaces we excluded built up areas and crop lands from our analysis using the Global Land Cover 2000 product (classes 16-23, <http://bioval.jrc.ec.europa.eu/products/glc2000/glc2000.php>).

Classes were identified using model-based clustering as implemented in the `mclust` package (Fraley & Raftery, 2002; Fraley *et al.*, 2012) for R (R Core Team, 2014). The algorithm first applies a hierarchical clustering to a subset of the data, the result of which is used to initialise a linear mixture model that classifies all data. A major advantage of this technique is that it returns an estimate of the Bayesian Information Criterion (BIC) for each number of clusters, allowing the user to select the optimal number of clusters in the data. We first applied the algorithm to the evergreenness index to identify classes of leaf habit. From the result of this analysis, we selected evergreen pixels, on which a second clustering was performed using the minimum NDVI to identify LAI classes within evergreen systems. The two classifications were combined in a supervised manner to produce a final classification.

Biogeographic realms

We used the biogeographic realms for plants as defined by Cox (2001). This scheme is based on Takhtajan's (1986) floral kingdoms, but separates the palaeotropical realm into African and Indo-Pacific realms, includes the Cape floral kingdom with the African realm (also see Linder *et al.* 2012), includes New Zealand with the Australian realm, and includes Patagonia with the South American realm. The classification thus yields four realms spanning tropical and austral regions: South American, African, Indo-Pacific and Australian. These names were proposed by Cox (2001) and, despite not being entirely accurate in some locations, were adopted here for pragmatic reasons; they are relatively unambiguous and short. Since Cox (2001) and Takhtajan (1986) do not provide digital

maps, the boundaries between Olson *et al.*'s (2001) zoographic realms were taken as a guide where they coincided with Cox's classification and were drawn by hand otherwise.

TTR

The Transport Resistance model is a model of plant growth and allocation developed by Thornley (1998). Thornley's model predicts biomass accumulation based on the acquisition of carbon by shoots, acquisition of nitrogen by roots, and the exchange of these resources between roots and shoots as determined by the demand and supply of each compartment. It explicitly separates the physiological processes of resource uptake from growth. Higgins *et al.* (2012b) developed an implementation of Thornley's Transport Resistance (henceforth TTR) model in which the modelled physiological processes are forced by environmental variables. Specifically, their implementation considers how carbon uptake might be limited by temperature, soil moisture, solar radiation and shoot nitrogen; how nitrogen uptake might be limited by temperature, soil moisture and soil nitrogen; and how growth and respiration might be influenced by temperature. The model predicts the accumulated biomass of an individual plant at a given location as a function of the plant's physiological properties (as represented by the TTR parameters) and the environmental forcing variables at that location. If we assume that an entity (in this study a phenome) exists in a physiological niche space, we can use information on the geographic distribution of environmental forcing variables to project that entity's geographic distribution. Higgins *et al.* (2012b) used such an approach to predict the distribution of tree species in Europe. In that study, the physiological properties described by the model were not known a priori and were inferred from observed species distributions. Here we employ the same approach for phenomes, using the observed phenome distributions as described in the previous section to infer their physiological niche.

To fit the model, we follow Higgins *et al.* (2012b) and assume that p_i , the probability of a phenome occurring at site i , is described by the complementary log-log function of the

modelled plant biomass at site i and that the likelihood of observing the presence absence data (y_i) at site i is described by the Bernoulli distribution. To find the set of parameters that maximise this likelihood over all sites, we used the differential evolution optimization algorithm (Mullen *et al.*, 2011). The algorithm mutates and recombines a population of candidate solutions over generations. We ran the algorithm for each phenome using populations of 100 candidate solutions for 500 generations. This procedure was repeated 5 times. Each subsequent iteration through the phenome list used solutions from the previous iterations to initiate the algorithm. To speed up computation, we randomly selected 2000 presence and 2000 absence points for each phenome per iteration. The estimated probability of a phenome occurring at site i was converted to presence-absence using a threshold, which was determined by maximising the overall accuracy of the map, i.e. the proportion true presences and absences (Guisan & Thuiller, 2005; Higgins *et al.*, 2012b).

The model runs on monthly time steps and therefore explicitly considers how seasonal fluctuations in the forcing variables interactively influence resource uptake and growth. The environmental forcing variables used in the simulations were monthly soil water and solar radiation (Trabucco & Zomer, 2010), monthly mean, maximum and minimum temperature (Hijmans *et al.*, 2005) and soil nitrogen as soil nitrogen density (Global Soil Data Task Group, 2000). The soil nitrogen data was available at a 5x5 arc-minutes grid, while all other variables were taken from 1-km grids.

Accuracy, projections and niche overlap

To describe the accuracy of the TTR model predictions, we compare the predicted presences and absences of each phenome in its native realm to the observed presences and absences using a confusion matrix. From the confusion matrix, we calculated overall accuracy, which is the proportion of correctly predicted presences plus the proportion of correctly predicted absences. We also calculate the kappa statistic (κ). This is a measure

of classification accuracy that takes into account that some of the overall accuracy may be due to chance, which is likely when one class (e.g. absences) is much more common than the other (e.g. presences). κ can be described as the proportion of disagreements expected by chance that did not occur (Rossiter, 2014). When κ is 1, there are no disagreements and when it is 0, all disagreements expected by chance occurred. There are no clear rules about what value for κ indicates a good fit; however, values above 0.4 have been suggested to indicate a good fit (Monserud & Leemans, 1992).

To test how well each phenome is able to predict the distribution of analogous phenomes in other (non-native) realms, we also used confusion matrices. That is, for each phenome we compared projections into the non-native realms to observed leaf habit in the non-native realms while excluding projections into the native realm. If projections from a phenome can predict the observed distribution of an analogous phenome in another realm, it suggests that these phenomes have similar physiological niches.

We also calculated niche overlap directly. Because the physiological niche as predicted by the TTR model is a multi-dimensional volume that is shaped by interactions between the modelled physiological processes and their environmental dependencies, overlap is difficult to quantify. We therefore follow methods developed by Warren *et al.* (2008) and Broennimann *et al.* (2012) in which the predicted probability of occurrence from the TTR model is used as a one-dimensional summary of the physiological niche to calculate overlap. Niche overlap is quantified using Schoener's D, which is a value between 0 (no overlap) and 1 (complete overlap). The calculation of niche overlap only includes environmental space that exists in both of the realms that are being compared (Broennimann *et al.*, 2012). To test if the overlap between the physiological niche of two phenomes is greater than expected by chance, we compare the niche of a phenome in its native realm to a randomly simulated niche in another realm. Where niche overlap between analogous phenomes of different realms is greater than expected by chance, evolutionary convergence is implied.

Results

Delineating phenomes

The simple NDVI-based index for evergreenness ($\frac{amp}{min}$) corresponds to existing maps of biome distributions (Figure 3.1a). For example, in Africa areas dominated by tropical forest and arid shrublands are evergreen, while surrounding savannas are deciduous. The cluster analysis on the evergreenness index identified the optimal solution as having 5 classes, the first two of which were small and clearly deciduous (a low minimum with a large amplitude). They were therefore merged with the third class. The resulting three classes: deciduous, evergreen and an intermediate class, are shown by the diagonal dividing lines in Figure 3.1b. We then performed a second cluster analysis on minimum NDVI that only included pixels in the evergreen and intermediate classes. This analysis identified 3 LAI classes as the optimal solution. The first one clearly represented low LAI systems (green in Figure 3.1b), while the other two were highly mixed in geographical space and we therefore merged them. This resulted in a final classification with four classes (Figure 3.1 b,c). The overlap class was not modelled as a separate leaf habit, but was interpreted as areas where the distribution of deciduous and evergreen vegetation overlaps. Ecologically such areas can be thought of as either having significant proportions of both evergreen and deciduous vegetation or consisting of evergreen-deciduous mosaics at a scale below the data resolution (0.083°). The final classification was therefore a combination of an unsupervised clustering approach and manual pruning of some clusters to produce a pragmatic and repeatable classification.

For each of the four biogeographic realms, the classification provided presence-absence data for three phenomes. The maps in Figure 3.1 show that by masking pixels with heavily modified land cover, most of the continental part of the Indo-Pacific realm and large parts of South America are excluded from the analysis.

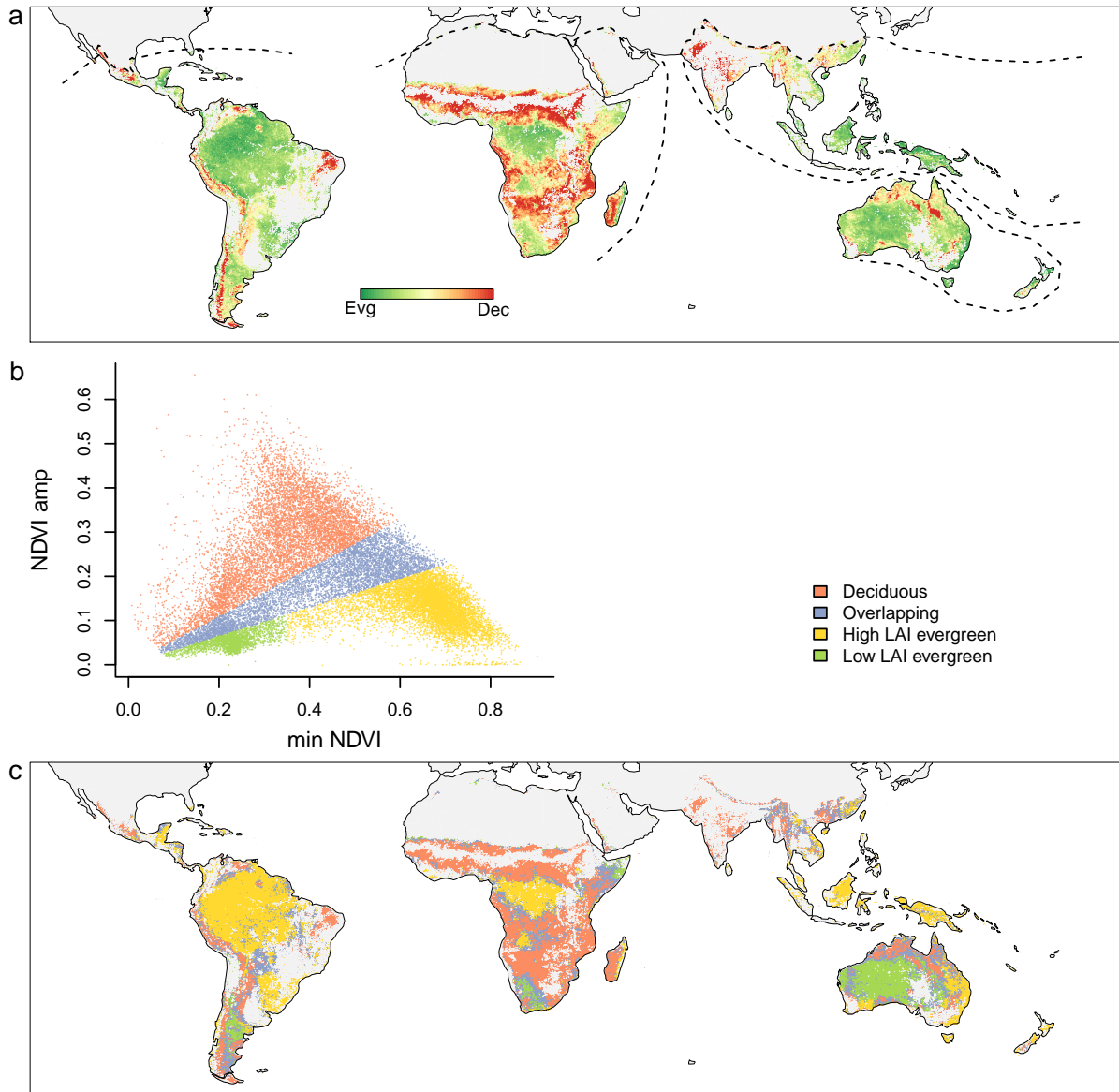


Figure 3.1: Evergreenness and phenome classification. **a**) Evergreenness expressed as the ratio of NDVI amplitude and minimum NDVI. Areas outside selected realms, bare areas, and intensively managed areas are shown in grey and were masked from the analysis. The dotted lines show the boundaries of biogeographic realms according to Cox (2001). **b**) Classes obtained from the evergreenness index ($\frac{amp}{min}$) and minimum NDVI using linear mixture models. **c**) The classes from **b** projected into geographical space.

Model accuracy

The proportion of correctly predicted presences and absences in the native realm indicates an overall model accuracy between 60 and 90% (Table 3.1). The proportion of false negatives reflects how often the model failed to predict phenome presence despite it being present in the observed data. When there are many false negatives, the model is likely to be unrealistic (Segurado2004) (often expressed as sensitivity: 1 - proportion false negatives). The proportion of false negatives was less than 10% for 10 of 12 phenomes. The κ values, which account for unequal number of presences and absences in the observed data, ranged between 0.31 and 0.76 for all except one phenome. The very low κ for the low LAI evergreen phenome in the Indo-Pacific realm was a result of the very small number of presence points (Table 3.1). Overall, these results indicate that the model correctly predicted presence or absence at the majority of pixels in the native realm and that model sensitivity was relatively high.

Physiological niche of phenomes

The predicted niche dimensions for each phenome in each realm are shown in Figure 3.2. Although for most niche axes the overlap between the same phenome in different realms is relatively large, there are distinct differences. For example, carbon uptake for the deciduous phenome in the Indo-Pacific and South America proceeds at lower maximum temperatures than in Africa and Australia. Growth in low LAI evergreens takes place at lower temperatures in South America than it does in other realms.

The results in Figure 3.2 are difficult to interpret because modelled growth (from which occurrence is estimated) is co-limited by all physiological processes and their environmental dependencies. In other words, growth is constrained by the most limiting physiological process and some of the niche boundaries in Figure 3.2 may therefore be misleading. However, the predicted probabilities of occurrence accounts for these co-limiting processes and

Table 3.1: Performance of the TTR model as comparisons between observed and predicted phenome distributions in the native realm. Columns show the total number of pixels where the phenome was present (n_P) and absent (n_A), the proportions of true positive and negative predictions (T_{pos} , T_{neg}), proportions of false positive and negative predictions (F_{pos} , F_{neg}), overall accuracy ($A_o = T_{pos} + T_{neg}$) and the kappa statistic (κ). The sensitivity is not shown but can be calculated as $1 - F_{neg}$. The phenome abbreviations are dec = deciduous, hle = high LAI evergreen and lle = low LAI evergreen. The realm abbreviations are AU = Australia, AF = Africa, IP = Indo-Pacific and SA = South America.

Phenome	Realm	n_A	n_P	T_{pos}	T_{neg}	F_{pos}	F_{neg}	A_o	κ
dec	AU	47687	37448	0.30	0.42	0.14	0.14	0.72	0.44
dec	AF	35367	149258	0.76	0.10	0.10	0.05	0.85	0.48
dec	IP	22218	34734	0.53	0.30	0.10	0.08	0.82	0.62
dec	SA	99132	67032	0.32	0.43	0.17	0.08	0.74	0.49
hle	AU	62203	22932	0.24	0.65	0.08	0.03	0.89	0.73
hle	AF	133939	50686	0.27	0.34	0.39	0.01	0.60	0.31
hle	IP	19385	37567	0.54	0.24	0.10	0.12	0.78	0.52
hle	SA	44236	121928	0.67	0.23	0.04	0.06	0.90	0.76
lle	AU	36593	48542	0.54	0.34	0.09	0.03	0.87	0.74
lle	AF	160889	23736	0.12	0.67	0.20	0.01	0.79	0.43
lle	IP	56756	196	0.00	0.89	0.10	0.00	0.90	0.03
lle	SA	151531	14633	0.08	0.77	0.14	0.01	0.86	0.47

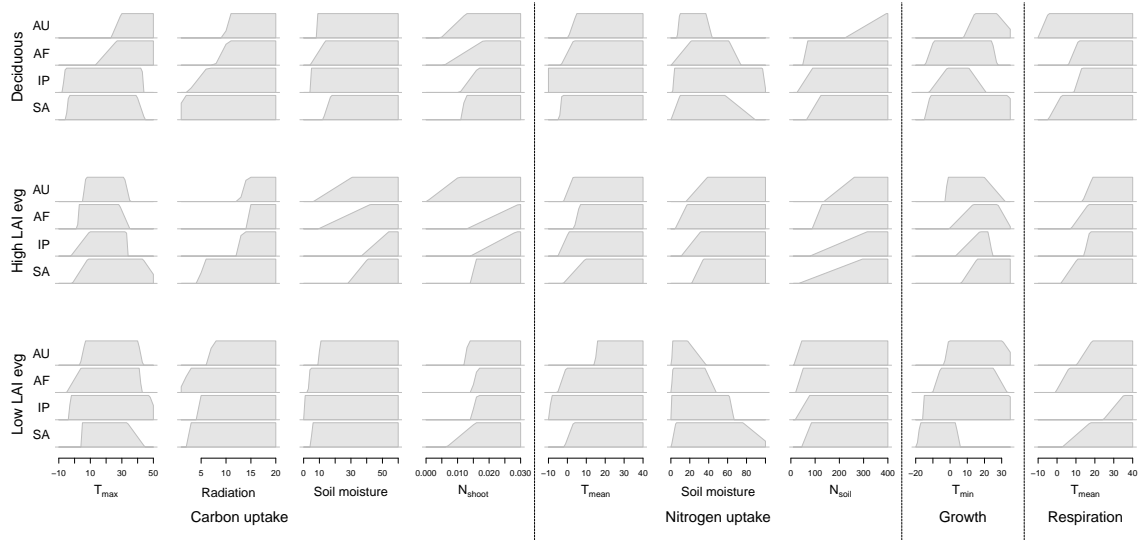


Figure 3.2: Physiological niche dimensions of phenomes from different realms, as estimated using the TTR model. Temperatures are in $^{\circ}\text{C}$, solar radiation is expressed as daily evaporation equivalents (mm day^{-1}), soil moisture is a percentage, shoot N is a concentration and soil N is g m^{-2} .

can therefore be used as a one-dimensional summary of the multi-dimensional physiological niche. We used the projected occurrence probabilities to calculate pairwise niche overlaps between each phenome, and every analogous phenome from other realms. The results in Table 3.2 show that niche overlap between analogous phenomes ranged from no overlap ($D=0$) to high overlap ($D=0.86$). Average overlap as expressed by Schoener's D was 0.49 ± 0.28 (SD). For some of the pairwise comparisons of evergreen phenomes, the null hypothesis of niche similarity could be rejected. In particular, some evergreen phenomes from different realms occupied different physiological niche spaces. For pairwise comparisons of deciduous phenomes this was not the case (all $p \geq 0.05$), suggesting no evidence against niche similarity of the deciduous phenomes from the different realms.

Table 3.2: Niche overlap and similarity between phenomes in their native realm and analogous phenomes from different realms. Niche overlap is quantified using Schoener's D. The p -values show the results of tests for niche similarity, where observed similarity (D) is compared to simulated random overlaps. The procedure tests the hypothesis that the niche occupied by a phenome in its native realm is more similar to the niche of an analogous phenome in a different realm than would be expected by chance. If $p < 0.05$, we reject the hypothesis of niche similarity. Significance at the 0.05 level is indicated with *. The test is performed by calculating overlap between the observed niche in the native realm and randomly simulating niches in the non-native realm (n→nn) and between the observed niche in the non-native realm and randomly simulated niches in the native realm (nn→n). The realm abbreviations are AU = Australia, AF = Africa, IP = Indo-Pacific and SA = South America.

native	non-native	Deciduous			High LAI evg			Low LAI evg		
		D	$p_{n \rightarrow nn}$	$p_{nn \rightarrow n}$	D	$p_{n \rightarrow nn}$	$p_{nn \rightarrow n}$	D	$p_{n \rightarrow nn}$	$p_{nn \rightarrow n}$
AU	AF	0.68	0.08	0.06	0.45	0.53	0.14	0.74	0.05	0.10
	IP	0.63	0.08	0.49	0.46	0.70	0.08	0.40	0.01*	0.09
	SA	0.60	0.60	0.48	0.73	0.58	0.08	0.36	0.01*	0.19
AF	AU	0.64	0.15	0.29	0.52	0.01*	0.60	0.26	0.19	0.05
	IP	0.80	0.05	0.11	0.80	0.02*	0.05	0.09	0.01*	0.22
	SA	0.81	0.06	0.14	0.74	0.38	0.22	0.22	0.11	0.19
IP	AU	0.45	0.05	0.07	0.00	1.00	0.84	0.02	0.08	0.01*
	AF	0.75	0.21	0.08	0.86	0.09	0.03*	0.02	0.42	0.01*
	SA	0.72	0.16	0.09	0.85	0.19	0.16	0.00	0.20	1.00
SA	AU	0.55	0.18	0.09	0.33	0.22	0.35	0.05	0.62	0.04*
	AF	0.72	0.22	0.06	0.48	0.04*	0.10	0.36	0.01*	0.08
	IP	0.75	0.32	0.18	0.60	0.25	0.12	0.13	0.01*	0.02*

Projecting phenome distributions

The physiological niche of each phenome as obtained from the TTR model were used to project the potential distribution of each phenome into its native realm and into the three non-native realms. The purple colours in Figure 3.3 show the projected presences and the yellow and brown colours show projected absences. By first focussing on the native realm for each phenome, we can see where the model correctly predicted presence and absence. For example, the projections in the top row of Figure 3.3 are based on the phenomes in the Australian realm and by looking at Australia in e.g. the top-right panel, it can be seen that the model correctly predicted the majority of presences and absences for the low LAI evergreens. The corresponding confusion matrices for each phenome projection in its native realm are given in Table 3.1.

The next step is to focus on projected phenome distributions outside the native realm. These resemble the distributions of global biomes. For example, high LAI evergreen vegetation as projected from each of the four realms largely falls in tropical forest regions (purple colours in the middle column of Figure 3.3). Similarly, the projected distribution of low LAI evergreen vegetation is confined to arid regions (purple colours in the third column of Figure 3.3). Overall, the projections into non-native realms are dominated by true positives and true negatives (high accuracy) as can be seen from the confusion matrices in Figure 3.3, indicating that the physiological niches of analogous phenome in different realms are, to an extent, similar. The high accuracy of the projections into non-native realms also suggest that the model adequately describes the physiological niche of the phenomes. This is further illustrated by projections from all realms correctly predicting deciduous vegetation in the relatively small Guyanan savannas of Venezuela and Brazil, which are surrounded by evergreen forest and where the climate could support forest.

Although overall accuracy is high, there are also large areas where the projected leaf habit does not match the observed. Projections from the deciduous phenomes of South America, Africa and the Indo-Pacific have high rates of false positives and thus over-predict

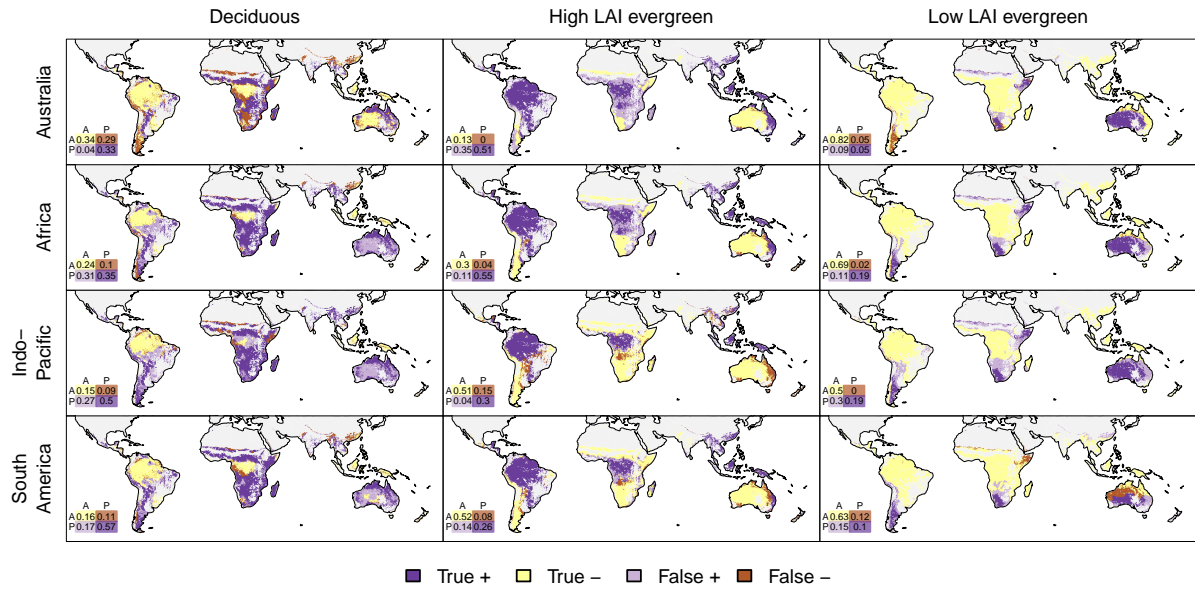


Figure 3.3: Projecting phenomes into non-native realms based on their physiological niche. Each row shows projections from one native realm into the other realms. For example, the top left panel shows where the deciduous phenome from the Australian realm is projected to occur. The colours show where the projected distributions agree and disagree with the observed distributions of analogous phenomes in the different realms. The confusion matrices only include pixels of projections into non-native realms. Confusion matrices for projections into native realms are given in Table 3.1. Confusion matrix columns are observed presence (P) and absence (A) and rows are projected presence (P) and absence (A).

the observed extent of deciduous vegetation. This is, in large part, due to projecting the deciduous phenome into the Australian interior, where the observed phenome is low LAI evergreen. Vice versa, the projection from the Australian deciduous phenome has a high rate of false negatives, failing to predict large areas of deciduous vegetation throughout Africa, but also in Patagonia, Southeast Asia and southern China.

High LAI evergreen phenome projections are also characterised by a high rate of false positives. Both the Australian and African high LAI evergreen phenomes over-predict the observed extent of this phenome in Africa. It is therefore projected to occur well beyond the extent of evergreen tropical forest and occupy most of the savanna regions throughout Africa and on Madagascar. Projections from South America and the Indo-Pacific are similar to observed leaf habit in Africa, but they fail to predict high LAI evergreens in parts of eastern Australia.

The low LAI evergreen projections have, on average, the highest rate of overall accuracy (79%, compared to 77% for high LAI evergreen and 66% for deciduous). This is, to a large extent, due to the high rate of correctly predicted absences. Projections from all realms overestimate the extent of low LAI evergreens in southern Africa and, to some extent, in the Sahel and eastern Australia. The Australian low LAI evergreen phenome does not predict an analogous phenome to occur in Patagonia where it is observed, while the projection from South America omits a large area of low LAI evergreens north-western Australia.

Predictability of phenome distribution

The projections from each column in Figure 3.3 can be overlaid to show where phenome projections from different realms coincide (Figure 3.4 a-c). These maps show, for each phenome, how many projections from different realms predicted the same leaf habit. For all phenomes the agreement is large, and areas where only one or two projections coincide

are relatively small. This suggests that the physiological niche of phenomes in different realms overlap considerably.

Figure 3.4 d overlays projections from the different phenomes (Figure 3.4 a-c). The red, yellow and green areas show where projections from all four realms agreed on the presence of a particular phenome. The blue areas show where projections from each realm predicted multiple phenomes to occur, i.e. where phenomes are predicted to overlap. The black areas show where the projection from at least one realm did not agree with projections from the other realms. These areas of disagreement are where the physiological niche of analogous phenomes from different realms differed, suggesting non-convergence of the physiological niche. The areas of disagreement are primarily in arid regions (Köppen climate group B) and in regions with temperate maritime climates (Köppen climate type Cfb) at the southern margins of South America, Africa, Australia and in New Zealand (Peel, 2007). Figure B.1 overlays the projections as in Figure 3.4 d, but excluding projections from the native realm. These two maps are identical in South America and Africa, but different in the Indo-Pacific and Australia, suggesting that in these two realms the projection from the native realm disagrees with projections from the foreign realms.

Discussion

We described the physiological niche of deciduous and two types of evergreen vegetation in each of four global biogeographic realms, using a physiologically based model of plant growth and observed distributions. Using the modelled physiological niche we projected the potential distribution of each phenome into geographical space, and analyse overlap with the observed distributions of analogous phenomes in other realms. The overlap between projected and observed distributions was substantial, indicating that analogous phenomes from different realms occupy similar physiological niches. However, major areas of mismatch between observed and projected distributions suggest considerable non-

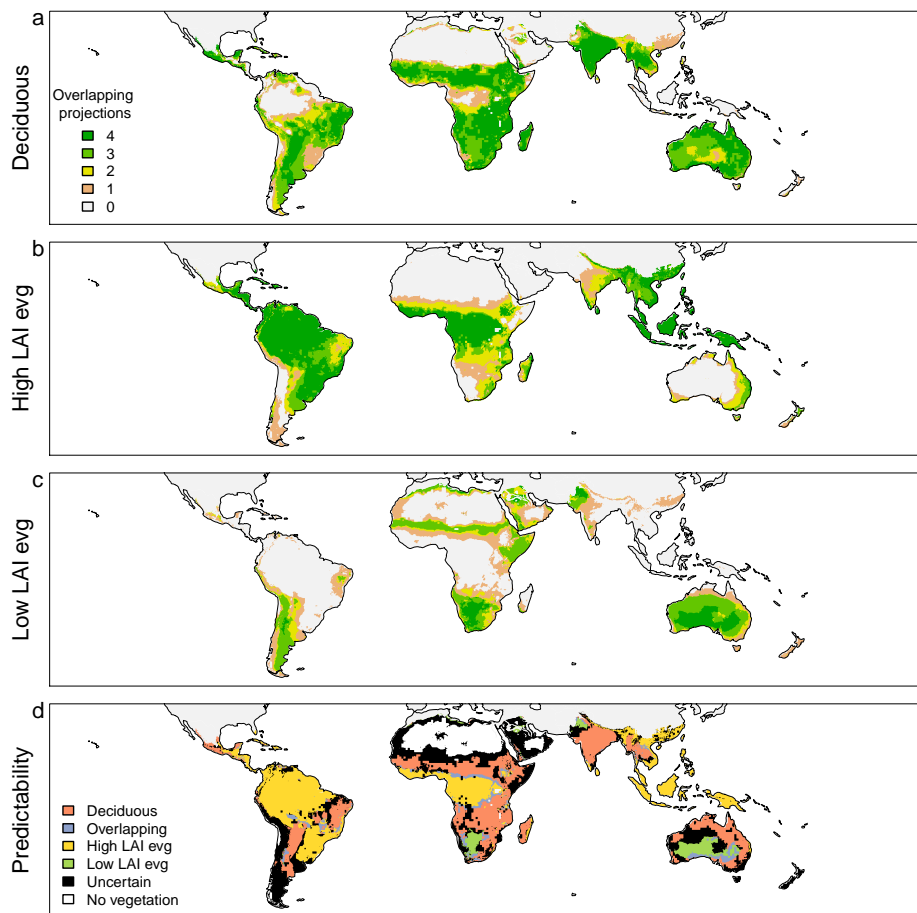


Figure 3.4: Panels **a-c** show, for each phenome, how many projections from different realms coincide. **d**) Areas where projections from every realm agree on a particular phenome (red, yellow, green), on overlapping phenomes (blue) or on areas devoid of vegetation (white). Areas in black are where the projection from at least one realm did not coincide with the projections from the other realms.

convergence of the physiological niche between realms.

Since model parameters are not known a-priori they are inferred from the observed distribution. Therefore, like in any species distribution model, the accuracy of observed ranges is crucial. Our map of a simple evergreenness index based on NDVI metrics largely corresponded to existing biome maps (Olson *et al.*, 2001; Friedl *et al.*, 2002). There only appears to be one global data set of proportion evergreen vegetation in the literature (DeFries *et al.*, 2000), but since this data set only includes vegetation that is dominated by trees and thus excludes shrublands, we did not attempt a formal comparison. Nevertheless, vegetation identified as evergreen trees in maps derived from this data (DeFries *et al.*, 2000; Woodward *et al.*, 2004) was largely consistent with our classification in those areas. A major advantage of using remotely sensed images over ground-based occurrence data is that the entire land surface can be examined. In addition to presence data, it therefore also provides absence data, which is often missing from distribution data sets.

Although process-based species distribution models are not a panacea (Dormann *et al.*, 2012), we expect that the process based model of plant growth provides several advantages over correlative models for this application. Firstly, by evaluating growth at monthly time steps using monthly environmental data, co-limitation can vary between months so that phenological processes are implicit to the model (Higgins *et al.*, 2012b). For example, the model can directly simulate that carbon uptake might be limited by low solar radiation in winter, but by dry soils in summer. In contrast, a correlative model would account for this by, for example, modelling the probability of occurrence as a function of rainfall in the coldest month of the year. Secondly, the shapes of the functions that describe the response of various physiological processes to environmental variables are fixed. This rigid structure ensures biologically realistic responses; for example, carbon uptake is constrained to have a uni-modal temperature dependency. Correlative models in contrast use flexible polynomial functions that may adopt any form (linear, exponential, uni- or multi-modal).

The proportion of false positive predictions, i.e. where the model predicts a phenome to

occur while it is not observed, was relatively high across projections for all phenomes (17% on average), was not specific to any particular realm and occurred in both native and non-native realms. This over-prediction of phenome ranges might arise when the phenome is not at equilibrium with the environment and does not fill its potential geographical range as predicted from physiological niche dimensions. Various processes may prevent or slow down range filling, for example dispersal rates (Svenning & Skov, 2004; Schurr *et al.*, 2007), but at the spatial (global) and organisational (phenome) scales that are studied here, it is reasonable to assume that phenomes have had enough time to fill their potential range. It is therefore more likely that ongoing biotic processes restrict the realised range. For example, deciduous vegetation might be excluded from the aseasonal tropics by light competition from evergreen trees, and ranges of evergreen tropical vegetation might be restricted by neighbouring flammable ecosystems (Bond *et al.*, 2005; Beerling & Osborne, 2006; Bond, 2008). Areas of false positive projections in the native realm therefore provide a guide of where range restriction might be ongoing. Such areas might be expected to have multiple stable states that switch depending on the strength of range restricting processes (Staver *et al.*, 2011; Higgins & Scheiter, 2012). Projections of high LAI evergreens in large areas of Africa where deciduous savannas are known to occur coincide with areas where a stable forest state is predicted to be possible (Moncrieff *et al.*, 2014c).

Mismatches between projected and observed phenomes were particularly frequent in projections into Australia, or in projections from Australia into other realms (Figure 3.3). The largest areas of mismatch stemmed from the projection of deciduous vegetation into the interior of Australia, which was low LAI evergreen according to the classification of satellite data. However, low LAI evergreen was also projected into the same area by all realms (only partly by South America), suggesting that Australia's interior might have been a mixture of deciduous and evergreen vegetation if plants from other realms occurred there.

Surprisingly, large mismatches did not occur in Northern Australian savannas, which have

been characterised as phenologically anomalous in a global context (Bowman & Prior, 2005; Bowman *et al.*, 2010). The woody component of Australian savannas is dominated by evergreens from the Myrtaceae family, while tropical savanna trees in Africa and South America are predominantly deciduous. In our classification northern Australia was highly mixed, including areas with deciduous vegetation, overlap between deciduous and high LAI evergreens and overlap between deciduous and low LAI evergreens (Figure 3.1). Such a mixed pattern is consistent with the sharp phenological contrast between northern Australia's evergreen trees and deciduous grasses, which results in a mixed NDVI signal (Donohue *et al.*, 2009; Ma *et al.*, 2013). Other realms all projected deciduous vegetation into northern Australia, while they did not consistently project either type of evergreen into northern Australia. This suggests that the physiological niche of deciduous vegetation from other realms would allow them to occur in northern Australia, so that Australian savannas might not have been dominated by evergreen trees if taxa from other realms had a chance to evolve there. In other words, evergreenness of Australian savanna trees might not be environmentally deterministic and might instead be a consequence of historical contingencies, such as the continental species pool (Lehmann *et al.*, 2014; Moncrieff *et al.*, 2014b). Although historical contingency provides scope for explanations that bypass optimality arguments and evolutionary convergence, it is not an explanation for eucalypt dominance in itself. Proximate explanations for eucalypt dominance may include superior competitive ability under frequent fires regimes (Bond *et al.*, 2012). Such biotic explanations are consistent with projections of Australia's native deciduous phenome into northern Australia, which suggests that the deciduous phenome can, physiologically, tolerate the environmental conditions there.

Although projections from the Indo-Pacific and South America correctly predicted high LAI evergreens in the Congo and Amazon basins, they failed to predict high LAI evergreens outside these basins, such as in South American Cerrado, African Miombo woodlands and north-eastern Australia. These under-predictions of the high LAI evergreen range in non-native realms likely stem from under-prediction of the phenome in its native realm.

The under-prediction in the native realm might in turn be due to classification errors. False negatives in South America occur in the Espinal region of Argentina and the Chaco region of Paraguay, both of which might be predominantly deciduous, while they were classified as overlapping deciduous and evergreen vegetation. Similarly, areas in the Indo-Pacific realm that were classified as overlapping deciduous and evergreen vegetation were projected to be only deciduous. The most likely explanation for the failure to predict high LAI evergreen where it was observed in the Indo-Pacific realm is the mosaic of evergreen and dry deciduous forests in the Indochinese region (Olson *et al.*, 2001). The boundaries between these forest types are likely to be gradual rather than sharp, potentially limiting the suitability of a dichotomous classification.

Suggested mechanisms that underlie the distribution of evergreen and deciduous vegetation have focussed on the concept of an optimal leaf lifespan, which assumes that leaf lifespan is an adaptive trait under selective pressure from the environmental regime. The optimal leaf lifespan is that which maximises whole plant carbon gain, and therefore fitness (Givnish, 2002). The cost benefit analyses used to model relative performance of different leaf habits explicitly include physiological processes related to carbon and nutrient gains and losses (Chabot & Hicks, 1982; Kikuzawa, 1991; Ackerly, 1999; Givnish, 2002). Similar, although not identical, processes are included in the TTR model. The interpretation of results from our analysis is based on the assumption that a phenome, or a leaf habit, has a physiological niche. Using this model we are able to predict 71% of the study area correctly (Figure 3.4 d), suggesting convergence in the physiological niche of phenomes for the majority of the study area.

Convergence of plant traits in environmentally similar areas has long been central to explanations for the distribution of vegetation types (Warming & Vahl, 1909; Mooney & Dunn, 1970a; Box, 1996). Recent studies have challenged the universality of convergence in emergent biome properties by showing that global biomes on different continents are not equivalent structurally (Moncrieff *et al.*, 2014b), functionally Lehmann *et al.* (2014) and

bio-climatically (Bond *et al.*, 2005; Moncrieff *et al.*, 2014a). It is important to recognise that non-convergence in such emergent ecosystem properties does not rule out evolutionary convergence of functional traits (Shipley, 2010). That is, traits under selective pressure may vary predictably along environmental gradients, while community composition, and associated vegetation structure might be influenced by stochastic processes including historical contingencies (Shipley, 2010). The physiological niche as estimated by the TTR model can be seen as a description of functional traits rather than as an emergent property of these traits, suggesting that dissimilar physiological niches imply that evolution has not converged on the same set of traits.

Biogeographically, such non-convergence can be detected as areas where phenome predictions are uncertain. These areas made up 29% of the study area and were concentrated in arid regions and temperate regions with maritime climates. Interestingly, in Africa the phenome-uncertain areas appeared similar to areas where two alternative vegetation stable states were predicted to be possible (Higgins & Scheiter, 2012). In that study, the simulated vegetation types were C₄ dominated grasslands or savannas and C₃ dominated forest, the distribution of which were estimated using a dynamic vegetation model. Since leaf habit in tropical and sub-tropical regions of Africa is tightly linked to biome, i.e. evergreen tropical forest and deciduous savannas, it is possible that bistable and phenome-uncertain patterns are caused by overlap in the same physiological niche dimensions. This may suggest that forecast shifts in the locations of bistable areas with increasing atmospheric CO₂ (Higgins & Scheiter, 2012) may be partly caused by differential responses of leaf habit to increased atmospheric CO₂.

Conclusion

We have shown that the analogous phenomes in different biogeographic realms largely occupy similar niche space, resulting in large agreement of projected phenome distributions from different realms. These results imply evolutionary convergence of the physiological

niche. We also identify instances where the physiological niches of two phenomes are dissimilar, which results in areas where projected phenomes are not consistent. This implies non-convergence of the physiological niche. Future work may focus on identifying the niche dimensions (physiological processes) that were responsible for the observed niche dissimilarity, which may provide further insight into the driving forces of the geographic distribution of leaf habit. The identified physiological processes should be matched against processes hypothesised to determine optimal leaf habit.

Chapter 4

Effects of leaf phenology and leaf habit on the carbon budget of African savanna trees

Robert Buitenwerf, Hendrik J. Combrink, Edmund C. February and Steven I. Higgins¹

¹Author declarations: RB and SIH designed the study and data analyses based on ideas from ECF and SIH. HJC co-designed and implemented the remote sensing data collection. RB collected all other data and performed all analyses. RB wrote the manuscript with assistance from SIH.

Abstract

The distribution of vegetation with evergreen and deciduous leaf habits along environmental gradients is thought to reflect evolutionary convergence to an optimal leaf habit. This hypothesis appears to be contradicted by the large range of leaf lifespans that characterise ecological communities. We explore how leaf habit and leaf phenology are related to carbon and water economies of woody African savanna species. We measured leaf lifespan, tracked canopy phenology using NDVI images and used functional traits and gas exchange rates to describe carbon and water economies of 9 study species. To examine the integrated effects of the measured traits, we parametrise a simple carbon gain model. Leaf lifespan ranged between 5 and 18 months, canopy NDVI peaked during the wet season for all species, but rates of leaf deployment and senescence varied considerably. Leaf lifespan was positively related to LMA and low photosynthetic rates, which is consistent with predictions from the leaf economic spectrum. Furthermore, early flushing species had fast-developing canopies, high mesophyll conductance and low leaf construction costs. Even though moisture imposes strong controls on vegetation activity in the study system, traits related to water use were not related to leaf phenology or leaf habit. The calculated annual carbon gain varied more than fivefold between species, was lowest for evergreen species and was moderately sensitive to differences in leaf habit and leaf phenology. The large variation in leaf phenology, leaf habit and carbon budgets of species in a highly seasonal environment suggests that divergent selection helps shape the phenological strategies of species.

Introduction

The distinct sorting of evergreen and deciduous vegetation along temperature, moisture and soil fertility gradients has long inspired biogeographers and ecologists to seek environmental explanations for these patterns (Mooney & Dunn, 1970a; Sarmiento *et al.*, 1985). If such patterns between leaf habit and environment indicate causal relationships, changes to the environmental regime, e.g. in the form of changing climates, increased atmospheric CO₂ concentrations or soil eutrication, may affect the dominant leaf habit of vegetation. The potential for major shifts in leaf habit to occur is demonstrated in the fossil record, which shows that deciduous forests dominated the Arctic and Antarctic throughout much of the past 250 million years (Spicer & Chapman, 1990; Royer *et al.*, 2003). On a more immediate time scale, global change has already affected the seasonal progression of leaf flush and senescence, by advancing and prolonging the growing season in seasonally cold systems (Menzel *et al.*, 2006; Zhu *et al.*, 2012; Zohner & Renner, 2014). This phenological change is likely to have major effects on the global carbon cycle, but a limited understanding of the driving mechanisms still presents a key uncertainty in projections of earth-atmosphere and dynamic vegetation models (Myhre *et al.*, 2013). Consequently, forecasts currently rely on correlations between climate variables and the cues that trigger plant responses such as leaf expansion (or flower initiation or seed germination). The correlative approach is a useful tool in making short-term phenological forecasts, but does not allow for changes in processes that might disrupt these correlations. For example, changing community composition may affect phenological strategies by altering competitive interactions (Fridley, 2012). In order to consider the relative ecological and evolutionary advantages of different leaf phenological strategies, it is therefore instructive to consider leaf phenological strategy as the joint effects of leaf habit and leaf phenology.

The first aspect of the phenological strategy, leaf habit, has been explored primarily in terms of how the evergreen-deciduous dichotomy is related to environmental drivers (Chabot & Hicks, 1982; Williams *et al.*, 1989; Kikuzawa, 1991; Ackerly, 1999; Kikuzawa

& Ackerly, 1999; Givnish, 2002; Kikuzawa & Lechowicz, 2011). These studies have employed cost-benefit analyses of the carbon budget, based on the assumption that plants optimise their leaf habit in order to maximise whole-plant carbon gain. The underlying assumption is that carbon gain is an indicator of fitness, such that the optimal leaf habit is expected to dominate. The benefit term in these models is simply the time-integrated amount of carbon gained through photosynthesis, while the costs include respiration and the construction costs of the leaf tissue, but in some models also includes construction and maintenance costs of root and stem tissue that supply the leaf with water and nutrients. These considerations have resulted in models that differ in how they represent the leaf construction costs and the whole-plant cost of photosynthesis (Chabot & Hicks, 1982; Williams *et al.*, 1989; Kikuzawa, 1991; Ackerly, 1999; Kikuzawa & Ackerly, 1999; Givnish, 2002), leading Givnish (2002) to argue that global patterns of dominant leaf habit, including regions where leaf habit appears to be inconsistent with the environmental regime, can only be predicted when accounting for whole-plant costs of photosynthesis.

Despite the long history of optimal leaf habit models, a global implementation is lacking. Such a model would predict convergence on the optimal leaf habit in a given location, which would appear at odds with observations of leaf lifespan, which may vary over an order of magnitude within a single community (Shiodera *et al.*, 2008; Kikuzawa & Lechowicz, 2011). The wide range of leaf habits under a common environmental regime is suggestive of non-convergence, and would imply that a range of lifespans or multiple lifespans are equally optimal, or that non-optimal leaf habits are not excluded by natural selection. This would imply a divergent selective force such as competition for resources or space that impose limiting similarity (MacArthur & Levins, 1967). For example, forest herbs may complete their entire growing season before the tree canopy closes (Al-Mufti *et al.*, 1977). Leaf phenology, as affected by competitive interactions, may therefore affect the leaf habit.

To quantify the interactions between leaf phenology, leaf habit and the carbon budget,

we estimate these variables for woody species in an African savanna. Although seasonal moisture limitation imposes a strong control on seasonal patterns of physiological activity (Williams *et al.*, 2009; Merbold *et al.*, 2009) and many woody species lose their leaves during part of the dry season, leaf habits and leaf phenology are known to vary considerably among species (Shackleton, 1999; Higgins *et al.*, 2011). We first describe leaf phenology and leaf habit using measurements of leaf lifespan and the seasonal progression of leaf phenology as derived from remotely sensed images. We then use measurements of functional traits including rates of gas exchange to characterise the carbon and water economies of species and use physiological and phenological data to parametrise a simple carbon gain model.

Methods

Study area

The study was conducted at eight sites along a 40 km transect (31.249 – 31.607 °E, -25.197 – -25.073 °S) in the Kruger National Park, South Africa. The transect spans a rainfall gradient between 553 and 746 mm yr⁻¹ mean annual rainfall, the majority of which falls between October and April. The wet season is also the hottest season, with average temperatures of approximately 25° C. All 8 sites were located on catenal crests and upper-slopes, on which weathering of the granite substrate has produced sandy and well drained soils (Venter *et al.*, 2003). The woody vegetation is dominated by *Terminalia sericea*, *Dichrostachys cinerea*, *Combretum apiculatum* and *Sclerocarya birrea*. The grass layer is dominated by tall Andropogonoid bunch grasses at the wettest sites, while the dryer sites have a sparser and shorter grass layer dominated by Panicoideae and Chloridoideae. A more in depth site description is given in Higgins *et al.* (2011). Nomenclature follows Schmidt *et al.* (2007).

Leaf phenology

Leaf phenology was described using the normalised difference vegetation index (NDVI), which quantifies greenness and is a proxy of the leaf area index. NDVI was calculated from multi-spectral aerial images that were taken with an ADC camera (Tetracam Inc., Chatsworth, California, USA) equipped with a 5 mm focal length wide-angle lens. The camera's sensor has a resolution of 2048 x 1536 pixels and is sensitive in the green to near-infrared part of the electromagnetic spectrum (520 – 920 nm). Using the camera manufacturer's proprietary Pixelwrench software (Tetracam Inc., Chatsworth, California, USA), three spectral bands were calculated: green, red (RED) and near-infrared (NIR) to produce a 3-band image, from which NDVI could be calculated.

The camera was mounted on a South African National Parks (SANParks) helicopter and on an unmanned aerial vehicle (UAV, AiDrones, Wildau, Germany). At all 8 sites images were captured on eleven dates during the 2011-2012 growing season. The first four dates: 22 September, 10 October, 7 November and 1 December were captured from the SANParks helicopter. Later images were captured from the UAV: 23 January (site 1), 10 February (sites 2-8), 1 March, 26 March, 18 April, 16 May and 13 June. Image capture started before any plants had produced fresh leaves. Images from the SANParks helicopter were captured at an altitude of approximately 200 m yielding an approximate resolution of 13 cm, while images from the UAV were taken from 100 m and yielded a resolution of approximately 6 cm. The ground area covered in a single image was approximately 100 x 130 m. During each image capturing session, several partly overlapping images were taken at each site. These were stitched together into a single composite image per site per date, using Autopano Giga 2.6 (Kolor SARL, Francin, France). Each composite image covered an area of approximately 340 x 340 m. Composites from different dates were then stacked and geo-referenced in Arcmap 10.1 (ESRI, Redlands, California, USA), using markers with known coordinates that were deployed in the field during image capture. From the 3-band images in the stack, we then calculated NDVI from the red (RED) and near-infrared (NIR)

reflectance as

$$NDVI = \frac{(RED - NIR)}{(RED + NIR)}. \quad (4.1)$$

Finally, from the geo-referenced NDVI stacks, we extracted NDVI time series for 340 tree canopies of 9 species. The outline of these tree canopies were mapped in the field using a differential GPS device that achieved an accuracy of approximately 0.1 m (Trimble, Sunnyvale, California, USA). The NDVI time series for each canopy were described using a back-to-back sigmoid function:

$$f(day, d_{on}, d_{off}, s_{on}, s_{off}, max, min) = 2lo - hi + \frac{(hi - lo)}{1 + \exp(s_{on} [d_{on} - x])} + \frac{(hi - lo)}{1 + \exp(s_{off} [x - d_{off}])}. \quad (4.2)$$

This function has been used to describe NDVI time series in this environment (Higgins *et al.*, 2011). Four of the parameters can be interpreted ecologically: d_{on} is the day on which greening proceeds most rapidly and s_{on} is the rate of NDVI increase on that day. Likewise, d_{off} is the day on which NDVI decreases most rapidly and s_{off} the rate of NDVI decrease on that day. The hi and lo parameters influence the maximum and minimum of the function. The day parameter represents time as the day of year. Since our NDVI observations spanned only 265 days we extended our time series to 1 year, by assuming that NDVI on day 366 was the same as on day 1 of the time series. This assumption was necessary to ensure that the fitted function declined back to baseline levels at the end of the dry season.

Parameters from Equation 4.2 were estimated in a hierarchical Bayesian model. All six parameters were estimated at the species level, but to account for variation between individual canopies, we modelled the lo parameter as an individual canopy effect so that it is interpreted as a random effect. We also included additive site effects for s_{on} and s_{off} ,

to allow the rates of greening and leaf senescence to vary between sites, accounting for unmeasured differences between sites e.g. in soil moisture. The d_{on} , s_{on} , d_{off} and s_{off} parameters were assigned normal and uninformative priors, while hi and lo were given normal priors truncated between 0 and 1 as our calculated NDVI values were constrained to that range. The variances of the normal priors were assumed to have uniform and uninformative priors.

Functional traits

Leaf lifespan

The lifespan of individual leaves was measured by tagging freshly expanded leaves with small cable ties and monitoring their survival throughout the season. The day that leaves were tagged was assumed to be the start of their lifespan, resulting in a slight underestimation of true leaf lifespan. This assumption is justified from a carbon economy perspective, since immature leaves are physiologically not yet fully functional (Kikuzawa & Lechowicz, 2011). Leaves that had been browsed by animals were excluded from the analysis, resulting in a total of 157 leaves for which the date of senescence could be assigned to a period between two successive monitoring dates. Since the exact date of senescence was not known, we fitted a survival function using the Kaplan-Meier estimator in the survival package (Therneau, 2014) in R (R Core Team, 2014), which provides an estimate of survival as a function of time.

Gas exchange: CO₂ and light response curves

To quantify the biochemical capacity to fix carbon, we measured the photosynthetic rate (A) at a range of CO₂ concentrations for each species. These measurements are referred to as CO₂ response curves, as photosynthesis increases rapidly with CO₂ at low concentrations, but levels off at high CO₂ through sequential rate limiting processes. These

processes include the maximum rate of carboxylation (V_{cmax}) and the maximum rate of RuBP regeneration (J_{max}), both of which can be estimated from the CO₂ response curve along with the mesophyll conductance (g_m) and the CO₂ compensation point (Γ^*), which is the CO₂ concentration at which carbon assimilation balances photo-respiration. Similarly, by measuring A at a range of light intensities, we can estimate the dark respiration during photosynthesis (R_{day}). All parameters were estimated at the species level in a hierarchical Bayesian model following Patrick *et al.* (2009) and Higgins *et al.* (2012a) using MCMC methods in JAGS (Plummer, 2014).

For each species, between three and seven CO₂ response curves and two light response curves were measured in the field. Measurements were taken on well-lit, fully expanded leaves from healthy looking individuals. All measurements were taken with a LI6400XT photosynthesis system that was fitted with a 6400-02B LED light source (LI-COR, Lincoln, Nebraska, USA). We measured rates of gas-exchange at 50, 100, 150, 250, 350, 500, 700, 900 and 1200 ppm of CO₂. During these measurements, the light intensity was set at 1500 or 2000 μmol of photosynthetically active photons $\text{m}^{-2} \text{s}^{-1}$ and leaf temperature was held constant at the ambient leaf temperature which was typically between 24 and 29 °C. Light curve measurements were taken at 2000, 1500, 1000, 750, 500, 250, 120, 60, 40, 20, 10 and 0 μmol of photons $\text{m}^{-2} \text{s}^{-1}$. During light response curves, the CO₂ concentration was held constant at 400 ppm, while leaf temperature was held constant at its ambient value, typically between 24 and 29 °C.

Gas exchange: optimal stomatal conductance

To characterise the water economy of species, we examine the response of water loss to environmental conditions. Transpiration has generally been modelled using empirically derived relationships between stomatal conductance and environmental variables (Ball *et al.*, 1987; Leuning, 1995). Theory on stomatal conductance is based on the assumption that stomata are regulated to optimise the balance of carbon gain and water loss (Cowan

& Farquhar, 1977). Optimal stomatal behaviour should therefore minimise the time-integrated sum of

$$E - \lambda A, \tag{4.3}$$

where E is water loss (transpiration), A is carbon assimilation (photosynthesis) and λ ($\text{mol H}_2\text{O mol}^{-1} \text{C}$) is the marginal water cost of fixing carbon (Medlyn *et al.*, 2011). Models based on this theory have proven difficult to implement until recently, when Medlyn *et al.* (2011, 2012) showed that the model for optimal stomatal conductance (Equation 4.3) can be approximated as

$$g_s^* \approx 1.6 \left(1 + \frac{g_1}{\sqrt{VPD}} \right) \frac{A}{C_a}, \tag{4.4}$$

where g_s^* is the optimal stomatal conductance to water. The measured terms in this model are VPD , the vapour pressure deficit between the leaf surface and the air in kPa, A is the rate of photosynthesis in $\text{mol}^{-1} \text{m}^{-2} \text{s}^{-1}$ and C_a is the concentration of CO_2 around the leaf. The g_1 parameter is estimated. There are two major advantages of this model. First its form is closely analogous to the empirical models of stomatal conductance, which means that it can easily be fitted to data. Second, the estimated parameters have a theoretical interpretation. The interpretation of g_1 is of particular interest, as Medlyn *et al.* (2011), suggest that it is proportional to λ , the marginal water cost of photosynthesis. Evidence that λ is relatively constant over time, i.e. that it is not sensitive to short term fluctuations in environmental conditions (Xu & Baldocchi, 2003; Medlyn *et al.*, 2011) suggests that it can be treated as a functional trait that describes the carbon-water economies of species. In economic terms, λ can be interpreted as an indicator of how much water a plant is prepared to spend for a given amount of carbon gain. Small values indicate a conservative strategy, while large values indicate a profligate strategy with large water loss per unit

carbon gain (Givnish, 1986; Medlyn *et al.*, 2011). To estimate g_1 , we fit the optimal stomatal conductance model (Equation 4.4) to measured values of VPD , A , C_a and g_s using the Differential Evolution algorithm as implemented in the DEoptim package (Ardia *et al.*, 2013) for R (R Core Team, 2014). We then use the g_1 estimate to calculate λ following Medlyn *et al.* (2011):

$$\lambda = 1.6 \left(\frac{g_1}{\sqrt{3\Gamma^*P}} \right)^2, \quad (4.5)$$

where Γ^* is the CO_2 compensation point in mol mol^{-1} and P is the atmospheric pressure in kPa.

The gas-exchange data needed to estimate λ was collected using the LI6400XT. In order to estimate the relationship between water loss and carbon gain, measurements of instantaneous photosynthesis were made over a range of stomatal conductances. This was achieved by measuring the same leaf at intervals over the course of the day during which increasing temperature and VPD caused stomata to close. A total of 1204 measurements were made on 135 leaves. Measurements were made during 20 days throughout the growing season and were always within a week after significant rainfall, in order to reduce effects of low soil water potentials on transpiration. The light intensity inside the chamber was set to match outside conditions, which ranged from $30 \mu\text{mol m}^{-2} \text{s}^{-1}$ shortly after sunrise to peak levels exceeding $2000 \mu\text{mol m}^{-2} \text{s}^{-1}$. The CO_2 concentration was set to 400 ppm, while temperature was set to approximate the ambient leaf temperature. Since leaves were typically in the chamber for less than 1 minute, the relative humidity was not regulated but was kept close to ambient levels by setting the rate of air flow through the system at $500 \mu\text{mol s}^{-1}$.

Morphological traits

We determined the leaf mass per area (LMA) and leaf tissue density from measurements of leaf area, weight and thickness. Wood density for six species were taken from Higgins *et al.* (2012a), while the remaining three were taken from the global wood density data base (Zanne *et al.*, 2009; Chave *et al.*, 2009). Wood density for *Balanites aegyptiaca* was used as an approximation for *Balanites maughamii*.

Leaf construction costs

Leaf construction costs can be defined as the amount of glucose required to construct the carbon skeleton of leaves, including glucose expended in tissue synthesis (Lambers *et al.*, 2008). This measure of leaf construction costs is strongly correlated with the energy content as measured by the heat of combustion of leaf tissue (Williams *et al.*, 1987; Villar & Merino, 2001). We measured heat of combustion using a CAL2K bomb calorimeter (Digital Data Systems, Randburg, South Africa). Approximately 50 green and mature leaves from several individuals and from different positions in the canopy were dried and ground together into a single bulk sample per species. For each species, a minimum of three calorific measurements were made.

To express leaf construction costs in carbon units, we converted heat of combustion (kJ g^{-1} leaf) to leaf construction costs (g glucose g^{-1} leaf) using the relationship described by Williams *et al.* (1987). We assumed an ash content of 6.5%, which is the average for leaf tissue (Williams *et al.*, 1987; Villar & Merino, 2001). We converted glucose units (g glucose g^{-1} leaf) to carbon units (mol C g^{-1} leaf) using the molar mass of glucose and then used LMA to convert from mass-based rates (mol C g^{-1} leaf) to area-based rates (mol C m^{-2} leaf).

Phenology vs. functional traits

To identify relationships between phenological variables and functional traits, we used partial least squares regression (PLSR), which is a multi-variate approach (Mevik & Wehrens, 2007; Carrascal *et al.*, 2009). In PLSR, each set of variables (here phenological and traits) are summarised into separate latent variables (similar to principal components). This step reduces the number of variables and removes the impact of collinearity between variables. The latent variables can therefore be interpreted as summaries of the phenological strategy and summaries of functional trait combinations. These two sets of latent variables are then regressed onto each other to determine relationships between phenological strategies and functional traits. Analyses were performed using the `plsdepot` package (Sanchez, 2012) in R (R Core Team, 2014).

Carbon gain model

Using the gas-exchange data, we parametrise a simple carbon gain model for each species. The model parameters are equivalent to those proposed by Givnish (2002), but it was estimated at daily time steps:

$$C_{gain} = \left(\sum_{t=1}^{365} A_t - \frac{1}{\lambda} E_t - R_t \right) - C. \quad (4.6)$$

Here the total annual carbon gain (C_{gain}) is the annual sum of daily carbon gain (A_t), daily respiration (R_t) and daily transpiration (E_t). By multiplying E with the carbon cost of water loss ($\frac{1}{\lambda}$), it is translated into carbon units. Leaf construction costs (C) were subtracted from the annual sum. A , E and R represent average daily rates, while rates of gas-exchange were measured in $\text{m}^2 \text{s}^{-1}$. To simplify matters, we assumed a 10 hr growing day throughout the year. This period can be seen to represent the number of daylight hours. R_t was defined by R_{day} as obtained from the CO_2 and light response measurements.

A_t was defined as A_{max} , which was the maximum measured net photosynthetic rate plus R_{day} . E_t was taken as the rate of E_{max} at maximum measured net photosynthesis. We assumed that the rates A_{max} and E_{max} were reduced by soil moisture availability. We also assumed that the moisture-constrained rates of A , E and R were further reduced by the photosynthetic activity of the whole plant, as indicated by our NDVI time series. The operational version of the model in Equation 4.6 is given by

$$C_{gain} = \left(\sum_{t=1}^{365} \left(\left(s_{light} \psi_t \left(A_{max} - \frac{1}{\lambda} E_{max} \right) \right) - s_{tot} R_{day} \right) NDVI_t \right) - C, \quad (4.7)$$

where ψ_t and $NDVI_t$ are soil moisture availability and NDVI on day t , s_{light} is the number of daylight seconds and s_{tot} is the number of seconds in a day. When there is no soil moisture ($\psi_t = 0$), daily carbon gain is $-R_{day}$ and when the plant does not have leaves ($NDVI_t = 0$), daily carbon gain is 0.

To calculate soil moisture availability, we used volumetric soil moisture that was recorded at 10 minute intervals at every field site using EC-5 probes (Decagon Devices, Pullman, Washington, USA). Volumetric soil moisture was multiplied by the soil bulk density (Wigley *et al.*, 2013) to yield gravimetric soil moisture. Gravimetric soil moisture was then converted to soil water potential as described in Chapter D and in Buitenwerf *et al.* (2014). Water potentials between 0 and -2 MPa were assumed to allow transpiration and the values in this range were rescaled to the range of 0-1 to yield a soil moisture availability index.

Since NDVI did not drop to 0 during the leafless period (Table 4.1), we rescaled NDVI values for each species to the 0-1 range, by assuming that 0.2 represents a leafless state (0) and the maximum NDVI value for the species represents maximum photosynthetic activity (1).

Relative abundance

To evaluate the relationship between carbon gain and ecological dominance we obtained a measure of relative abundance. We used data from a large and long-term fire experiment in the Kruger National Park. The experiment consists of plots on which various fire return intervals have been maintained since the 1950s. These sets of plots are replicated four times in each of four landscape types. The experimental setup and geographic layout is fully described in Biggs *et al.* (2003). We use data collected during the 1990s, which was the most recent survey that covered all landscape types. Woody individuals were counted in diagonal, 2-m wide belt transects on every plot. Full details of the data and data collection procedures are described in Higgins *et al.* (2007). We excluded data from the Mopani landscape, as the community composition and climate are very different from our study sites. We also excluded data from the fire exclusion plots, as this is a highly artificial fire regime in this ecosystem. We use the abundance data to calculate relative abundance of the study species in each plot. We sum the relative abundances to provide an estimate of ecological dominance for each of the study species. By summing, instead of averaging, we ensure a fair score for species with a narrow distribution (i.e. they do not occur on many of the plots) that dominate where they are present (i.e. high relative abundance). Averaging would lead to a score close to zero for such species.

Results

Leaf phenology

Canopy greenness was distinctly seasonal and reached a maximum during the wet season for all measured species (Figure 4.1a). Despite these general similarities, leaf phenology varied substantially between species. Three species (*E. divinorum*, *E. natalensis* and *G. senegalensis*) retained green canopies throughout the dry season with minimum NDVI

values of around 0.3 (Table 4.1). Their evergreen leaf habit was confirmed by maximum leaf lifespans that exceeded one year (Figure 4.1b), although the median leaf lifespan of *G. senegalensis* was very similar to that of most deciduous species, suggesting a more intricate variation in leaf deployment and leaf senescence that is not easily captured by the deciduous-evergreen dichotomy. Similarly, differences between the six deciduous species were evident from the seasonal development of NDVI. For example, *S. birrea* and *A. nigrescens* greened up faster than other species, while *S. birrea* also shed its leaves more rapidly at the end of the season.

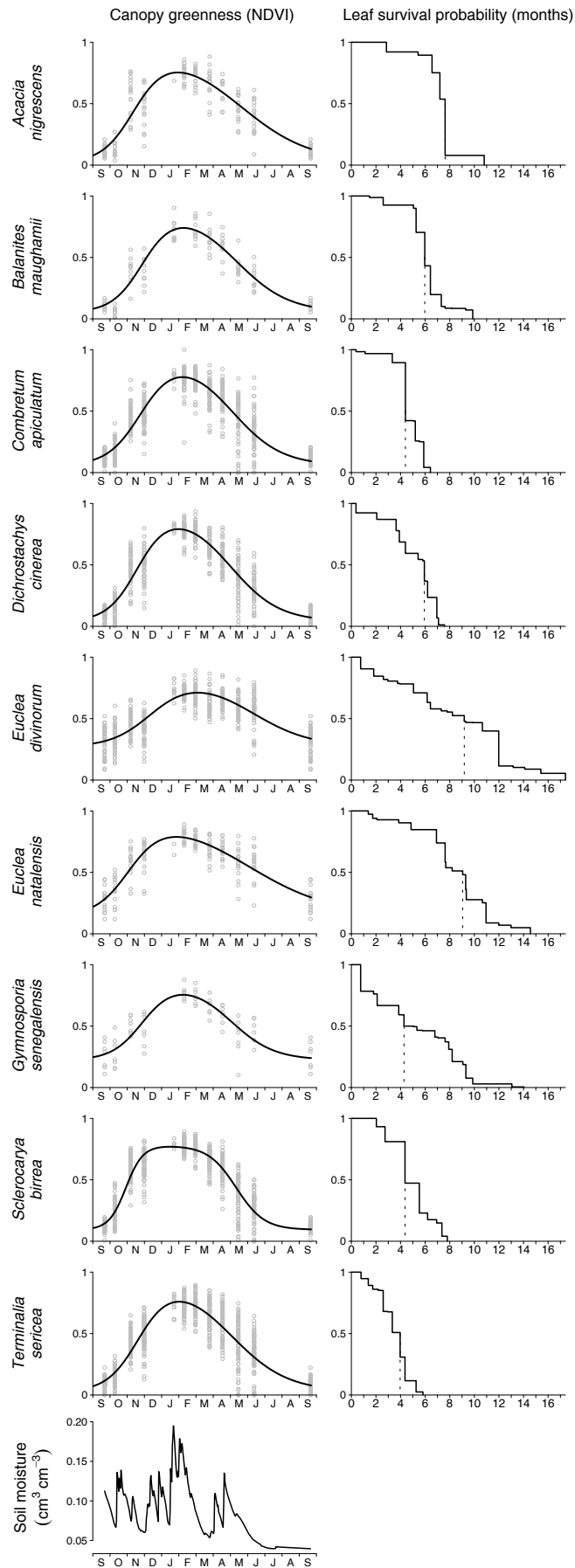


Figure 4.1: Canopy greenness and leaf lifespan for nine species. **a)** Canopy greenness over time as measured by NDVI. The line shows the fitted function of Equation 4.2. **b)** Leaf lifespan as the survival probability calculated from the Kaplan-Meier function. The vertical dotted lines shows the median leaf lifespan. **c)** Time series of volumetric soil moisture content as the average across the 8 sampling sites.

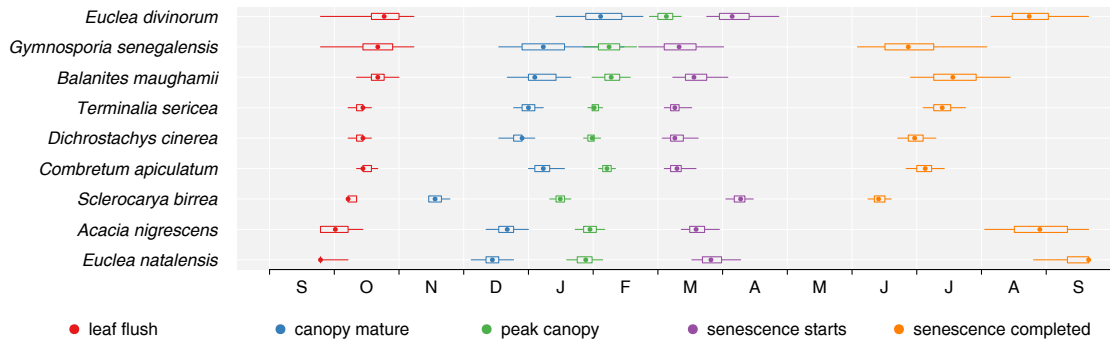


Figure 4.2: Temporal separation of phenological events. The variables were derived from the parameters in Equation 4.2, which were estimated from NDVI time series. The dot shows the median, the boxes show the 25th and 75th percentiles and the whiskers show the 95% credible interval.

To extract further ecologically relevant information from the NDVI signal, we derived five additional phenological variables from the model in Equation 4.2. We propagated the errors from the MCMC parameter estimates in Equation 4.2, allowing full posterior distributions to be estimated for these derived variables. The credible intervals of the derived variables were used to assess phenological overlap between species (Figure 4.2). The first variable shows that the date of leaf flush varied by almost a month between species. The variability in leaf flush date was generally lower for early flushing than for late flushing species. The date of mature canopy marks the end of the greening period (and therefore the start of the period with a mature canopy) and shows that early flushing species also tended to attain full canopies sooner. Despite distinct differences in leaf flush date and date of mature canopy, the date of peak canopy (peak NDVI) was very similar for most species except for *E. divinorum*, which reached peak NDVI more than one month after all other species. Leaf senescence started later for early and late flushing species than for intermediate flushing species. The period between the start and the end of leaf senescence was at least 2 months, but lasted for up to 5 months for some species.

The results in Figures 4.1 and 4.2 show that the leaf phenological strategy cannot be easily

described by a single variable or parameter. We therefore summarised variables using a multi-variate approach (PLSR) that included five of the six parameters from Equation 4.2. Maximum NDVI (*max*) was excluded as it varied little between species and, due to data normalisation in the PLSR algorithm, disproportionately influenced the ordination. We included the integral of the NDVI curve (*int*) and the median and maximum leaf lifespan estimates shown in Figure 4.1 in the PLSR analysis. The first two PLSR axes explained 60% of the variance in the original phenological variables and summarises them in two dimensions (Figure 4.3a). The first axis spans a gradient of “evergreenness”, where long leaf lifespans are associated with a high dry-season NDVI (*min*) and large integral of NDVI (*int*). The second axis captures variation in the dates and rates of leaf onset and leaf offset, where early leaf-on days (*d_{on}*) were associated with rapid onsets (*s_{on}*) and offsets (*s_{off}*). Some species (e.g. *C. apiculatum*, *D. cinerea* and *T. sericea*) clustered together, indicating they adopt similar phenological strategies, while *S. birrea* adopts a unique strategy within this assemblage.

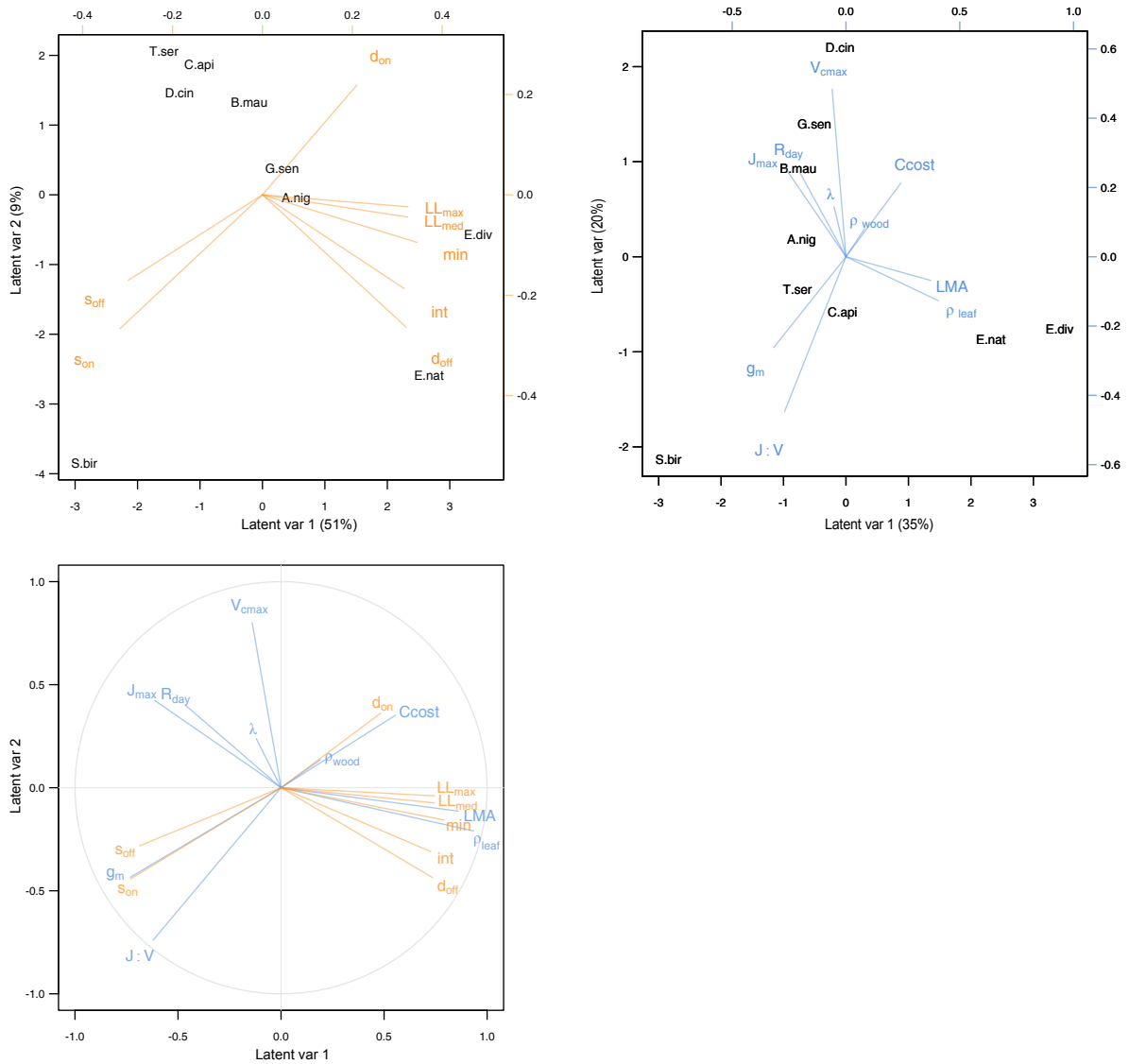


Figure 4.3: The relationship between species, phenological variables and physiological variables as obtained from partial least squares regression (PLSR). **a)** Species ordination and variable loadings in phenological space. **b)** Species ordination and variable loadings in physiological space. **c)** The correlation between PLSR latent variables from **b)** and the original phenological and physiological variables. Longer lines indicate greater correlations, where the circle indicates where correlation coefficients would equal 1. Species abbreviations are A.nig = *Acacia nigrescens*, B.mau = *Balanites maughamii*, C.api = *Combretum apiculatum*, D.cin = *Dichrostachys cinerea*, E.div = *Euclea divinorum*, E.nat = *Euclea natalensis*, G.sen = *Gymnosporia senegalensis*, S.bir = *Sclerocarya birrea*, T.ser = *Terminalia sericea*. Variable abbreviations are d_{on} = leaf-on day, d_{off} = leaf-off day, int = NDVI integral, LL_{max} = maximum leaf lifespan, LL_{med} = median leaf lifespan, min = minimum NDVI, s_{on} = leaf onset rate, s_{off} = leaf offset rate, Ccost = construction costs, g_m = mesophyll conductance, J_{max} = maximum electron transport rate, J:V = maximum electron transport rate : maximum carboxylation rate, λ = marginal water cost of fixing carbon, LMA = leaf mass per area, ρ_{leaf} = leaf tissue density, ρ_{wood} = wood density, R_{day} = dark respiration during photosynthesis, V_{cmax} = maximum carboxylation rate.

Functional traits

The MCMC chains used to estimate physiological parameters (V_{cmax} , J_{max} , g_m and R_{day}) from the CO₂ and light response curves converged and the fitted model described the data well (Figure C.1). Parameter estimates varied substantially between species, particularly for J_{max} and g_m . The uncertainty in parameter estimates was relatively large, which might be partly explained by intra-specific and site variation, since we estimated parameters at the species level but used data from multiple individuals per species.

Observed stomatal conductance was reasonably well described by the model for optimal stomatal conductance in Equation 4.4 ($R^2 = 0.43-0.90$, Figure C.2). The λ and g_1 parameters varied by three and two-fold respectively, suggesting that species differed considerably in their water use strategies (Table 4.1). The variation in λ obtained from Equation 4.5 was primarily explained by variation in g_1 ($R^2=0.99$) and not by variation in Γ^* and P .

LMA of different species varied by over threefold (78-257), wood density by nearly twofold (0.60-1.15 g cm³) and leaf construction costs between 16.05 and 18.95 kJ g⁻¹. Values for each species are listed in Table 4.1.

The physiological variables listed in rows 10-19 of Table 4.1 were summarised in two PLSR latent variables, which explained 55% of the variance in the original variables (Figure 4.3b). In physiological space, two gradients can be distinguished. First, high LMA and high leaf tissue density were associated with low respiration (R_{day}) and low electron transport capacity (J_{max}), indicating that thicker and/or denser leaves had lower metabolic rates. The second gradient revealed that high leaf construction costs were strongly associated with low mesophyll conductance (g_m). Surprisingly, there was no relationship between g_m and leaf tissue density. The water cost of carbon gain (λ) was only moderately associated with the latent variables, but it was positively correlated with R_{day} ($p<0.01$, $R^2=0.65$).

Table 4.1: Measured phenological and physiological traits. Species abbreviations are acanig = *Acacia nigrescens*, balmau = *Balanites maughamii*, comapi = *Combretum apiculatum*, diccin = *Dichrostachys cinerea*, eucdiv = *Euclea divinorum*, eucnat = *Euclea natalensis*, gymsen = *Gymnosporia senegalensis*, sclbir = *Sclerocarya birrea*, terser = *Terminalia sericea*.

Trait	Unit	acanig	balmau	comapi	diccin	eucdiv	eucnat	gymsen	sclbir	terser
d_{on}	day since 1 Jan 2011	316	332	329	322	347	307	331	302	324
d_{off}	day since 1 Jan 2011	504	497	489	487	524	518	488	497	487
s_{on}	NDVI day ⁻¹	0.0351	0.0367	0.0336	0.0372	0.0282	0.0338	0.0368	0.0667	0.0353
s_{off}	NDVI day ⁻¹	0.0162	0.0214	0.0227	0.0231	0.0191	0.0137	0.0261	0.0403	0.0201
min	NDVI	0.14	0.10	0.10	0.07	0.32	0.28	0.24	0.09	0.08
max	NDVI	0.75	0.74	0.78	0.80	0.71	0.79	0.75	0.77	0.76
int	NDVI day	172	155	161	159	194	210	179	167	156
LL _{med}	days	233	182	134	181	280	276	131	133	121
LL _{max}	days	330	301	196	231	531	444	428	238	178
LMA	g m ²	78	84	108	165	257	187	111	99	330
ρ_{leaf}	g cm ³	0.343	0.330	0.438	0.395	0.576	0.511	0.295	0.287	0.335
Ccost	kJ g ⁻¹	16.05	17.61	17.11	18.95	18.01	18.28	16.99	16.72	17.01
ρ_{wood}	g cm ³	1.15	0.69	0.96	0.88	0.78	0.81	0.62	0.60	0.71
g_i	$\mu\text{mol m}^2 \text{s}^{-1}$	3.98	2.33	4.71	3.49	1.80	0.94	1.57	7.27	3.31
R_{day}	$\mu\text{mol m}^2 \text{s}^{-1}$	1.87	3.80	2.34	2.69	1.73	1.29	2.11	2.43	1.71
V_{cmax}	$\mu\text{mol m}^2 \text{s}^{-1}$	92	83	79	131	82	82	124	79	103
J_{max}	$\mu\text{mol m}^2 \text{s}^{-1}$	123	108	108	149	93	109	140	132	142
$\frac{J_{max}}{V_{cmax}}$		1.34	1.30	1.37	1.14	1.13	1.32	1.13	1.66	1.37
λ	mol H ₂ O mol ⁻¹ CO ₂	1076	3189	1642	1804	1155	1635	1030	1512	908
g_1	kPa ^{0.5}	2.73	4.74	3.34	3.57	2.90	3.45	2.75	3.23	2.57

Phenology and functional traits

The relationships between phenological variables and functional traits are shown in Figure 4.3c. As expected, species with large LMA had longer leaf lifespans, higher minimum NDVI, larger NDVI integrals and later leaf-off days. Moreover, this evergreen strategy was associated with low respiration rates and a low electron transport capacity compared to deciduous species. Early and rapidly flushing species were associated with greater mesophyll conductance and low leaf construction costs. Therefore, species that rapidly attained a full canopy appeared to have lower leaf construction costs.

Carbon gain model

Annual carbon gain as calculated from Equation 4.6 varied more than fivefold between species (Table 4.2, Figure 4.4). To test the sensitivity of carbon gain to phenology on the outcome, we ran the model without the NDVI term (i.e. $NDVI_t = 1$). Carbon gain estimated using constant NDVI was closely and linearly related to carbon gain estimated using varying NDVI ($p < 0.001$, $R^2 = 0.94$). There was a positive relationship between annual carbon gain and relative abundance ($p = 0.07$, $R^2 = 0.31$, Figure 4.4).

Discussion

Models designed to explain the spatial distribution of dominant leaf habit explore carbon gain as a function of leaf-level gas-exchange processes and environmental variables. They do not consider that leaf phenology may be acted on by divergent selection such as competitive interactions and how this might influence carbon gain. We examined how carbon gain may be affected by phenology and describe interactions between leaf phenology, leaf habit and functional traits that are related to the carbon and water economies. We found that both leaf phenology and functional traits varied substantially between species and

Table 4.2: Annual carbon gain calculated using Equation 4.6.

Species	Carbon gain (g g ⁻¹ leaf yr ⁻¹)
<i>Acacia nigrescens</i>	10.2
<i>Balanites maughamii</i>	4.8
<i>Combretum apiculatum</i>	4.6
<i>Dichrostachys cinerea</i>	8.1
<i>Euclea divinorum</i>	1.9
<i>Euclea natalensis</i>	4.4
<i>Gymnosporia senegalensis</i>	3.2
<i>Sclerocarya birrea</i>	5.2
<i>Terminalia sericea</i>	5.3

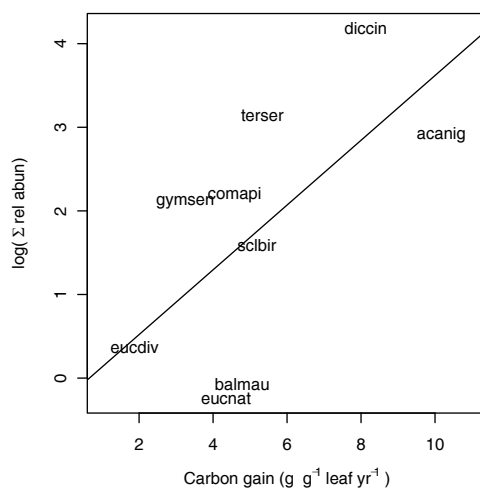


Figure 4.4: Relationship between ecological dominance and annual carbon gain. The line shows a linear regression fit, $P = 0.07$, $R^2 = 0.31$.

that aspects of leaf phenology were strongly related to the carbon economy but not to water use strategy.

Phenological strategies

The variation in leaf habit was large, ranging from evergreens with long-lived (>1 yr) leaves to leaf-exchanging deciduous species with average leaf lifespans of 3-4 months; less than half the leaf-bearing period. Although differences in leaf lifespan were large, all species had uni-modal canopy greenness, indicating that leaf area and photosynthetic activity were highest during the wet season independent of leaf habit. For evergreen species with long-lived leaves, this peak may be explained by median leaf-lifespans that were shorter than one year, suggesting that part of the canopy was shed during the dry season. Nutrient resorption from senescing leaves, which implies the disassembly of chlorophyll, is significant in this ecosystem (Ratnam *et al.*, 2008). This would also reduce greenness, although it is not clear when this process starts in these evergreen species. Despite the large overlap in peak growing seasons, the timing of leaf flush and senescence and the rates at which canopy greenness increase and decrease, varied considerably between species. The earliest flushing deciduous species deployed leaves 3 weeks before the last one and leaf senescence varied between 2 and 5 months. Although leaf flush before seasonal rain, referred to as pre-emptive flushing, is a well know phenomenon in seasonally dry environments (Borchert, 1994) and has also been recorded in this savanna (Archibald & Scholes, 2007; Higgins *et al.*, 2011), we did not observe any pre-emptive flushing, potentially because the first rains of the season came very early during our study (6 September). Despite large overlap in peak growing season (Figure 4.1), divergent timing of phenological events (Figure 4.2) suggests that phenological niche separation might be substantial in this system.

Because many phenological variables varied independently of each other, phenological strategies in this environment are not effectively captured by dichotomies such as evergreen vs. deciduous or early vs. late flusher. Similar conclusions have been drawn for South

American savannas, where the assignment of species to functional groups based on leaf phenology was found to be rather arbitrary, and that strategies are sorted along continuous axes of phenology and seasonal activity (Goldstein *et al.*, 2008; Cianciaruso *et al.*, 2013).

Functional traits

The range in functional trait values that we observed in this savanna allowed us to describe relationships between different traits and compare them to previously described relationships such as the leaf economic spectrum (LES) (Wright *et al.*, 2004). For example, LMA in our study ranged between 78 and 257, which spans approximately 50% of the global range for woody angiosperms (Poorter *et al.*, 2009). The association between high LMA, low respiration rates (R_{day}), low electron transport capacity (J_{max}) and, to a lesser extent, low carboxylation capacity (V_{cmax}) is consistent with findings from the LES. The LES shows that, across biomes, LMA is negatively related to respiration and photosynthetic capacity (Wright *et al.*, 2004). The predictive ability of these relationships within communities has been questioned (Wright & Sutton-Grier, 2012), but seem to hold within this savanna, perhaps because our study area includes 50% of the global variation in LMA. Leaf construction costs was only weakly related to LMA in this study. Interestingly, species with high construction costs had low mesophyll conductances. The mesophyll conductance is the rate at which CO₂ diffuses from the stomatal cavity to the location of Rubisco, inside the chloroplast, and low mesophyll conductance therefore limits the rate of carbon assimilation. Low mesophyll conductance is typically associated with dense leaf tissue (Niinemets *et al.*, 2011), but we did not detect this in our data. Overall, these results show that traits related to the carbon economy differed substantially between species.

As was the case for carbon-related traits, variation in traits related to water use strategy was substantial. Estimates for the g_1 parameter from the optimal stomatal conductance model (Equation 4.4) ranged between 2.57 and 4.74 in this study. This is well within the

range reported for woody plants from various biomes, but low compared to Australian savanna species (6 Eucalypt and non-Eucalypt species) that averaged 6.6 ± 0.6 (Medlyn *et al.*, 2011). Because g_1 is proportional to the water cost of carbon gain (λ), this difference suggests that African savanna species might use water more conservatively than Australian savanna species. However, our estimates of λ from Equation 4.5 were consistent with the reported range for tropical savanna species (Lloyd & Farquhar, 1994; Thomas *et al.*, 1999), suggesting that water use strategy is highly variable within communities, but on average similar in savannas on different continents. Our multi-variate analysis (Figure 4.3) suggested that the variation in λ was not well explained and was not strongly related to most other traits. However, it was positively related to respiration rate, indicating that species with higher metabolic activity are prepared to lose more water per unit carbon gain. Because species with higher metabolic activity have a greater operational carbon demand, it follows that under dry conditions large transpirational capacity is required in order to maintain metabolic activity. We have not seen such a relationship between λ and respiration reported in the literature, and more species would need to be sampled to assess the generality of this relationship.

To our knowledge, there are no previous records of the marginal water cost of photosynthesis and the described relationships between structural and gas-exchange traits for woody African savanna species, preventing direct comparisons of our results. Considerable work has been done in Australian savannas (Eamus, 1999; Eamus & Prior, 2001); however, Australia is anomalous phenologically and taxonomically with its largely evergreen Myrtaceae-dominated savannas (Bowman & Prior, 2005; Bowman *et al.*, 2010). Comparisons between continents should be made with caution as recent work has shown that the interactions between savanna vegetation and environmental drivers differs markedly between continents, despite the vegetation being structurally similar (Moncrieff *et al.*, 2014b; Lehmann *et al.*, 2014). Part of these differences might be accounted for by historical contingencies, including differences in continental species pools.

Phenology and functional traits

We found that high LMA was associated with long leaf lifespan and evergreenness (where evergreenness was indicated by several phenological variables) and with low photosynthetic and metabolic rates (Figure 4.3). These results provide further evidence that patterns predicted from the LES trade-offs can emerge over the relatively small spatial scale covered in this study. We further found that early leaf flush and rapid canopy development were associated with a high mesophyll conductance and with low leaf construction costs.

Water use strategy as measured by the water cost of carbon gain (λ) was not related to any of the phenological variables or to leaf lifespan. It has been suggested that in biomes with a high evaporative demand and a predictable periodic water supply (e.g. tropical savannas) non-conservative water use should be the most successful strategy, whereas in biomes with a high evaporative demand but unpredictable episodic water supply (i.e. deserts) conservative water use should be more successful (Lloyd & Farquhar, 1994). Lloyd & Farquhar (1994) extend this hypothesis to propose that plants with a rapid phenological development over a short period (i.e. drought deciduous plants) should have less conservative water use (high λ) than plants with slower phenological development over longer periods. This prediction is contested by Eamus & Prior (2001), who point out that empirical data presented in Thomas *et al.* (1999) shows that, for 6 Australian rainforest and savanna species, drought deciduous species had the lowest values for λ . Although our study did not include evergreen species with very long-lived leaves, the absence of a relationship between phenological strategy and water use strategy in our study suggests that such a relationship, if it exists, is currently not well understood.

Carbon gain

To assess whether our estimates of annual carbon gain using Equation 4.7 were similar to reported values we compared our estimates to net assimilation rates as reported in

Larcher (2003). Because net assimilation rates are in $\text{g dry matter m}^{-2} \text{ day}^{-1}$, we used our measurements of LMA and growing season length from the NDVI time series to calculate an approximate annual carbon gain. This yielded annual carbon gains in the range of 1-15 $\text{g g}^{-1} \text{ yr}^{-1}$, which is similar to the range we estimated: 1.9-10.2 $\text{g g}^{-1} \text{ yr}^{-1}$ (Table 4.2). This suggests that the range of carbon gain estimates from Equation 4.7 are realistic.

By expressing carbon gain per gram of leaf, we can contrast the carbon gain of a leaf with its construction cost. Our calculation of species-specific carbon gain shows a fivefold difference, with the three evergreen species having the lowest carbon gain. Although the linear relationship between maximum leaf lifespan and carbon gain was weak ($p=0.2$, $R^2=0.11$), when phenology (NDVI) was excluded from the model the least productive and the three most productive species retained the same rank, while the intermediate five species changed rank. Together these results suggest that the leaf phenological strategy has a moderate effect on carbon gain and that differences in carbon gain were primarily due to differences in physiological rates.

The maximum lifespan in our study was approximately 1.5 years, but the majority of leaves from evergreen species only lived for up to 1 year (Figure 4.1, Table 4.1), which negates some advantages that evergreens are hypothesised to have over deciduous leaf habits (Givnish, 2002). First, evergreens can potentially extend growing seasons by taking advantage of early rainfall when deciduous species have not yet deployed leaves. This advantage holds for the 1-year leaves common to the evergreen species in our study. Second, evergreens should have lower amortized construction costs, because they only need to replace part of the canopy each year. This is only true when lifespan exceeds one year and therefore does not apply to 1-year leaves. Third, amortized nutrient replacement costs should also be lower, but again, energetic costs of capturing new nutrients can only be lower in evergreens if lifespan exceeds one year (unless total nutrient uptake is lower) (Aerts, 1995). Fourth, evergreen leaves need to be tougher to survive mechanical stresses over their lifespan, which might provide the additional benefit of deterring herbivores. Deterrence might be

especially important in our study system, with a native assemblage of mammalian herbivores that require food throughout the dry season, when many species are leafless. On the other hand, these savannas are characterised by frequent dry-season fires (Govender *et al.*, 2006) that instantaneously consume leaves in the flame zone, irrespective of their traits.

The theory of optimal leaf habit (Givnish, 2002) predicts that the leaf habit with the highest return in a given environment should dominate that environment. Despite the limited effect of phenological strategy on carbon gain, carbon gain of species was related to their relative abundance. Species in our sample spanned the entire range of relative abundances in this system and included the three most abundant species, suggesting that annual carbon gain as calculated using our model may partly explain ecological dominance. A larger sample size would be needed to assess the generality of this finding.

Conclusion

The studied savanna system is characterised by a highly seasonal moisture supply, relatively infertile soils, frequent fires and a full assemblage of native herbivores. It is not immediately clear which plant strategies (Grime, 1977) should be expected to dominate in such an environment, whether seasonal moisture limitation and severe disturbance regime should lead to convergence in traits or, whether seasonally favourable growth conditions result in a competitive environment in which trait divergence should be expected. We find that, although peak growing season of all studied species largely overlap, there are considerable differences in leaf phenology, leaf habit and physiological traits related to the carbon and water economies. These differences suggest non-convergence in individual traits, but the resulting differences in annual carbon gain also suggests non-convergence in the integrated effects of trade-offs between traits and their environmental dependencies, i.e. the physiological niche. While it is likely that divergent selective forces such as competitive interactions (MacArthur & Levins, 1967) play a role in this system, other

mechanisms of coexistence such as the storage effect (Chesson & Warner, 1981; Chesson, 2000) could also provide a plausible explanation for the coexistence of dissimilar phenological strategies. For example, evergreens may benefit disproportionately in years with very early rain or heavier dry-season rains, so that annual carbon gain in those years exceeds that of deciduous species.

Chapter 5

Synthesis

Overview

Local climates arise from complex interactions between global and local drivers that affect the balances of incoming and outgoing energy and moisture at sub-daily to decadal time scales. Terrestrial plants affect many of these interactions at all spatial and temporal scales. For example, as introduced in Chapter 1 of this thesis, plants have altered the long-term carbon cycle and, thereby, the global energy balance for the past 360 million years. On shorter time scales, plants also affect the global energy balance, through carbon sequestration into biomass and soils, effects on albedo and evapotranspiration. On regional to local scales the transpiration of water vapour into the atmosphere affects relative humidity and cloud formation. In mountainous regions throughout the world abundant emissions of isoprenes by plants give rise to a “blue haze”, but also have a major impact on atmospheric ozone formation (Went, 1960; Sharkey *et al.*, 2007). The radiative forcing by plants is not limited to the processes listed here, but many of the impacts that plants have on the climate, atmospheric composition, geochemical cycling and the global energy balance are directly affected by the presence and functioning of leaves. Therefore, out of all plant organs, leaves seem to have an inordinately large effect on the functioning of the Earth system. Of course, the ability to bear planar leaves with a high energy load necessitates the possession of well developed roots and vascular shoots to supply the leaves with moisture necessary to maintain sub-lethal temperatures through evaporative cooling. Nonetheless, changes in the amount, spatial distribution, timing and duration of leaf deployment is certain to affect the global energy balance.

In this thesis, I have aimed to fill several gaps in the knowledge on global patterns of leaf phenology, evergreen and deciduous leaf habits and the combined effect of these concepts on the carbon balance of individual plants. One of the main challenges in developing a framework in which to understand the drivers and consequences of leaf deployment is the enormous disparity of scale between the various drivers and consequences. For example, the density of stomata on leaves is regulated by the atmospheric CO₂ concen-

tration (Woodward, 1987), which is globally largely invariant. Because stomata regulate the balance between carbon uptake and water loss, physiological functioning at the smallest scale is affected by a global driver, but at the same time feed back to regulate the global carbon and energy balances. In Chapters 2 and 3 of this thesis, I have attempted to address spatial patterns in leaf phenology and leaf habit at the largest scales, while recognising that these patterns emerge from leaf-level and organism-level processes, which are in turn affected by both global and local drivers. To gain further insight into how leaf deployment is related to other aspects of plant strategies and how these interactions affect plant fitness, I measured leaf- and organism-level processes of trees in an African savanna. In the following sections, I shortly summarise the main findings of each chapter, review potential weaknesses and elaborate on how the findings have contributed to fulfilling the aims described in Chapter 1. Finally, I ask which new questions have emerged and provide suggestions for how these could be addressed.

Findings and implications

In Chapter 2, I quantified seasonal patterns of leaf deployment for the entire terrestrial surface (except Antarctica) and calculated changes over the past three decades. The analysis showed that in most parts of the world change in at least one of the calculated phenological metrics was severe. The algorithms that were developed in this chapter improve on previous methods in several ways. By fitting a spline through the NDVI time series, the NDVI signal can be described very flexibly, allowing the same method to be applied to areas with very different seasonal fluctuations in NDVI. This could not have been achieved with a single parametric function as often used in regional studies, which would be too rigid to describe the global variety in seasonal NDVI signals. A potential advantage of parametric functions could be that, when an appropriate function is selected, the parameters may be biologically interpretable. This problem was overcome by deriving 21 phenological metrics from the spline function, which is considerably more detailed

than previous studies. The real advantage of parametric functions is therefore that the uncertainty in the parameter estimates can be quantified. Although the spline fit can be assessed for each location, a less than perfect fit cannot be propagated as uncertainty to the derived phenological metrics. This makes it difficult to assess, for a single pixel, what the uncertainty envelope around each phenological metric is. This problem was partly overcome by expressing change at each location relative to the phenological variance of all locations with similar phenology.

The patterns of change that are described in Chapter 2 are only a small subset of the results from the analysis, but the maps and figures presented in Chapter 2 and Appendix A provide a convenient means to extract information about change in specific phenological metrics or at specific geographic locations. Although certain kinds of change, such as earlier leaf deployment and extended growing seasons in Europe and North America, have already been clearly linked to global warming (Menzel *et al.*, 2006; Menzel, 2013b), the mechanisms behind detected phenological change in seasonally dry regions of the southern hemisphere have not been investigated. Since vegetation activity is strongly limited by soil moisture during the dry season, drought deciduousness is a common strategy in these systems. While detailed information on the cues that trigger leaf deployment is not readily available for these systems, several studies have shown that leaf deployment by trees in seasonally dry ecosystems does not necessarily require soil moisture (Borchert, 1994; Archibald & Scholes, 2007; Higgins *et al.*, 2011). Nonetheless, it is likely that for many species soil moisture provides a cue for leaf deployment, particularly for grasses (Archibald & Scholes, 2007; Higgins *et al.*, 2011). Moreover, recent work shows that deciduous species can be induced to retain leaves when soil moisture is provided throughout the dry season (Stevens *et al.*, 2015), suggesting that moisture availability affects rates of leaf senescence. The timing and size of precipitation events in these ecosystems is intrinsically more uncertain than the seasonal progression of temperatures in Boreal and temperate regions, so that attributing changes in leaf phenology to changes in climate is likely to be more difficult. It is also important to consider that all the observed phenological change

takes place against a backdrop of increasing atmospheric CO₂. Recent work shows that increased atmospheric CO₂ can delay leaf senescence by conserving soil moisture in grassland communities (Reyes-Fox *et al.*, 2014). Later leaf-off dates over a large part of the terrestrial surface (Figure A.2) might therefore indicate a CO₂ effect, particularly in areas where plant growth at the end of the growing season is constrained by moisture limitation. However, to convincingly attribute the observed change will require detailed regional studies and experiments, as in different areas the seasonal progression of vegetation activity may be limited by different resources and environmental variables.

In Chapter 3, I examine overlap in the physiological niche of one deciduous and two evergreen phenomes in different biogeographic realms to assess convergence. In 71% of the study area, all four realms predicted the same phenome distributions, suggesting that the physiological niches of analogous phenomes in different realms largely overlap. The large niche overlap of analogous phenomes in areas with different evolutionary histories implies convergence. However, it is not clear how exactly the physiological niche and the leaf habit are related. For example, does the leaf habit determine the physiological niche, does the physiological niche determine leaf habit, or does the answer lie in relationships between leaf habit and individual niche axes and potential trade-offs between all bivariate interactions? Some clues may be found in the similarities and differences between the different models used in this thesis. Carbon balance models such as the model developed in Chapter 4 or in Givnish (2002) use estimates of physiological parameters to determine the optimal leaf habit. On the other hand, the model used in Chapter 3 uses observations of leaf habit to estimate physiological parameters. Similar physiological parameters are included in both models, for example, both include estimates of carbon assimilation and respiration and negative effects of low soil moisture on carbon gain. There are also differences, e.g. the carbon balance model in Chapter 4 aims to consider effects of nutrient availability on the carbon balance through estimates of water loss and leaf construction costs, whereas the model of plant growth in Chapter 3 explicitly considers nitrogen uptake by the roots. The inclusion of both similar and different physiological processes in models attempting

to explain leaf habit from physiological properties and models describing the physiological properties of different leaf habits suggests that there are multiple relationships between leaf habit and the physiological niche. These relationships potentially form a set of trade-offs within which balances may shift along environmental gradients.

Such trade-offs between leaf habit and aspects of the physiological niche would be consistent with hypotheses about optimal leaf habit (Givnish, 2002), but also with the trade-offs between leaf lifespan and physiological and anatomical traits described in the leaf economic spectrum (LES) (Wright *et al.*, 2004). The large amount of unexplained variation in the LES could account for the relatively large area (29%) in which projected phenomes differed depending on realm, but this non-convergence seems to contradict the theory on optimal leaf habit. This theory predicts that for each set of environmental conditions one leaf habit will yield a greater carbon gain than the other and for that reason should dominate. A possible explanation for phenome-uncertain areas identified in Chapter 3 is that both leaf habits can achieve equal carbon gain in these areas. Which of the two possible leaf habits dominates an area would then depend on other processes, such as historical contingencies. To test whether the potential carbon gain of evergreen and deciduous plants in the phenome-uncertain areas is equal, an experiment could be performed in which species of both leaf habits are grown in (simulated) phenome-uncertain environments. An alternative test would be to establish if invasions by exotic species can cause the dominant leaf habit of an ecosystem to switch.

Equal carbon gain for deciduous and evergreen leaf habits can also be used to explain the areas where all realms consistently predicted both leaf habits to occur. However, an alternative explanation for the areas of overlapping leaf habits could be that one leaf habit yields a greater carbon gain, but that this does not always translate to ecological dominance. Such a situation could be imagined in regions with unpredictable climates or disturbance regimes, where one leaf habit may be favoured in some years and another leaf habit may be favoured in other years. This type of dynamic has been described as the

storage effect (Chesson & Warner, 1981; Chesson, 2000) and it would be interesting to test if the ratio of evergreen and deciduous leaf habits in a location is related to the regularity of resource pulses (e.g. rainfall) or disturbance (e.g. fire) in that location. The ratio between leaf habits should become more equal as the temporal availability of resources becomes less predictable.

In systems where the climate and the disturbance regime follow more regular cycles, the co-existence of evergreen and deciduous leaf habits may be explained by biotic interactions. If competition for resources is intense during certain parts of the year, less competitive species may persist by using the “shoulder” seasons, i.e. times of the year when competitors are dormant, to fulfil most of their annual carbon requirement. A classic example of such phenological niche separation comes from under-storey herbs in deciduous forests, which can complete their entire growing season before the tree canopy closes (Al-Mufti *et al.*, 1977). Recent work has shown that invasive species can occupy a part of the phenological niche that is not utilised by native species (Fridley, 2012; Wolkovich & Cleland, 2014) and this raises the question of why native species have not evolved to utilise the available niche space. Assuming that evolutionary rates have not prevented species from expanding into the the entire available niche space, the answer may lie in the strength of competitive interactions that drive divergence in the phenological niche.

The research presented in Chapter 4 was partly based on previous findings by Higgins *et al.* (2011), who showed that plants had different phenological niches in a seasonally dry African savanna. The study by Higgins *et al.* (2011) divided observed canopies into functional groups based on their phenology, but did not identify whether these functional groups were unique to sets of species or whether there was large intra-specific variation. The work in Chapter 4 provides phenological information for a set of common species and shows that inter-specific variation is larger than intra-specific variation. Despite variation in leaf phenology and leaf habit, physiological activity in this ecosystem is highly limited by moisture during part of the year, and accordingly the growing seasons of all species

were shown to largely overlap in Chapter 4. Outside this overlapping growing season, the time windows during which growth is possible are narrow as very low soil moisture during the dry season probably prevents photosynthesis. The period during which evergreen plants, early flushing plants or plants that retain leaves for long into the dry season may gain an advantage over competitors is therefore limited. However, if phenological niche separation driven by competition is responsible for the variation in leaf phenology and leaf habit, the amount of carbon gained during these narrow time windows is apparently large enough to drive selection for different phenological strategies. Whether the within-community divergence in phenology and leaf habit as described in Chapter 4 results from inter-specific competition for resources was left unanswered by the study.

If competition plays a role in the divergent leaf phenologies and leaf habits, it is possible that plant fitness is not directly affected by the period during which carbon uptake is possible, but rather by other processes that regulate the carbon balance. One such process might be the uptake of soil nutrients. For example, if carbon gain during the wet season becomes limited by soil nitrogen, competition for nitrogen should increase. Species with low transpirational capacity (e.g. evergreens) may be disadvantaged under intense competition, as their limited ability to cycle water should reduce the capacity to take up N through mass flow. For such species, it may be essential to access soil N stocks when other, more competitive, species are still dormant. The benefits may be especially large at the start of the season, when the first rain of the season allows soil microbes to mineralise a supply of litter substrate that has been building up during the dry season when conditions were too dry for microbial activity (Higgins *et al.*, 2015).

Conclusion

The work in this thesis has addressed three specific questions about leaf phenology and leaf habit. In the previous sections I have posed several specific questions that emerged

from the findings in this thesis and made suggestions for how these questions may be addressed to further the understanding of leaf habit and leaf phenology. In a broader sense, the main challenge is to develop a framework that incorporates the concepts of leaf phenology and leaf habit and links relationships between leaf deployment, environmental gradients and biotic interactions across spatial and temporal scales (Pau *et al.*, 2011). One avenue of research that is likely to improve such a framework is the description of relationships between leaf deployment and other functional traits. Quantifying these relationships should lead to an understanding of the trade-offs between leaf deployment and other functional traits, which ultimately drive ecological interactions such as competition and therefore form the selective basis of (phenological) niche divergence. The work in Chapter 4 contributes to this endeavour by carefully cataloguing many traits for a small set of species, while other recent studies have contributed by including many species, but inevitably fewer functional traits (Panchen *et al.*, 2014).

The proposed framework is based on the assumption that leaf phenology and leaf habit have adaptive significance and that selection acts on these traits and on their trade-offs with other traits. While adaptive significance seems likely given the accumulated evidence on the sorting of leaf habit along environmental gradients (Givnish, 2002) and the relationships between leaf lifespan and other functional traits (Wright *et al.*, 2004), large scale studies of leaf phenology have traditionally treated leaf phenology as a phenotypically plastic trait that is highly responsive to environmental fluctuations. This notion most likely stems from the strong correlations between climatic and phenological seasonality in deciduous regions of the world, but it is important to consider that species respond to environmental cues differentially and that the genetic make-up of different species may set different limits for phenological plasticity. It should also be considered that leaf phenology is, to an extent, phylogenetically conserved (Davies *et al.*, 2013), i.e. genetically closely related species resemble each other phenologically. It will be important to establish to what extent the different aspects of leaf phenology as described in Chapter 2 are phylogenetically conserved, to what extent they are evolutionary adaptive and to what extent phenotypic

plasticity may buffer the effects of changing environments.

Finally, I make a case for better integration of atmospheric CO₂ effects on phenology, as CO₂ has driven the evolution of plant form and functioning throughout history (Woodward, 1987; Beerling *et al.*, 2001; Osborne *et al.*, 2004). Evidence from recent CO₂ enrichment experiments suggests significant effects of elevated CO₂ on leaf phenology but, importantly, also reveal that responses vary among species (Cleland *et al.*, 2006; Reyes-Fox *et al.*, 2014). It is not clear if CO₂ responses can be predicted from other traits or if CO₂ responses may be phylogenetically conserved. CO₂ effects on phenology are undoubtedly complex because of the myriad pathways through which CO₂ affects plant and ecosystem functioning (Körner, 2006; Ainsworth & Rogers, 2007). For example, elevated CO₂ may increase photosynthetic rates, decrease transpiration rates leading to conservation of soil moisture, lower stomatal density and smaller leaves (Woodward, 1987; Ainsworth & Long, 2005; Körner, 2006; Ainsworth & Rogers, 2007). All these effects and their interactions are likely to have an impact on resource use and competition, which co-regulate phenological strategies and determine the balance between convergence and divergence. Future CO₂ enrichment experiments should aim to include dominant species from all major biomes, which should help to determine if large-scale phenological change may be partly driven by elevated CO₂. Until such time, careful thought experiments will need to provide tentative explanations for the observed changes and generate the hypotheses that need testing most urgently.

Summary

Summary

The seasonal timing and duration of leaf deployment by plants has major implications for the exchange of energy and matter between the Earth surface and the atmosphere. Since the Devonian the spread of leafy terrestrial plants has made a major impact on the composition of the atmosphere and the cycling of carbon and mineral nutrients. Presently, plants are still a key link in various feedback loops that determine the climate. Plants negatively force the global energy balance by capturing CO₂ from the atmosphere during photosynthesis, which in most plants takes place primarily in the leaves. During photosynthesis water vapour is transpired into the atmosphere, which cools the surface, but also affects other atmospheric processes such as cloud formation that in turn affect the global energy balance. Leaves also directly affect the energy balance, by regulating the proportions of absorbed and reflected solar radiation i.e. the albedo. Whether the albedo of a vegetated surface is higher or lower than the substrate depends on both the vegetation type and the substrate type. All these processes by which vegetation affects the global energy balance and thus the climate, fluctuate seasonally with the temporal patterns of leaf deployment. Since both the climate and the seasonal timing of leaf deployment (leaf phenology) have been changing over the past decades, an understanding of the mechanisms that underlie the timing and duration of leaf deployment by plants is crucial to anticipate changes in the energy and carbon fluxes between the atmosphere and the terrestrial surface.

An additional reason for pursuing a better understanding of the extent and severity of leaf phenological change arises from the cascading effect on biotic interactions. Effects on, for example, food webs can be dramatic if species rely on the timing of leaf flush and associated availability of resources to complete their life cycle or reproductive cycle. Such temporal mismatching of previously synchronised seasonal cycles may greatly increase the extinction risk for affected species. For example, the hatching date of butterfly eggs may be directly regulated by leaf flush and therefore adaptable, while the arrival date of migratory passerine birds that rely on the caterpillar peak to raise their brood may be

constrained by different, non-changing, factors. As a result, mismatches in the timing of food availability and food requirement may reduce reproductive output. Changes in the temporal dynamics of leaf deployment may also affect competitive interactions between plant species, potentially leading to changes in community structure and composition.

While observational studies on the leaf phenology of common European and North American plant species have clearly shown changes in response to climatic change over the past decades, a larger scale overview of the extent and severity of phenological change is lacking. Particularly the southern hemisphere has remained understudied despite the availability of remotely sensed time series that date back to the early 1980s. In Chapter 2, I use a remotely sensed 31-year time series of normalised difference vegetation index (NDVI) to quantify phenological change globally. Change was determined for 21 phenological metrics that were derived from a spline fit through the NDVI time series using a novel method. In addition to quantifying absolute change, e.g. leaf flush in Julian days, I quantified relative change by scaling the change in each location (pixel) by the variance of change over all locations that were phenologically similar, so that change is expressed in standard deviation (SD) units. These phenologically similar areas, phenomes, were identified using a cluster analysis that yielded 99 phenomes. Change for each metric at each location was presented in global maps, which show that over 54% of the terrestrial surface change exceeded 2 SD for at least one phenological metric. By summarising the average change of 99 phenomes and over 21 phenological metrics into 9 global syndromes of change, it becomes apparent that different kinds of phenological change are distinctly clustered in space. Over large areas, e.g. the Boreal, the kind of change is relatively homogeneous, while in other regions, e.g. West Africa, the kind of change is highly variable over relatively short distances. The detected phenological change was consistent with previous studies at regional scales, primarily in the northern hemisphere, but substantial change in the southern hemisphere was not detected previously. The high phenological resolution of this analysis (21 metrics) revealed that qualitatively different phenological changes can lead to quantitatively similar change in summary variables such as growing season length

and total photosynthetic activity, a proxy for primary productivity. No changes in net primary productivity, a variable commonly used in remote sensing studies, may therefore mask underlying phenological change. Although previous studies have clearly attributed phenological change to climatic change and increased atmospheric CO₂, these studies also show that complex interactions between multiple drivers affect leaf phenology. Attribution of the detected phenological change would be the next important step, although identifying the interacting processes that affect leaf phenology is likely to warrant a regional approach.

Chapter 2 describes shifts in timing of leaf deployment and senescence, but does not address potential effects of climate change or increased atmospheric CO₂ on the the duration of leaf deployment i.e. leaf habit. In order to assess potential effects of global change on the distribution of evergreen and deciduous vegetation, it is necessary to uncover the mechanisms that determine these patterns. Current explanations for the geographic distribution of deciduous and evergreen leaf habits assume evolutionary convergence on an optimal leaf habit that maximises carbon gain in a given environment. In Chapter 3, I examine convergence by quantifying the physiological niche of evergreen and deciduous vegetation in four global biogeographic realms and calculate the niche overlap and niche similarity of evergreen and deciduous vegetation in these realms. Large overlap implies convergence of the physiological niche. I start by defining the distribution of one deciduous phenome and two evergreen phenomes, i.e. with high and low leaf area index, to distinguish between closed-canopy evergreen forests and thicket and sparsely vegetated arid shrubland. To describe the physiological niche of each of these phenomes in each biogeographic realm I used a process-based model of plant growth. The model estimates plant growth as a function of respiration, carbon uptake by the shoot, nitrogen uptake by the root, and the transport of these resources between the root and the shoot. Each of these physiological processes has environmental dependencies which were estimated from global environmental data sets and phenome presence-absence data. For example, carbon uptake is limited by solar radiation and affected by temperature. The model was able to predict the observed

distributions of the phenomes in their native realm with an average accuracy of 81%, indicating that the model accurately described the physiological niche of these phenomes. I assessed the niche overlap between analogous phenomes of different realms by projecting the potential distribution of each phenome into each non-native realm and examining the overlap in geographic ranges. In 71% of the study area projections from all four realms predicted the same phenome, suggesting a high level convergence. The remaining 29%, where projections from all realms did not coincide, indicate that the phenome type is uncertain in those areas, possibly because of historical contingencies or alternative stable states. These results imply that the biogeography of leaf habit is, for the largest part, driven by evolutionary convergence, but that there are also large regions where there is no convergence. Therefore, the leaf habit in these regions potentially depends on divergent selective forces such as competition, so that potential effects of global change on the geographic distribution of leaf habits will be difficult to predict.

After exploring global changes in leaf phenology in Chapter 2 and the distribution of evergreen and deciduous leaf habits in Chapter 3, I take an integrative approach in Chapter 4, where I evaluate the interactions between leaf habit, leaf phenology and other functional traits that are related to the carbon economy of plants using empirical data. For nine woody species in a seasonally dry South African savanna, I quantify leaf phenology using near-surface remotely sensed NDVI images, leaf habit by measuring the lifespan of tagged leaves and several functional traits including rates of gas exchange. Leaf lifespan varied from 5 to 18 months between species, implying both deciduous and evergreen leaf habits. Leaf phenology also differed substantially between species, for example in the rate of canopy development. Relationships between leaf lifespan, photosynthetic and metabolic rates and the leaf mass per area were consistent with relationships described in the literature on the leaf economic spectrum. One trait of particular interest was the marginal water cost of carbon gain ($\frac{\delta E}{\delta A} = \lambda$), which can be interpreted as the amount of water that a plant is prepared to spend for a given amount of carbon. I estimated λ using a recently published model for optimal stomatal conductance and found that it was not related to

leaf phenology and leaf habit, while a relationship might be expected given the seasonally dry environment in which most species would be described as drought deciduous and leaf phenology is expected to be strongly affected by water availability. In a subsequent analysis I used the collected data on phenology, soil moisture, photosynthetic and metabolic rates and λ to parametrise a simple carbon gain model for each species. The calculated annual carbon gain varied more than fivefold between species, was lowest for evergreen species and was moderately sensitive to differences in leaf habit and leaf phenology. The large variation in leaf phenology, leaf habit and carbon budgets of species in a highly seasonal environment suggests that convergence to an optimal leaf habit may be opposed by divergent selection as a result of limiting similarity or the storage effect.

In this thesis, I examine change in global leaf phenology and the geographic distribution of leaf habit, as leaf phenology and leaf habit regulate the functioning of biological communities and the Earth system. I show severe phenological change during the past three decades over large parts of the terrestrial surface, which is likely to have substantial impacts on species that rely on leaf phenological cycles for their survival or reproduction. At very large scales, convergence in the physiological niche of evergreen or deciduous vegetation from biogeographically distinct realms suggests convergence on the same leaf habit in similar environments across different realms. Convergence implies that the relative advantages and disadvantages of different leaf habits in a given environment can be predicted from environmental data, so that once these advantages and disadvantages are quantified, a predictive model in which the outcome of future environmental scenarios can be evaluated is feasible. However, the work in this thesis also suggests that for nearly one third of the austral and tropical regions convergence might not apply, suggesting that both deciduous and evergreen leaf habits could be successful in these areas. At much smaller scales, species within a community were found to have largely overlapping growing seasons but considerably different leaf habits and leaf phenology. Overall, the findings in this thesis largely support convergence to a dominant leaf habit at large scales, but also provides evidence for divergent selection of leaf habit at large scales and certainly on smaller scales.

Non-convergence suggests that biotic interactions such as competition are likely to affect leaf habit.

Zusammenfassung

Der saisonale Einsatz und die Dauer des Blattaustriebs von Pflanzen haben maßgeblichen Einfluss auf den Austausch von Energie und Materie zwischen der Erdoberfläche und der Atmosphäre. Seit dem Devon hat die Ausbreitung von Wurzelbildenden Landpflanzen die Zusammensetzung der Atmosphäre und die globalen Kohlenstoff- und Nährstoffkreisläufe entscheidend beeinflusst. Auch heutzutage nehmen Landpflanzen noch immer eine Schlüsselrolle in verschiedenen Rückkopplungsprozessen ein die das Klima der Erde bestimmen. Pflanzen reduzieren die globale Energiebilanz durch die Fixierung von atmosphärischem Kohlenstoffdioxid durch die Photosynthese. Zusätzlich wird während der Photosynthese Wasserdampf in die Atmosphäre abgegeben, was global gesehen zu einer Abkühlung die Erdoberfläche beiträgt und gleichzeitig atmosphärische Prozess wie, zum Beispiel, die Wolkenbildung beeinflusst. Ein weiterer Einfluss von laubtragender Vegetation auf die globale Energiebilanz besteht darin, dass Blätter das Verhältnis zwischen absorbiertem und reflektiertem Sonnenlicht (die Albedo) verändern. Ob dabei die Albedo einer Fläche durch die Vegetation erhöht (also mehr Sonnenlicht reflektiert) oder verringert (also mehr Sonnenlicht absorbiert) wird, hängt von jeweiligen Vegetationstyp und der Art des Substrats ab. Alle hier genannten Prozessen durch die Vegetation die globale Energiebilanz, und damit das Klima, beeinflusst unterliegen Jahreszeitlichen Schwankungen, abhängig von Beginn und Länge des Blattaustriebs Da sich sowohl das Klima als auch der jahreszeitliche Beginn und die Länge des Blattaustriebs (die Blattphänologie) in den letzten Jahrzehnten geändert haben, ist ein genaues Verständnis der Mechanismen welche die Blattphänologie bestimmen, grundlegend um Veränderungen in der globalen Energiebilanz und dem globalen Kohlenstoffkreislaufs zwischen Erdoberfläche und Atmosphäre vorherzusagen.

Ein zusätzlicher Grund für die Erforschung von Veränderungen in der Blattphänologie besteht in der kumulativen Natur biotischer Abhängigkeiten. Beispielsweise können die Folgen für Nahrungsnetze verheerend sein, wenn Tierarten von der Verfügbarkeit von Blättern zu einer bestimmten Zeit abhängig sind, um ihren Reproduktionszyklus zu voll-

den. Durch Brüche in solchen zeitlichen Abhängigkeiten, kann sich die Austerbegefahr für betroffene Arten stark erhöhen. Zum Beispiel hängt das Schlüpfen der Raupen bestimmter Schmetterlingsarten direkt von dem Blattaustrieb ab. Während diese Arten durch die direkte Abhängigkeit flexibel auf Änderung im Einsetzen des Blattaustriebes reagieren können, könnte das Ankunftsdatum von Zugvögeln die auf die Raupen als Nahrung angewiesen sind zusätzliche von anderen Faktoren bestimmt werden und dadurch unflexibel sein. Dadurch entsteht eine zeitliche Diskrepanz zwischen Nahrungsverfügbarkeit und Nahrungsbedarf. Veränderungen in der zeitlichen Dynamik der Blattphänologie können des Weiteren Konkurrenzbeziehungen zwischen verschiedenen Pflanzenarten beeinflussen, was möglicherweise zu Änderungen in Struktur und Zusammensetzung von Artengemeinschaften führen.

Obwohl Untersuchungen der Blattphänologie von Europäischen und Nordamerikanischen Pflanzenarten einen deutlichen Zusammenhang zwischen Änderungen in der Blattphänologie und dem Klimawandel in den letzten Jahrzehnten gezeigt haben, steht eine großflächige Beurteilung des Ausmaßes und der Schwere der Änderungen weiterhin aus. Insbesondere die Südhalbkugel ist in bisherigen Studien weitestgehend unterrepräsentiert, obwohl Fernerkundungsdaten bis in die frühen 1980er Jahre verfügbar sind. In Kapitel 2 dieser Arbeit nehme ich diesen Mangel auf und benutze eine Zeitreihe des globalen "normalized difference vegetation index" (NDVI) der letzten 31 Jahre um Änderungen in der Blattphänologie in diesem Zeitraum zu quantifizieren. Änderungen im NDVI wurden für 21 Messwerte bestimmt. Diese Messwerte wurden durch "spline fit" durch die NDVI Zeitreihe mittels einer neuen Methode abgeleitet. Zusätzlich zur Quantifizierung der absoluten Veränderung, also des Blattaustriebs in Tagen, quantifiziere ich die relative Änderung in jedem Untersuchungsbereich (Pixel) in Form der Varianz der Änderung aller Untersuchungsbereiche die phänologisch identisch waren (Phänome). Dies erlaubt die Änderung in Einheiten der Standardabweichung auszudrücken. Durch eine Clusteranalyse bestimmt, wurden insgesamt 99 verschiedene Phänome bestimmt. Die Änderung jeder Messgröße in den Untersuchungsbereichen wurde durch globale Karten dargestellt die zeigen, dass die

Änderung der Blattphänologie auf über 54 % der Landoberfläche mehr als 2 Einheiten Standardabweichung für mindestens eine Messgröße beträgt. Durch das Zusammenfassen der 99 Phänome und mehr als 21 Messgrößen zu 9 globalen Klassen wird klar, dass verschiedenen Typen von Änderung räumliche Gruppierungen bilden. Über weite Flächen, zum Beispiel die boreale Zone, veränderte sich die Blattphänologie homogen, während die Änderung in anderen Teilen der Welt, z.B. West-Afrika, auch über kurze Distanz stark variiert. Die hier festgestellten Änderungen in der Blattphänologie stimmen mit den Ergebnissen vorangegangener regionaler Studien, durchgeführt hauptsächlich auf der Nordhalbkugel, überein. Gleichzeitig zeigt diese Studie auch substantielle Änderungen der Blattphänologie die bisher unbekannt waren, besonders auf der Südhalbkugel. Die mit 21 Messgrößen hohe phänologische Auflösung zeigte, dass qualitativ sehr unterschiedliche Änderungen der Blattphänologie zu quantitativ sehr ähnlichen Änderungen in zusammenfassenden Kennwerten, wie zum Beispiel die Länge der Wachstumsperiode oder der totalen Photosyntheseaktivität führen können. Dies bedeutet auch, dass ein gleichbleiben der Nettoprimärproduktion, einer in fernerkundlichen Studien oft verwendete Kennzahl, tatsächlich vorhandene Veränderungen der Phänologie nur unzureichend abbildet. Obwohl vorhergehende Studien einen klaren Zusammenhang zwischen Änderungen der Phänologie und dem Klimawandel sowie dem erhöhtem CO₂-Gehalt der Atmosphäre gezeigt haben, haben diese Studien ebenfalls deutlich gemacht, dass die Blattphänologie von einem komplizierten Zusammenspiel mehrere Faktoren abhängt. Eine Klärung der Ursachen der hier festgestellten Änderungen in der Phänologie ist sicherlich der nächste wichtige Schritt, aber um die komplizierten Prozesses zu verstehen, ist ein regionaler Ansatz geboten.

Kapitel 2 beschreibt Veränderungen im zeitlichen Beginn des Blattaustriebs und Blattabwurfs. Um den möglichen Einfluss des Global change auf die Verbreitung von immergrüner und laubwerfender Vegetation einschätzen zu können ist es unerlässlich die Mechanismen die Blattaustrieb und Blattabwurf steuern zu verstehen. Aktuelle Erklärungen für die geographische Verbreitung verschiedener Blattabwurfstrategien basieren auf der Annahme evolutionärer Konvergenz auf eine optimale Strategie, welche den Kohlenstoffgewinn

in einer gegebenen Umgebung maximiert. In Kapitel 3 untersuche ich diese Konvergenz durch Quantifizierung der physiologischen Nische immergrüner und laubabwerfender Vegetation in vier biogeographischen Reichen, und berechne zusätzlich “niche overlap” und “niche similarity” von immergrüner und laubwerfender Vegetation in diesen Reichen. Ein großer niche overlap und große niche similarity, also eine große Ähnlichkeit der Nische, deuten auf eine Konvergenz der physiologischen Nische hin. Zunächst definiere ich die geographische Verbreitung eines laubabwerfenden und zweier immergrünen Phänome, um zwischen immergrünen Wäldern mit geschlossenem Kronendach und spärlicher buscharziger Vegetation zu unterscheiden. Um die physiologische Nische jedes dieser Phänome in jedem biogeographischen Reich zu charakterisieren simuliere ich Pflanzenwachstum mit Hilfe eines prozessbasierenden Modells. Mit Hilfe dieses Modells wird das Pflanzenwachstum als Funktion von Respiration, Kohlenstoffaufnahme durch den oberirdischen Pflanzenteil, Stickstoffaufnahme durch die Wurzeln und den Transport von Ressourcen zwischen den unterschiedlichen Pflanzenkompartimenten simuliert. Jeder dieser physiologischen Prozesse ist abhängig von verschiedenen Umweltfaktoren, welche für diese Studie von globalen Daten abgeleitet wurden. Dies bedeutet zum Beispiel, dass die Kohlenstoffaufnahme durch die Sonneneinstrahlung begrenzt und außerdem von der Außentemperatur abhängig ist. Das Modell ermöglichte eine Vorhersage der richtigen Ausbreitung der Phänome mit 81%iger Genauigkeit, was darauf hindeutet, dass das Modell die physiologische Nische der Phänome akkurat beschreibt. In dieser Studie habe ich den niche overlap zwischen jeweils vergleichbaren Phänomenen aus den unterschiedlichen biogeographischen Reichen getestet. Dazu wurde die potentielle Verbreitung jedes Phänoms in allen anderen biogeographischen Reichen simuliert und die Schnittmenge der geographischen Ausbreitung bestimmt. In 71 % des Untersuchungsgebietes sagen Simulationen von alle vier Reichen dasselbe Phänom voraus. Dies deutet auf eine hohe Konvergenz der Phänome hin. Die verbleibenden 29%, in denen sich die Verbreitung der Phänome zwischen den Reichen unterschieden, deuten höchstwahrscheinlich darauf hin, dass der Phänom-typ in diesen Regionen unsicher ist. Dies ist möglicherweise auf historischen Gegebenheiten oder auf “alternative stable

states”, also der Tatsache das unter den gegebenen Bedingungen mehrere Phänome ökologisch möglich sind zurückzuführen. Die Ergebnisse dieses Kapitels deuten darauf hin, dass evolutionäre Konvergenz eine wichtige Rolle in der Biogeographie von Blattabwurfstrategien (immergrün/laubwerfend) spielt, aber sie zeigen auch, dass in weiten Teilen der Welt andere Faktoren wichtig sind. Diese Faktoren werden wahrscheinlich Auswirkungen auf die Veränderung der geographischen Verbreitung der verschiedenen Blattabwurfstrategien im Rahmen des “global change” haben.

Nachdem ich in Kapitel 2 globale Änderungen der Blattphänologie und in Kapitel 3 die Verbreitung immergrüner und laubwerfender Vegetation erörtert habe, wähle ich in Kapitel 4 einen übergeordneten Ansatz und untersuche die Zusammenhänge zwischen Blattabwurfstrategie, Blattphänologie und anderen funktionellen Merkmalen die den Kohlenstoffhaushalt von Pflanzen beeinflussen, basierend auf empirischen Daten. In diesem Kapitel untersuche ich Blattphänologie und Blattabwurfstrategie von neun verschiedenen Gehölzarten in einer von Regen- und Trockenzeit geprägten Savanne in Südafrika. Messungen der Blattphänologie beruhen auf NDVI Messungen die mit Hilfe eines Oberflächen-nahen UAV (Unmanned Aerial Vehicle) durchgeführt wurden, die Messungen zur Blattabwurfstrategie beruhen auf Daten zur Blattlebensdauer, die mit Hilfe von im Feld markierten Blättern ermittelt wurde. Die Blattlebensdauer schwankte zwischen 5 und 18 Monaten je nach Art, sowohl für laubwerfende als auch für immergrüne Arten. Die Blattphänologie schwankte ebenfalls stark zwischen den untersuchten Arten. Das hier gefundene Verhältnis zwischen Blattlebensdauer, Photosynthese- und Stoffwechselrate und das Blattmasse:Blattfläche-Verhältnis stimmen mit Literaturwerten überein. Ein Merkmal von besonderem Interesse ist der “marginal water cost of carbon gain” ($\frac{\delta E}{\delta A} = \lambda$). Dieser Wert gibt die Menge Wasser an die benötigt wird um eine bestimmte Menge Kohlenstoff zu fixieren. Hier schätze ich λ mit Hilfe eines existierenden Modells für Stomata-Durchlässigkeit. Interessanterweise, wurde hier kein Zusammenhang zwischen Stomataöffnung und Blattphänologie oder Blattabwurfstrategie gefunden. Dies ist überraschend, da das saisonale Klima im Untersuchungsgebiet einen Zusammenhang zwischen Wasserverfügbarkeit und Blattabwurfstra-

ategie nahelegt. In einer weiterführenden Analyse benutze ich die gesammelten Daten zu Blattphänologie, Bodenfeuchte, Photosynthese- und Stoffwechselrate und λ um die Kohlenstoffbilanz für jede der neun Arten zu modellieren. Der errechnet jährliche Kohlenstoffgewinn schwankte um mehr als das fünffache zwischen den untersuchten Arten und war am niedrigsten in immergrünen Arten. Des Weiteren zeigte der Kohlenstoffgewinn eine schwache Abhängigkeit von Blattabwurfstrategie und Blattphänologie. Die großen Unterschiede in Blattabwurfstrategie, Blattphänologie und Kohlenstoffbilanz im Untersuchungsgebiet deuten darauf hin, dass eine optimale Anpassung dieser Merkmale an die saisonale Umgebung durch Faktoren mit entgegengesetztem Selektionsdruck verhindert wird.

In dieser Arbeit untersuche ich Veränderungen der Blattphänologie und die globale Verbreitung von Blattabwurfstrategien. Dies ist von besonderem Interesse, da diese beiden Merkmale entscheidend an der Regulation der Biosphäre beteiligt sind. Ich zeige schwerwiegenden Änderungen in der Blattphänologie über die letzten drei Dekaden für weite Teile der Erdoberfläche auf. Diese Änderungen werden wahrscheinlich substantiellen Einfluss auf die Überlebensfähigkeit von Arten haben, die für ihr Überleben oder ihre Fortpflanzung von einer gleichbleibenden Blattphänologie abhängig sind. Auf globaler Ebene deutet die Konvergenz der physiologischen Nische von immergrüner und laubwerfender Vegetation aus verschiedenen biogeographischen Reichen auf eine Konvergenz gleicher Blattabwurfstrategien unter ähnlichen Umgebungsbedingungen hin. Eine solche Konvergenz impliziert, dass Vor- und Nachteile verschiedener Blattabwurfstrategien vorhersehbar sind. Dies bedeutet, dass sobald diese Vor- und Nachteile bekannt sind ein Model entwickelt werden kann, welches die geographische Verbreitung von Blattabwurfstrategien unter zukünftigen klimatischen Bedingungen vorhersagt. Allerdings zeigen die hier dargelegten Ergebnisse auch, dass eine solche Konvergenz in weiten Teilen der Tropen und der Südhalbkugel nicht zutrifft. Unter gegebenen Umweltbedingungen können immergrüne und laubwerfende Pflanzenarten in diesen Regionen gleichermaßen erfolgreich sein können, oder aber die Verbreitung der Blattabwurfstrategien ist dort maßgeblich von historischen Gegebenheiten

abhängig. Auf lokaler Ebene hatten Arten einer Artengemeinschaft größtenteils überlappende Wachstumsperioden, unterschieden sich aber deutlich in Blattabwurfstrategie und Blattphänologie. Insgesamt unterstützen die Ergebnisse dieser Arbeit die Hypothese einer großräumigen Konvergenz auf eine Blattabwurfstrategie unter gegebenen Umweltbedingungen, aber liefern auch Beweise für eine divergente Selektion in großem und kleinem Maßstab. Divergenz deutet darauf hin, dass biotische Interaktionen in Modelle für Blattabwurfstrategien miteinbezogen werden sollten.

Bibliography

- Ackerly, D. (1999). Self-shading, carbon gain and leaf dynamics: a test of alternative optimality models. *Oecologia*, 119, 300–310.
- Aerts, R. (1995). The advantages of being evergreen. *Trends in Ecology & Evolution*, 10, 402–407.
- Ainsworth, E.A. & Long, S.P. (2005). What have we learned from 15 years of free-air CO₂ enrichment (FACE)? A meta-analytic review of the responses of photosynthesis, canopy properties and plant production to rising CO₂. *New Phytologist*, 165, 351–372.
- Ainsworth, E.A. & Rogers, A. (2007). The response of photosynthesis and stomatal conductance to rising [CO₂]: mechanisms and environmental interactions. *Plant, Cell and Environment*, 30, 258–270.
- Al-Mufti, M.M., Sydes, C.L., Furness, S.B., Grime, J.P. & Band, S.R. (1977). A quantitative analysis of shoot phenology and dominance in herbaceous vegetation. *Journal of Ecology*, 65, 759–791.
- Archer, S., Boutton, T.W. & Hibbard, K.A. (2001). Trees in grasslands: biogeochemical consequences of woody plant expansion. In: *Global Biogeochemical Cycles in the Climate System* (eds. Schulze, E.D., Heimann, M., Harrison, S., Holland, E., Lloyd, J., Prentice, I.C. & Schimel, D.). Academic Press, chap. 9, pp. 115–137.
- Archibald, S. & Scholes, R.J. (2007). Leaf green-up in a semi-arid African savanna - separating tree and grass responses to environmental cues. *Journal of Vegetation Science*, 18, 583–594.
- Ardia, D., Mullen, K.M., Peterson, B.G. & Ulrich, J. (2013). *DEoptim: Differential Evolution in R*. Version 2.2-2.
- Assouline, S., Tessier, D. & Bruand, A. (1998). A conceptual model of the soil water retention curve. *Water Resources Research*, 34, 223–231.

- Baldocchi, D.D., Xu, L. & Kiang, N. (2004). How plant functional-type, weather, seasonal drought, and soil physical properties alter water and energy fluxes of an oak-grass savanna and an annual grassland. *Agricultural and Forest Meteorology*, 123, 13–39.
- Ball, J.T., Woodrow, I.E. & Berry, J.A. (1987). A model predicting stomatal conductance and its contribution to the control of photosynthesis under different environmental conditions. *Progress in Photosynthesis Research*, IV, 221–224.
- Bartholomé, E. & Belward, A.S. (2005). GLC2000: a new approach to global land cover mapping from Earth observation data. *International Journal of Remote Sensing*, 26, 1959–1977.
- Beerling, D.J. (2005). Leaf evolution: Gases, genes and geochemistry. *Annals of Botany*, 96, 345–352.
- Beerling, D.J. (2007). *The Emerald Planet*. Oxford University Press, Oxford.
- Beerling, D.J. & Osborne, C.P. (2006). The origin of the savanna biome. *Global Change Biology*, 12, 2023–2031.
- Beerling, D.J., Osborne, C.P. & Chaloner, W.G. (2001). Evolution of leaf-form in land plants linked to atmospheric CO₂ decline in the late Palaeozoic era. *Nature*, 410, 352–354.
- Berner, R.A. (1997). The rise of plants and their effect on weathering and atmospheric CO₂. *Science*, 276, 544–546.
- Berner, R.A. (1998). The carbon cycle and carbon dioxide over Phanerozoic time: the role of land plants. *Philosophical Transactions of the Royal Society B: Biological Sciences*, 353, 75–82.
- Biggs, R., Biggs, H.C., Dunne, T.T., Govender, N. & Potgieter, A.L.F. (2003). Experimental burn plot trial in the Kruger National Park: history, experimental design and suggestions for data analysis. *Koedoe*, 46, 1–15.
- Bonan, G.B. (2008). Forests and climate change: forcings, feedbacks, and the climate benefits of forests. *Science*, 320, 1444–1449.
- Bond, W.J. (2008). What Limits Trees in C4 Grasslands and Savannas? *Annual Review of Ecology, Evolution, and Systematics*, 39, 641–659.
- Bond, W.J., Cook, G.D. & Williams, R.J. (2012). Which trees dominate in savannas? The escape hypothesis and eucalypts in northern Australia. *Austral Ecology*, 37, 678–685.

- Bond, W.J., Woodward, F.I. & Midgley, G.F. (2005). The global distribution of ecosystems in a world without fire. *New Phytologist*, 165, 525–538.
- Borchert, R. (1994). Soil and stem water storage determine phenology and distribution of tropical dry forest trees. *Ecology*, 75, 1437–1449.
- Both, C., Bouwhuis, S., Lessells, C.M. & Visser, M.E. (2006). Climate change and population declines in a long-distance migratory bird. *Nature*, 441, 81–83.
- Bouma, J. (1989). Using soil survey data for quantitative land evaluation. In: *Advances in Soil Science* (ed. Stewart, B.A.). Springer-Verlag, New York, vol. 9 of *Advances in Soil Science*, pp. 177–213.
- Bouyoucos, G.J. (1962). Hydrometer method improved for making particle size analyses of Soils. *Agronomy Journal*, 54, 464–465.
- Bowman, D.M.J.S., Balch, J.K., Artaxo, P., Bond, W.J., Carlson, J.M., Cochrane, M.A., D’Antonio, C.M., DeFries, R.S., Doyle, J.C., Harrison, S.P., Johnston, F.H., Keeley, J.E., Krawchuk, M.A., Kull, C.A., Marston, J.B., Moritz, M.A., Prentic, I.C., Roos, C.I., Scott, A.C., Swetnam, T.W., van der Werf, G.R. & Pyne, S.J. (2009). Fire in the Earth system. *Science*, 324, 481–484.
- Bowman, D.M.J.S., Brown, G.K., Braby, M.F., Brown, J.R., Cook, L.G., Crisp, M.D., Ford, F., Haberle, S., Hughes, J., Isagi, Y., Joseph, L., McBride, J., Nelson, G. & Ladiges, P.Y. (2010). Biogeography of the Australian monsoon tropics. *Journal of Biogeography*, 37, 201–216.
- Bowman, D.M.J.S. & Prior, L.D. (2005). TURNER REVIEW No. 10. Why do evergreen trees dominate the Australian seasonal tropics? *Australian Journal of Botany*, 53, 379–399.
- Box, E.O. (1996). Plant functional types and climate at the global scale. *Journal of Vegetation Science*, 7, 309–320.
- Broennimann, O., Fitzpatrick, M.C., Pearman, P.B., Petitpierre, B., Pellissier, L., Yoccoz, N.G., Thuiller, W., Fortin, M.J., Randin, C., Zimmermann, N.E., Graham, C.H. & Guisan, A. (2012). Measuring ecological niche overlap from occurrence and spatial environmental data. *Global Ecology and Biogeography*, 21, 481–497.
- Buitenwerf, R., Bond, W.J., Stevens, N. & Trollope, W.S.W. (2012). Increased tree densities in South African savannas: >50 years of data suggests CO₂ as a driver. *Global Change Biology*, 18, 675–684.

- Buitenwerf, R., Kulmatiski, A. & Higgins, S.I. (2014). Soil water retention curves for the major soil types of the Kruger National Park. *Koedoe*, 56, 1–9.
- Buitenwerf, R., Rose, L. & Higgins, S. (2015). Three decades of multi-dimensional change in global leaf phenology. *Nature Climate Change*, In Print.
- Carrascal, L.M., Galván, I. & Gordo, O. (2009). Partial least squares regression as an alternative to current regression methods used in ecology. *Oikos*, 118, 681–690.
- Chabot, B.F. & Hicks, D.J. (1982). The ecology of leaf life spans. *Annual Review of Ecology and Systematics*, 13, 229–259.
- Chave, J., Coomes, D., Jansen, S., Lewis, S.L., Swenson, N.G. & Zanne, A.E. (2009). Towards a worldwide wood economics spectrum. *Ecology Letters*, 12, 351–66.
- Chen, I.c., Hill, J., Ohlemüller, R., Roy, D.B. & Thomas, C.D. (2011). Rapid range shifts of species associated with high levels of climate warming. *Science*, 333, 1024–1026.
- Chesson, P.L. (2000). Mechanisms of maintenance of species diversity. *Annual Review of Ecology and Systematics*, 31, 343–358.
- Chesson, P.L. & Warner, R.R. (1981). Environmental variability promotes coexistence in lottery competitive systems. *The American Naturalist*, 117, 923–943.
- Chielewski, F.M. (2013). *Phenology: An Integrative Environmental Science*, Springer, Dordrecht, chap. Phenology in agriculture and horticulture, pp. 539–261. 2nd edn.
- Chuine, I., Morin, X. & Bugmann, H. (2010). Warming, photoperiods, and tree phenology. *Science*, 329, 277–278.
- Ciais, P., Reichstein, M., Viovy, N., Granier, A., Ogée, J., Allard, V., Aubinet, M., Buchmann, N., Bernhofer, C., Carrara, A., Chevallier, F., De Noblet, N., Friend, A.D., Friedlingstein, P., Grünwald, T., Heinesch, B., Keronen, P., Knohl, A., Krinner, G., Loustau, D., Manca, G., Matteucci, G., Miglietta, F., Ourcival, J.M., Papale, D., Pilegaard, K., Rambal, S., Seufert, G., Soussana, J.F., Sanz, M.J., Schulze, E.D., Vesala, T. & Valentini, R. (2005). Europe-wide reduction in primary productivity caused by the heat and drought in 2003. *Nature*, 437, 529–533.
- Cianciaruso, M.V., Silva, I.A., Manica, L.T. & Souza, J.a.P. (2013). Leaf habit does not predict leaf functional traits in cerrado woody species. *Basic and Applied Ecology*, 14, 404–412.

- Cleland, E., Chiariello, N., Loarie, S., Mooney, H. & Field, C. (2006). Diverse responses of phenology to global changes in a grassland ecosystem. *Proceedings of the National Academy of Sciences of the United States of America*, 103, 13740–13744.
- Cleland, E.E., Chuine, I., Menzel, A., Mooney, H.a. & Schwartz, M.D. (2007). Shifting plant phenology in response to global change. *Trends in Ecology and Evolution*, 22, 357–365.
- Cowan, I. & Farquhar, G.D. (1977). Stomatal function in relation to leaf metabolism and environment. In: *Integration of activity in the higher plant* (ed. Jennings, D.). Cambridge University Press, Cambridge, pp. 471–505.
- Cox, B. (2001). The biogeographic regions reconsidered. *Journal of Biogeography*, 28, 511–523.
- Craine, J.M. (2009). *Resource Strategies of Wild Plants*. Princeton University Press, Princeton.
- Davies, T.J., Wolkovich, E.M., Kraft, N.J.B., Salamin, N., Allen, J.M., Ault, T.R., Betancourt, J.L., Bolmgren, K., Cleland, E.E., Cook, B.I., Crimmins, T.M., Mazer, S.J., McCabe, G.J., Pau, S., Regetz, J., Schwartz, M.D. & Travers, S.E. (2013). Phylogenetic conservatism in plant phenology. *Journal of Ecology*, 101, 1520–1530.
- DeFries, R.S., Hansen, M.C., Townshend, J.R.G., Janetos, A.C. & Loveland, T.R. (2000). A new global 1-km dataset of percentage tree cover derived from remote sensing. *Global Change Biology*, 6, 247–254.
- DeFries, R.S., Townshend, J.R.G. & Hansen, M.C. (1999). Continuous fields of vegetation characteristics at the global scale at 1-km resolution. *Journal of Geophysical Research*, 104, 16911–16923.
- Donohue, R.J., McVicar, T.R. & Roderick, M.L. (2009). Climate-related trends in Australian vegetation cover as inferred from satellite observations, 1981–2006. *Global Change Biology*, 15, 1025–1039.
- Dormann, C.F., Schymanski, S.J., Cabral, J., Chuine, I., Graham, C., Hartig, F., Kearney, M., Morin, X., Römermann, C., Schröder, B. & Singer, A. (2012). Correlation and process in species distribution models: bridging a dichotomy. *Journal of Biogeography*, 39, 2119–2131.
- Dwyer, E., Pereira, J., Grégoire, J.M. & DaCamara, C.C. (2000). Characterization of the spatio-temporal patterns of global fire activity using satellite imagery for the period April 1992 to March 1993. *Journal of Biogeography*, 27, 57–69.

- Eamus, D. (1999). Ecophysiological traits of deciduous and evergreen woody species in the seasonally dry tropics. *Trends in Ecology & Evolution*, 14, 11–16.
- Eamus, D. & Prior, L.D. (2001). Ecophysiology of trees of seasonally dry tropics: comparisons among phenologies. *Advances in Ecological Research*, 32, 113–197.
- Ellis, E.C. & Ramankutty, N. (2008). Putting people in the map: anthropogenic biomes of the world. *Frontiers in Ecology and the Environment*, 6, 439–447.
- Farquhar, G.D., von Caemmerer, S. & Berry, J.A. (1980). A biochemical model of photosynthetic CO₂ assimilation in leaves of C₃ species. *Planta*, 149, 78–90.
- Field, C.B., Jackson, R.B. & Mooney, H.A. (1995). Stomatal responses to increased CO₂: implications from the plant to the global scale. *Plant, Cell and Environment*, 18, 1214–1225.
- Flato, G.J., Marotzke, J., Abiodun, B., Braconnot, P., Chou, S.C., Collins, W., Cox, P., Driouech, F., Emori, S., Eyring, V., Forest, C., Gleckler, P., Guilyardi, E., Jakob, C., Kattsov, V., Reason, C. & Rummukainen, M. (2013). Evaluation of climate models. In: *Climate Change 2013: The Physical Science Basis. Contribution of Working Group I to the Fifth Assessment Report of the Intergovernmental Panel on Climate Change* (eds. Stocker, T.F., Qin, D., Plattner, G.K., Tignor, M., Allen, S.K., Boschung, J., Nauels, A., Xia, Y., Bex, V. & Midgley, P.M.). Cambridge University Press, Cambridge, chap. 9, pp. 741–866.
- Foley, J.a., Coe, M.T., Scheffer, M. & Wang, G. (2003). Regime Shifts in the Sahara and Sahel: Interactions between Ecological and Climatic Systems in Northern Africa. *Ecosystems*, 6, 524–532.
- Fraley, C. & Raftery, A.E. (2002). Model-based clustering, discriminant analysis, and density estimation. *Journal of the American Statistical Association*, 97, 611–631.
- Fraley, C., Raftery, A.E., Murphy, T.B. & Scrucca, L. (2012). *mclust Version 4 for R: Normal Mixture Modeling for Model-Based Clustering, Classification, and Density Estimation*.
- Fredlund, D.G. & Xing, A. (1994). Equations for the soil-water characteristic curve. *Canadian Geotechnical Journal*, 31, 521–532.
- Freedman, J.M., Fitzjarrald, D.R., Moore, K.E. & Sakai, R.K. (2001). Boundary layer clouds and vegetation-atmosphere feedbacks. *Journal of Climate*, 14, 180–197.

- Fridley, J.D. (2012). Extended leaf phenology and the autumn niche in deciduous forest invasions. *Nature*, 485, 359–362.
- Friedl, M., McIver, D., Hodges, J., Zhang, X., Muchoney, D., Strahler, A., Woodcock, C., Gopal, S., Schneider, A., Cooper, A., Baccini, A., Gao, F. & Schaaf, C. (2002). Global land cover mapping from MODIS: algorithms and early results. *Remote Sensing of Environment*, 83, 287–302.
- van Genuchten, M.T. (1980). A Closed-form Equation for Predicting the Hydraulic Conductivity of Unsaturated Soils. *Soil Science Society of America Journal*, 44, 892–898.
- Givnish, T.J. (1986). Optimal stomatal conductance, allocation of energy between leaves and roots, and the marginal cost of transpiration. In: *On the economy of plant form and function* (ed. Givnish, T.J.). Cambridge University Press, Cambridge, pp. 171–213.
- Givnish, T.J. (2002). Adaptive significance of evergreen vs. deciduous leaves: solving the triple paradox. *Silva Fennica*, 36, 703–743.
- Global Soil Data Task Group (2000). *Global Gridded Surfaces of Selected Soil Characteristics (IGBP-DIS)*. International Geosphere Biosphere Programme - Data and Information System, Oak Ridge National Laboratory, Oak Ridge, Tennessee, U.S.A.
- Goldstein, G., Meinzer, F.C., Bucci, S.J., Scholz, F.G., Franco, A.C. & Hoffmann, W.A. (2008). Water economy of Neotropical savanna trees: six paradigms revisited. *Tree Physiology*, 28, 395–404.
- Govender, N., Trollope, W.S.W. & Van Wilgen, B.W. (2006). The effect of fire season, fire frequency, rainfall and management on fire intensity in savanna vegetation in South Africa. *Journal of Applied Ecology*, 43, 748–758.
- Grime, J.P. (1977). Evidence for the existence of three primary strategies in plants and its relevance to ecological and evolutionary theory. *American Naturalist*, 111, 1169–1194.
- Guisan, A. & Thuiller, W. (2005). Predicting species distribution: offering more than simple habitat models. *Ecology Letters*, 8, 993–1009.
- Haxeltine, A. & Prentice, I.C. (1996). BIOME3: An equilibrium terrestrial biosphere model based on ecophysiological constraints, resource availability, and competition among plant functional types. *Global Biogeochemical Cycles*, 10, 693–709.
- Higgins, S.I., Bond, W.J., Combrink, H.J., Craine, J.M., February, E.C., Govender, N., Lannas, K., Moncreiff, G. & Trollope, W.S.W. (2012a). Which traits determine shifts

- in the abundance of tree species in a fire-prone savanna? *Journal of Ecology*, 100, 1400–1410.
- Higgins, S.I., Bond, W.J., February, E.C., Bronn, A., Euston-Brown, D.I.W., Enslin, B., Govender, N., Rademan, L., O'Reagan, S., Potgieter, A.L.F., Scheiter, S., Sowry, R., Trollope, L. & Trollope, W.S.W. (2007). Effects of four decades of fire manipulation on woody vegetation structure in savanna. *Ecology*, 88, 1119–1125.
- Higgins, S.I., Delgado-Cartay, M.D., February, E.C. & Combrink, H.J. (2011). Is there a temporal niche separation in the leaf phenology of savanna trees and grasses? *Journal of Biogeography*, 38, 2165–2175.
- Higgins, S.I., Keretsetse, M. & February, E.C. (2015). Feedback of trees on nitrogen mineralisation to restrict the advance of trees in c_4 savannas. *Submitted*.
- Higgins, S.I., O'Hara, R.B., Bykova, O., Cramer, M.D., Chuine, I., Gerstner, E.M., Hickler, T., Morin, X., Kearney, M.R., Midgley, G.F. & Scheiter, S. (2012b). A physiological analogy of the niche for projecting the potential distribution of plants. *Journal of Biogeography*, 39, 2132–2145.
- Higgins, S.I. & Scheiter, S. (2012). Atmospheric CO₂ forces abrupt vegetation shifts locally, but not globally. *Nature*, 488, 209–212.
- Hijmans, R.J., Cameron, S.E., Parra, J.L., Jones, P.G. & Jarvis, A. (2005). Very high resolution interpolated climate surfaces for global land areas. *International Journal of Climatology*, 25, 1965–1978.
- IPCC (2013). Summary for Policymakers. In: *Climate Change 2013: The Physical Science Basis. Contribution of Working Group I to the Fifth Assessment Report of the Intergovernmental Panel on Climate Change* (eds. Stocker, T.F., Qin, D., Plattner, G.K., Tignor, M., Allen, S.K., Boschung, J., Nauels, A., Xia, Y., Bex, V. & Midgley, P.M.). Cambridge University Press, Cambridge, pp. 3–29.
- de Jong, R., Verbesselt, J., Schaepman, M.E. & de Bruin, S. (2012). Trend changes in global greening and browning: contribution of short-term trends to longer-term change. *Global Change Biology*, 18, 642–655.
- Keeling, C.D., Chin, J.F.S. & Whorf, T.P. (1996). Increased activity of northern vegetation inferred from atmospheric CO₂ measurements. *Nature*, 382, 146–149.
- Kelly, A.E. & Goulden, M.L. (2008). Rapid shifts in plant distribution with recent climate change. *Proceedings of the National Academy of Sciences of the United States of America*, 105, 11823–11826.

- Kenrick, P. & Crane, P.R. (1997). The origin and early evolution of plants on land. *Nature*, 389, 33–39.
- Kikuzawa, K. (1991). A cost-benefit analysis of leaf habit and leaf longevity of trees and their geographical pattern. *American Naturalist*, 138, 1250–1263.
- Kikuzawa, K. & Ackerly, D. (1999). Significance of leaf longevity in plants. *Plant Species Biology*, 14, 39–45.
- Kikuzawa, K. & Lechowicz, M. (2011). *Ecology of leaf longevity*. Springer, Tokyo.
- Körner, C. (2006). Plant CO₂ responses: an issue of definition, time and resource supply. *New Phytologist*, 172, 393–411.
- Körner, C. & Basler, D. (2010). Phenology under global warming. *Science*, 327, 1461–1462.
- Lambers, H., Chapin III, F.S. & Pons, T.L. (2008). *Plant Physiological Ecology*. Springer, New York.
- Larcher, W. (2003). *Physiological Plant Ecology*. 4th edn. Springer, Berlin.
- Lehmann, C.E.R., Anderson, T.M., Sankaran, M., Higgins, S.I., Archibald, S., Hoffmann, W.A., Hanan, N.P., Williams, R.J., Fensham, R.J., Felfili, J., Hutley, L.B., Ratnam, J., San Jose, J., Montes, R., Franklin, D., Russell-Smith, J., Ryan, C.M., Durigan, G., Hiernaux, P., Haidar, R., Bowman, D.M.J.S. & Bond, W.J. (2014). Savanna vegetation-fire-climate relationships differ among continents. *Science*, 343, 548–552.
- Leuning, R. (1995). A critical appraisal of a combined stomatal-photosynthesis model for C₃ plants. *Plant, Cell & Environment*, 18, 339–355.
- Linder, H.P., de Klerk, H.M., Born, J., Burgess, N.D., Fjeldså, J. & Rahbek, C. (2012). The partitioning of Africa: statistically defined biogeographical regions in sub-Saharan Africa. *Journal of Biogeography*, 39, 1189–1205.
- Lloyd, J. & Farquhar, G.D. (1994). ¹³C discrimination during CO₂ assimilation by the terrestrial biosphere. *Oecologia*, 99, 201–215.
- Long, S.P., Ainsworth, E.A., Rogers, A. & Ort, D.R. (2004). Rising atmospheric carbon dioxide: plants FACE the future. *Annual Review of Plant Biology*, 55, 591–628.
- Ma, X., Huete, A., Yu, Q., Coupe, N.R., Davies, K., Broich, M., Ratana, P., Beringer, J., Hutley, L.B., Cleverly, J., Boulain, N. & Eamus, D. (2013). Spatial patterns and temporal dynamics in savanna vegetation phenology across the North Australian Tropical Transect. *Remote Sensing of Environment*, 139, 97–115.

- MacArthur, R. & Levins, R. (1967). The limiting similarity, convergence, and divergence of coexisting species. *American Naturalist*, 101, 377–385.
- Medlyn, B.E., Duursma, R.A., Eamus, D., Ellsworth, D.S., Colin Prentice, I., Barton, C.V.M., Crous, K.Y., de Angelis, P., Freeman, M. & Wingate, L. (2012). CORRIGENDUM - Reconciling the optimal and empirical approaches to modelling stomatal conductance. *Global Change Biology*, 18, 3476–3476.
- Medlyn, B.E., Duursma, R.A., Eamus, D., Ellsworth, D.S., Prentice, I.C., Barton, C.V.M., Crous, K.Y., De Angelis, P., Freeman, M. & Wingate, L. (2011). Reconciling the optimal and empirical approaches to modelling stomatal conductance. *Global Change Biology*, 17, 2134–2144.
- Menzel, A. (2013a). Europe. In: *Phenology: An Integrative Environmental Science* (ed. Schwartz, M.D.). Springer, Dordrecht, chap. 4, pp. 53–65. 2nd edn.
- Menzel, A. (2013b). *Phenology: An Integrative Environmental Science*, Springer, Dordrecht, chap. Plant phenological "fingerprints", pp. 335–350. 2nd edn.
- Menzel, A. & Fabian, P. (1999). Growing season extended in Europe. *Nature*, 397, 659.
- Menzel, A., Sparks, T.H., Estrella, N., Koch, E., Aasa, A., Ahas, R., Alm-Kübler, K., Bissolli, P., Braslavská, O., Briede, A., Chmielewski, F.M., Crepinsek, Z., Curnel, Y., Dahl, A.s., Defila, C., Donnelly, A., Filella, Y., Jatczak, K., Måge, F., Mestre, A., Nordli, Ø., Peñuelas, J., Pirinen, P., Remišová, V., Scheifinger, H., Striz, M., Susnik, A., van Vliet, A.J.H., Wielgolaski, F.E., Zach, S. & Züst, A. (2006). European phenological response to climate change matches the warming pattern. *Global Change Biology*, 12, 1969–1976.
- Merbold, L., Ardö, J., Arneth, A., Scholes, R.J., Nouvellon, Y., de Grandcourt, A., Archibald, S., Bonnefond, J.M., Boulain, N., Brueggemann, N., Bruemmer, C., Cappelare, B., Ceschia, E., El-Khidir, H.A.M., El-Tahir, B.A., Falk, U., Lloyd, J., Kergoat, L., Le Dantec, V., Mougín, E., Muchinda, M., Mukelabai, M.M., Ramier, D., Roupsard, O., Timouk, F., Veenendaal, E.M. & Kutsch, W.L. (2009). Precipitation as driver of carbon fluxes in 11 African ecosystems. *Biogeosciences*, 6, 1027–1041.
- Mevik, B.H. & Wehrens, R. (2007). The pls package: principal component and partial least squares regression in R. *Journal of Statistical Software*, 18, 1–24.
- Moncrieff, G.R., Hickler, T. & Higgins, S.I. (2014a). Intercontinental divergence in the climate envelope of major plant biomes. *Global Ecology and Biogeography*, p. DOI: 10.1111/geb.12257.

- Moncrieff, G.R., Lehmann, C.E.R., Schnitzler, J., Gambiza, J., Hiernaux, P., Ryan, C.M., Shackleton, C.M., Williams, R.J. & Higgins, S.I. (2014b). Contrasting architecture of key African and Australian savanna tree taxa drives intercontinental structural divergence. *Global Ecology and Biogeography*, 23, 1235–1244.
- Moncrieff, G.R., Scheiter, S., Bond, W.J. & Higgins, S.I. (2014c). Increasing atmospheric CO₂ overrides the historical legacy of multiple stable biome states in Africa. *New Phytologist*, 201, 908–915.
- Monserud, R.A. & Leemans, R. (1992). Comparing global vegetation maps with the Kappa statistic. *Ecological Modelling*, 62, 275–293.
- Mooney, H.A. & Dunn, E.L. (1970a). Convergent evolution of Mediterranean-climate evergreen sclerophyll shrubs. *Evolution*, 24, 292–303.
- Mooney, H.A. & Dunn, E.L. (1970b). Photosynthetic systems of mediterranean-climate shrubs and trees of California and Chile. *American Naturalist*, 104, 447–453.
- Morgan, J.A., Milchunas, D.G., LeCain, D.R., West, M. & Mosier, A.R. (2007). Carbon dioxide enrichment alters plant community structure and accelerates shrub growth in the shortgrass steppe. *Proceedings of the National Academy of Sciences of the United States of America*, 104, 14724–9.
- Morin, X., Lechowicz, M.J., Augspurger, C., O’Keefe, J., Viner, D. & Chuine, I. (2009). Leaf phenology in 22 North American tree species during the 21st century. *Global Change Biology*, 15, 961–975.
- Mullen, K.M., Ardia, D., Gil, D.L., Windover, D. & Cline, J. (2011). DEoptim: An R package for global optimization by differential evolution. *Journal of Statistical Software*, 40, 1–26.
- Myhre, G., Shindell, D., Breon, F.M., Collins, W., Fuglestedt, J., Huang, J., Koch, D., Lamarque, J.F., Lee, D., Mendoza, B., Nakajima, T., Robock, A., Stephens, G., Takemura, T. & Zhang, H. (2013). Anthropogenic and Natural Radiative Forcing. In: *Climate Change 2013: The Physical Science Basis. Contribution of Working Group I to the Fifth Assessment Report of the Intergovernmental Panel on Climate Change* (eds. Stocker, T., Qin, D., Plattner, G.K., Tignor, M., Allen, S., Boschung, J., Nauels, A., Xia, Y., Bex, V. & Midgley, P.). Cambridge University Press, Cambridge, chap. 8, pp. 659–740.

- Nemani, R.R., Keeling, C.D., Hashimoto, H., Jolly, W.M., Piper, S.C., Tucker, C.J., Myneni, R.B. & Running, S.W. (2003). Climate-driven increases in global terrestrial net primary production from 1982 to 1999. *Science*, 300, 1560–1563.
- Nicotra, A.B., Atkin, O.K., Bonser, S.P., Davidson, A.M., Finnegan, E.J., Mathesius, U., Poot, P., Purugganan, M.D., Richards, C.L., Valladares, F. & van Kleunen, M. (2010). Plant phenotypic plasticity in a changing climate. *Trends in Plant Science*, 15, 684–692.
- Niinemets, U., Flexas, J. & Peñuelas, J. (2011). Evergreens favored by higher responsiveness to increased CO₂. *Trends in Ecology & Evolution*, 26, 136–42.
- Olson, D.M., Dinerstein, E., Wikramanayake, E.D., Burgess, N.D., Powell, G.V.N., Underwood, E.C., D'amico, J.A., Itoua, I., Strand, H.E., Morrison, J.C., Loucks, C.J., Allnutt, T.F., Ricketts, T.H., Kura, Y., Lamoreux, J.F., Wettengel, W.W., Hedao, P. & Kassem, K.R. (2001). Terrestrial ecoregions of the world: a new map of life on earth. *BioScience*, 51, 933–938.
- Olsson, L., Eklundh, L. & Ardö, J. (2005). A recent greening of the Sahel—trends, patterns and potential causes. *Journal of Arid Environments*, 63, 556–566.
- Osborne, C.P., Beerling, D.J., Lomax, B.H. & Chaloner, W.G. (2004). Biophysical constraints on the origin of leaves inferred from the fossil record. *Proceedings of the National Academy of Sciences of the United States of America*, 101, 10360–10362.
- Panchen, Z.A., Primack, R.B., Nordt, B., Ellwood, E.R., Stevens, A.D., Renner, S.S., Willis, C.G., Fahey, R., Whittmore, A., Du, Y. & Davis, C.C. (2014). Leaf out times of temperate woody plants are related to phylogeny, deciduousness, growth habit and wood anatomy. *The New phytologist*, 203, 1208–1219.
- Parmesan, C. (2006). Ecological and Evolutionary Responses to Recent Climate Change. *Annual Review of Ecology, Evolution, and Systematics*, 37, 637–669.
- Parmesan, C. & Yohe, G. (2003). A globally coherent fingerprint of climate change impacts across natural systems. *Nature*, 421, 37–42.
- Paruelo, J.M., Garbulsky, M.F., Guerschman, J.P. & Jobbágy, E.G. (2004). Two decades of Normalized Difference Vegetation Index changes in South America: identifying the imprint of global change. *International Journal of Remote Sensing*, 25, 2793–2806.
- Patrick, L.D., Ogle, K. & Tissue, D.T. (2009). A hierarchical Bayesian approach for estimation of photosynthetic parameters of C₃ plants. *Plant, Cell & Environment*, 32, 1695–1709.

- Pau, S., Wolkovich, E.M., Cook, B.I., Davies, T.J., Kraft, N.J.B., Bolmgren, K., Betancourt, J.L. & Cleland, E.E. (2011). Predicting phenology by integrating ecology, evolution and climate science. *Global Change Biology*, 17, 3633–3643.
- Peel, M.C. (2007). Updated world map of the Köppen-Geiger climate classification. *Hydrology and Earth System Sciences*, 11, 1633–1644.
- Pinzon, J.E. & Tucker, C.J. (2014). A non-stationary 1981-2012 AVHRR NDVI_{3g} time series. *Remote Sensing*, 6, 6929–6960.
- Plummer, M. (2014). *JAGS*, <http://mcmc-jags.sourceforge.net/>.
- Poorter, H., Niinemets, U., Poorter, L., Wright, I.J. & Villar, R. (2009). Causes and consequences of variation in leaf mass per area (LMA): a meta-analysis. *New Phytologist*, 182, 565–588.
- Post, E., Forchhammer, M.C., Bret-Harte, M.S., Callaghan, T.V., Christensen, T.R., Elberling, B., Fox, A.D., Gilg, O., Hik, D.S., Høye, T.T., Ims, R.A., Jeppesen, E., Klein, D.R., Madsen, J., McGuire, A.D., Rysgaard, S., Schindler, D.E., Stirling, I., Tamstorf, M.P., Tyler, N.J.C., van der Wal, R., Welker, J., Wookey, P.A., Schmidt, N.M. & Aastrup, P. (2009). Ecological dynamics across the Arctic associated with recent climate change. *Science*, 325, 1355–1358.
- Poulter, B., Frank, D., Ciais, P., Myneni, R.B., Andela, N., Bi, J., Broquet, G., Canadell, J.G., Chevallier, F., Liu, Y.Y., Running, S.W., Sitch, S. & van der Werf, G.R. (2014). Contribution of semi-arid ecosystems to interannual variability of the global carbon cycle. *Nature*, 509, 600–603.
- Prentice, I.C., Farquhar, G.D., Fasham, M.J.R., Goulden, M.L., Heimann, M., Jaramillio, V.J., Kheshgi, H.S., Le Quéué, C., Scholes, R.J. & Wallace, D.W.R. (2001). The carbon cycle and atmospheric carbon dioxide. In: *Climate Change 2001: The Scientific Basis* (eds. Houghton, J.T., Ding, Y., Griggs, D.J., Noguer, M., van der Linden, P.J., Dai, X., Maskell, K. & Johnson, C.A.). Cambridge University Press, Cambridge, chap. 3, pp. 183–237.
- R Core Team (2014). *R: A Language and Environment for Statistical Computing*. R Foundation for Statistical Computing, Vienna, Austria.
- Randerson, J.T., Liu, H., Flanner, M.G., Chambers, S.D., Jin, Y., Hess, P.G., Pfister, G., Mack, M.C., Treseder, K.K., Welp, L.R., Chapin, F.S., Harden, J.W., Goulden, M.L., Lyons, E., Schuur, J.C.N.E.A.G. & Zender, C.S. (2006). The impact of boreal forest fire on climate warming. *Science*, 314, 1130–1132.

- Ratnam, J., Sankaran, M., Hanan, N.P., Grant, R.C. & Zambatis, N. (2008). Nutrient resorption patterns of plant functional groups in a tropical savanna: variation and functional significance. *Oecologia*, 157, 141–51.
- Ray, D.K., Ramankutty, N., Mueller, N.D., West, P.C. & Foley, J.A. (2012). Recent patterns of crop yield growth and stagnation. *Nature Communications*, 3, 1–7.
- Reyes-Fox, M., Steltzer, H., Trlica, M.J., McMaster, G.S., Andales, A.A., LeCain, D.R. & Morgan, J.A. (2014). Elevated CO₂ further lengthens growing season under warming conditions. *Nature*, 510, 259–262.
- Ritchie, J.C., Eyles, C.H. & Haynes, C.V. (1985). Sediment and pollen evidence for an early to mid-Holocene humid period in the eastern Sahara. *Nature*, 314, 352–355.
- Rodríguez-Iturbe, I. & Porporato, A. (2004). *Ecohydrology of Water-controlled Ecosystems: Soil Moisture and Plant Dynamics*. Cambridge University Press, Cambridge.
- Root, T.L., Price, J.T. & Hall, K.R. (2003). Fingerprints of global warming on wild animals and plants. *Nature*, 421, 57–60.
- Rossiter, D. (2014). Statistical methods for accuracy assesment of classified thematic maps. Tech. rep., University of Twente, Enschede, The Netherlands.
- Royer, D.L., Osborne, C.P. & Beerling, D.J. (2003). Carbon loss by deciduous trees in a CO₂-rich ancient polar environment. *Nature*, 424, 60–62.
- Running, S.W., Nemani, R.R., Heinsch, F.A., Zhao, M., Reeves, M. & Hashimoto, H. (2004). A continuous satellite-derived measure of global terrestrial primary production. *BioScience*, 54, 547–560.
- Samanta, A., Costa, M.H., Nunes, E.L., Vieira, S.A., Xu, L. & Myneni, R.B. (2011). Comment on "Drought-induced reduction in global terrestrial net primary production from 2000 through 2009". *Science*, 333, 1093.
- Sanchez, G. (2012). *plsdepot: Partial Least Squares (PLS) Data Analysis Methods*. R package version 0.1.17.
- Sarmiento, G., Goldstein, G. & Meinzer, F. (1985). Adaptive strategies of woody species in neotropical savannas. *Biological Reviews*, 60, 315–355.
- Scheffer, M., Carpenter, S.R., Lenton, T.M., Bascompte, J., Brock, W., Dakos, V., van de Koppel, J., van de Leemput, I.A., Levin, S.A., van Nes, E.H., Pascual, M. & Vandermeer, J. (2012). Anticipating critical transitions. *Science*, 338, 344–348.

- Schmida, A. (1985). Biogeography of the desert floras of the world. In: *Hot Deserts and Arid Shrublands* (eds. Evenari, M., Noy-Meir, I. & Goodall, D.W.). Elsevier, Amsterdam, vol. 12a of *Ecosystems of the World*, chap. 2, pp. 23–77.
- Schmidt, E., Lötter, M. & McClelland, W. (2007). *Trees and shrubs of Mpumalanga and Kruger National Park*. 2nd edn. Jacana, Johannesburg.
- Schurr, F.M., Midgley, G.F., Rebelo, A.G., Reeves, G., Poschlod, P. & Higgins, S.I. (2007). Colonization and persistence ability explain the extent to which plant species fill their potential range. *Global Ecology and Biogeography*, 16, 449–459.
- Schwartz, M. & Crawford, T. (2001). Detecting energy-balance modifications at the onset of spring. *Physical Geography*, 22, 394–409.
- Schwartz, M. & Reiter, B. (2000). Changes in North American spring. *International Journal of Climatology*, 932, 929–932.
- Schwartz, M.D. (1996). Examining the spring discontinuity in daily temperature ranges. *Journal of Climate*, 9, 803–808.
- Shackleton, C.M. (1999). Rainfall and topo-edaphic influences on woody community phenology in South African savannas. *Global Ecology and Biogeography*, 8, 125–136.
- Sharkey, T.D., Bernacchi, C.J., Farquhar, G.D. & Singsaas, E.L. (2007). Fitting photosynthetic carbon dioxide response curves for C₃ leaves. *Plant, cell & environment*, 30, 1035–1040.
- Shiodera, S., Rahajoe, J.S. & Kohyama, T. (2008). Variation in longevity and traits of leaves among co-occurring understorey plants in a tropical montane forest. *Journal of Tropical Ecology*, 24, 121–133.
- Shipley, B. (2010). *From Plant Traits to Vegetation Structure*. Cambridge University Press, Cambridge.
- Spicer, R.A. & Chapman, J.L. (1990). Climate change and the evolution of high-latitude terrestrial vegetation and floras. *Trends in Ecology & Evolution*, 5, 279–284.
- Staver, A.C., Archibald, S. & Levin, S.A. (2011). The global extent and determinants of savanna and forest as alternative biome states. *Science*, 334, 230–232.
- Stevens, N., Archibald, S.A., Nickless, A., Swemmer, A. & Scholes, R.J. (2015). Evidence for facultative deciduousness in semi-arid african savannas. *Austral Ecology*, In Press.

- Svenning, J.C. & Skov, F. (2004). Limited filling of the potential range in European tree species. *Ecology Letters*, 7, 565–573.
- Takhtajan, A.L. (1986). *The Floristic Regions of the World*. University of California Press, Berkeley.
- Therneau, T.M. (2014). *A Package for Survival Analysis in S*. R package version 2.37-7.
- Thomas, C.D., Cameron, A., Green, R.E., Bakkenes, M., Beaumont, L.J., Collingham, Y.C., Erasmus, B.F.N., De Siqueira, M.F., Grainger, A., Hannah, L., Hughes, L., Huntley, B., Van Jaarsveld, A.S., Midgley, G.F., Miles, L., Ortega-Huerta, M.A., Peterson, A.T., Phillips, O.L. & Williams, S.E. (2004). Extinction risk from climate change. *Nature*, 427, 145–148.
- Thomas, D.S., Eamus, D. & Bell, D. (1999). Optimization theory of stomatal behaviour: II. Stomatal responses of several tree species of north Australia to changes in light, soil and atmospheric water content and temperature. *Journal of Experimental Botany*, 50, 393–400.
- Thornley, J.H.M. (1998). Modelling shoot root relations: the only way forward? *Annals of Botany*, 81, 165–171.
- Trabucco, A. & Zomer, R. (2010). *Global Soil Water Balance Geospatial Database*. CGIAR Consortium for Spatial Information.
- Venter, F.J., Scholes, R.J. & Eckhardt, H.C. (2003). *The Kruger Experience: Ecology And Management Of Savanna Heterogeneity*. Island Press, Washington DC.
- Villar, R. & Merino, J. (2001). Comparison of leaf construction costs in woody species with differing leaf life-spans in contrasting ecosystems. *New Phytologist*, 151, 213–226.
- Vogel, S. (2012). *The Life of a Leaf*. The University of Chicago Press, Chicago.
- Walther, G.R., Post, E., Convey, P., Menzel, A., Parmesan, C., Beebee, T.J.C., Fromentin, J.M., Hoegh-Guldberg, O. & Bairlain, F. (2002). Ecological responses to recent climate change. *Nature*, 416, 389–395.
- Warming, E. & Vahl, M. (1909). *Oecology of plants - an introduction to the study of plant communities*. Oxford Clarendon Press, Oxford.
- Warren, D.L., Glor, R.E. & Turelli, M. (2008). Environmental niche equivalency versus conservatism: quantitative approaches to niche evolution. *Evolution*, 62, 2868–2883.
- Went, F.W. (1960). Blue hazes in the atmosphere. *Nature*, 187, 641–643.

- Werger, J.A. (1978). The Karoo-Namib region. In: *Biogeography and ecology of southern Africa* (ed. Werger, J.A.). Dr. W. Junk Publishers, The Hague, vol. 31 of *Monographiae Biologicae*, chap. 9, pp. 231–302.
- White, M.A., de Beurs, K.M., Didan, K., Inouye, D.W., Richardson, A.D., Jensen, O.P., O’Keefe, J., Zhang, G., Nemani, R.R., van Leeuwen, W.J.D., Brown, J.F., Wit, D., Schaepman, M., Lin, X., Dettinger, M., Bailey, A.S., Kimball, J., Schwartz, M.D., Baldocchi, D.D., Lee, J.T. & Lauenroth, W.K. (2009). Intercomparison, interpretation, and assessment of spring phenology in North America estimated from remote sensing for 1982–2006. *Global Change Biology*, 15, 2335–2359.
- White, M.A., Hoffman, F., Hargrove, W.W. & Nemani, R.R. (2005). A global framework for monitoring phenological responses to climate change. *Geophysical Research Letters*, 32, L04705.
- Wickens, G.E. (1998). *Ecophysiology of economic plants in arid and semi-arid lands*. vol. Ecophysiology of economic plants in arid and semi-arid lands of *Adaptations of Desert Organisms*. Springer-Verlag, Berlin.
- Wigley, B.J., Bond, W.J. & Hoffman, M.T. (2010). Thicket expansion in a South African savanna under divergent land use: local vs. global drivers? *Global Change Biology*, 16, 964–976.
- Wigley, B.J., Coetsee, C., Hartshorn, A.S. & Bond, W.J. (2013). What do ecologists miss by not digging deep enough? Insights and methodological guidelines for assessing soil fertility status in ecological studies. *Acta Oecologica*, 51, 17–27.
- Williams, C.A., Hanan, N., Scholes, R.J. & Kutsch, W. (2009). Complexity in water and carbon dioxide fluxes following rain pulses in an African savanna. *Oecologia*, 161, 469–80.
- Williams, K., Field, C.B. & Mooney, H.A. (1989). Relationships among leaf construction cost, leaf longevity, and light environment in rain-forest plants of the genus *Piper*. *American Naturalist*, 133, 198–211.
- Williams, K., Percival, F., Merino, J. & Mooney, H.A. (1987). Estimation of tissue construction cost from heat of combustion and organic nitrogen content. *Plant, Cell & Environment*, 10, 725–734.
- Wolkovich, E.M. & Cleland, E.E. (2014). Phenological niches and the future of invaded ecosystems with climate change. *AoB plants*, 6, 1–16.

- Woodward, F.I. (1987). Stomatal numbers are sensitive to increases in CO₂ from pre-industrial levels. *Nature*, 327, 617–618.
- Woodward, F.I., Lomas, M.R. & Kelly, C.K. (2004). Global climate and the distribution of plant biomes. *Philosophical transactions of the Royal Society of London. Series B*, 359, 1465–1476.
- Wright, I.J., Reich, P.B., Westoby, M. & Ackerly, D.D. (2004). The worldwide leaf economics spectrum. *Nature*, 428, 821–827.
- Wright, J.P. & Sutton-Grier, A. (2012). Does the leaf economic spectrum hold within local species pools across varying environmental conditions? *Functional Ecology*, 26, 1390–1398.
- Xu, L. & Baldocchi, D.D. (2003). Seasonal trends in photosynthetic parameters and stomatal conductance of blue oak (*Quercus douglasii*) under prolonged summer drought and high temperature. *Tree Physiology*, 23, 865–877.
- Zanne, A., Lopez-Gonzalez, G., Coomes, D., Ilic, J., Jansen, S., Lewis, S., Miller, R., Swenson, N., Wiemann, M. & Chave, J. (2009). Data from: Towards a worldwide wood economics spectrum. dryad digital repository.
- Zhao, M. & Running, S.W. (2010). Drought-induced reduction in global terrestrial net primary production from 2000 through 2009. *Science*, 329, 940–943.
- Zhou, L., Tucker, C.J., Kaufmann, R.K., Slayback, D., Shabanov, N.V. & Myneni, R.B. (2001). Variations in northern vegetation activity inferred from satellite data of vegetation index during 1981 to 1999. *Journal of Geophysical Research*, 106, 20069–20083.
- Zhu, W., Tian, H., Xu, X., Pan, Y., Chen, G. & Lin, W. (2012). Extension of the growing season due to delayed autumn over mid and high latitudes in North America during 1982–2006. *Global Ecology and Biogeography*, 21, 260–271.
- Zohner, C.M. & Renner, S.S. (2014). Common garden comparison of the leaf-out phenology of woody species from different native climates, combined with herbarium records, forecasts long-term change. *Ecology Letters*, 17, 1016–1025.

Acknowledgements

First of all I would like to thank my supervisor Professor Steve Higgins. It has been a pleasure working with you and I have benefited greatly from your guidance and advice over the past years. Thank you for taking me on, giving me the confidence, freedom and support to explore my (too many) interests and sharing your ideas and expertise. It has been fun spending some out-of-office time in Kruger and Dunedin and I hope these opportunities will keep coming up in the future.

Secondly I wish to thank Associate Professor Ed February, without whom the best part of this PhD, collecting data in Kruger, would not have been possible. Thanks for including me in your lab at UCT, allowing me to use the facilities and making sure that operations in the field could always continue smoothly.

I would also like to thank Professor Thomas Hickler, who kindly adopted me and facilitated that I could finish my studies at Goethe University.

I have have been inspired by many people since I started the journey of becoming an ecologist, nearly 13 years ago. I will not try to mention every person from whom I have learnt valuable lessons during that period here, but I wish to acknowledge some people in particular without whose guidance I might not have made it this far. In more or less chronological order: Prof Jan Bakker, thank you for re-kindling my enthusiasm for discovery, guiding it toward the world of plants and enabling me to travel to exciting new places. Esther Chang, for broadening my views and introducing me to sushi. Prof Han

Olf, for sending me off to do fieldwork in Hllhuwe-iMfolozi without too much of a plan and stimulating me to reach further. Nikki Stevens, for sharing your knowledge and passion and for encouraging me to push ahead in science. Tony Swemmer for forcing me to learn R, giving me the freedom to explore and making sure I had a pay slip at the end of most months. Prof William Bond, you are an inspiration, thank you for generously sharing ideas, the notion that science works best when you have fun, and creating a job when I needed one.

Life over the past years would have been a lot less fun without Alex Zizka, Glenn Moncrieff (I cannot wait to have an office that does not bear the marks of your lunches), Liam Langan, Laura Rose, Henri & Leigh Combrink, Navashni Govender & Eddie Riddell, Laurence Kruger, Carla Staver, Leigh-Ann Woolley & Ryan the Ozzie, Kyle & Terry Harris, Jolande & Robert Hoogendijk, Edward Buitenwerf & Marlieke Engelen, Paola Vimercati, Ivana Kirchmair, Jay Iwasaki, Lars Ludwig, Rheiny Scholtz, Karen Vickers, Simon Scheiter and Ulla, Ben and Daniel Higgins.

For help with data collection I would like to thank: Alex Zizka for (various attempts at) climbing trees to count cable-tied leaves and many other less exciting things including help with my *zusammenfassung*, Vera Zizka for counting 22509.1 (?) stomata, Paola Vimercati for dutifully weighing decomposing grass that was eventually mowed prematurely, Jenny Toivio and Julia Fischer for measuring the water potential of many hundreds of cups of soil, Glenn Moncrieff for recording the most anomalous gas exchange rates in my dataset, Isabelle Stiefvater for sifting through many thousands of NDVI images, Shaamielah Davids for grinding and incinerating dead leaves, Henri Combrink for safely flying the remote controlled helicopter (almost) throughout the entire growing season and Michele Hofmeyer for keeping my plants at the Skukuza nursery watered and green until they perished as elephant snacks.

I must also express my gratitude to the Zizka family: Georg, Sabine, Alex and Vera, who have provided me with a home during my time in Frankfurt (I mean, Offenbach)

ACKNOWLEDGEMENTS

and generously shared their time and space. The Botany Department at the University of Otago has hosted me for nearly a year, generously providing support and office space. In particular I wish to thank Prof Kath Dickinson, for making us feel welcome and for providing exceptionally kind and much needed support in times of duress.

I wish to thank my parents, whom must have wondered and worried at times about what I was up to and where I would end up. Pa en Ma, jullie onvoorwaardelijke steun heeft alle verschil gemaakt.

Lastly, I thank Ashley Percy for unconditional support, patience and for following me to the ends of the Earth.

Appendix A

Three decades of multi-dimensional change in global leaf phenology

APPENDIX A. PHENOLOGICAL CHANGE

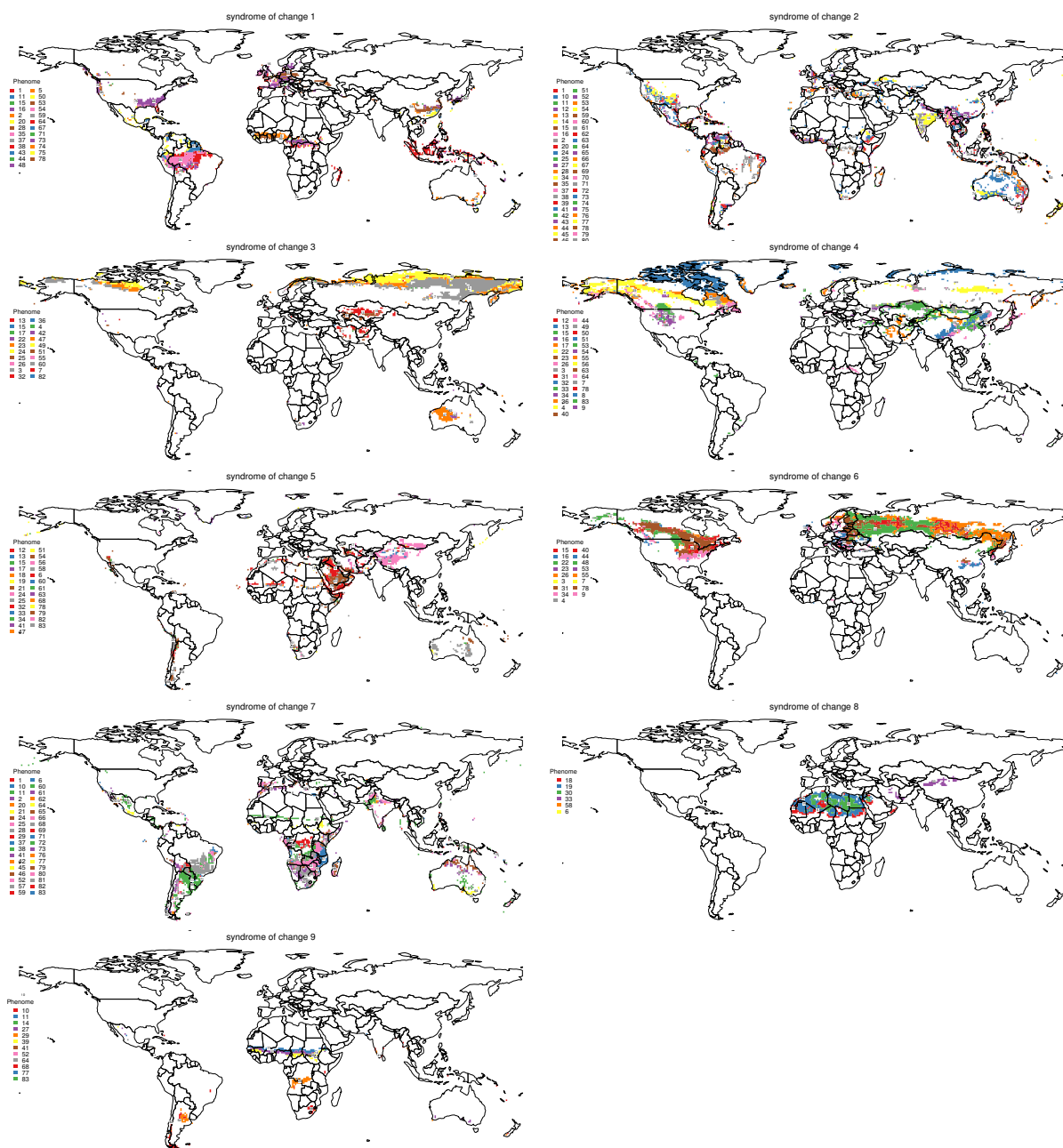


Figure A.1: The location of individual phenomes, grouped by syndrome of change (as shown in Figure 2.3a). Labels represent the phenome number and correspond with the numbers in Figure A.3.

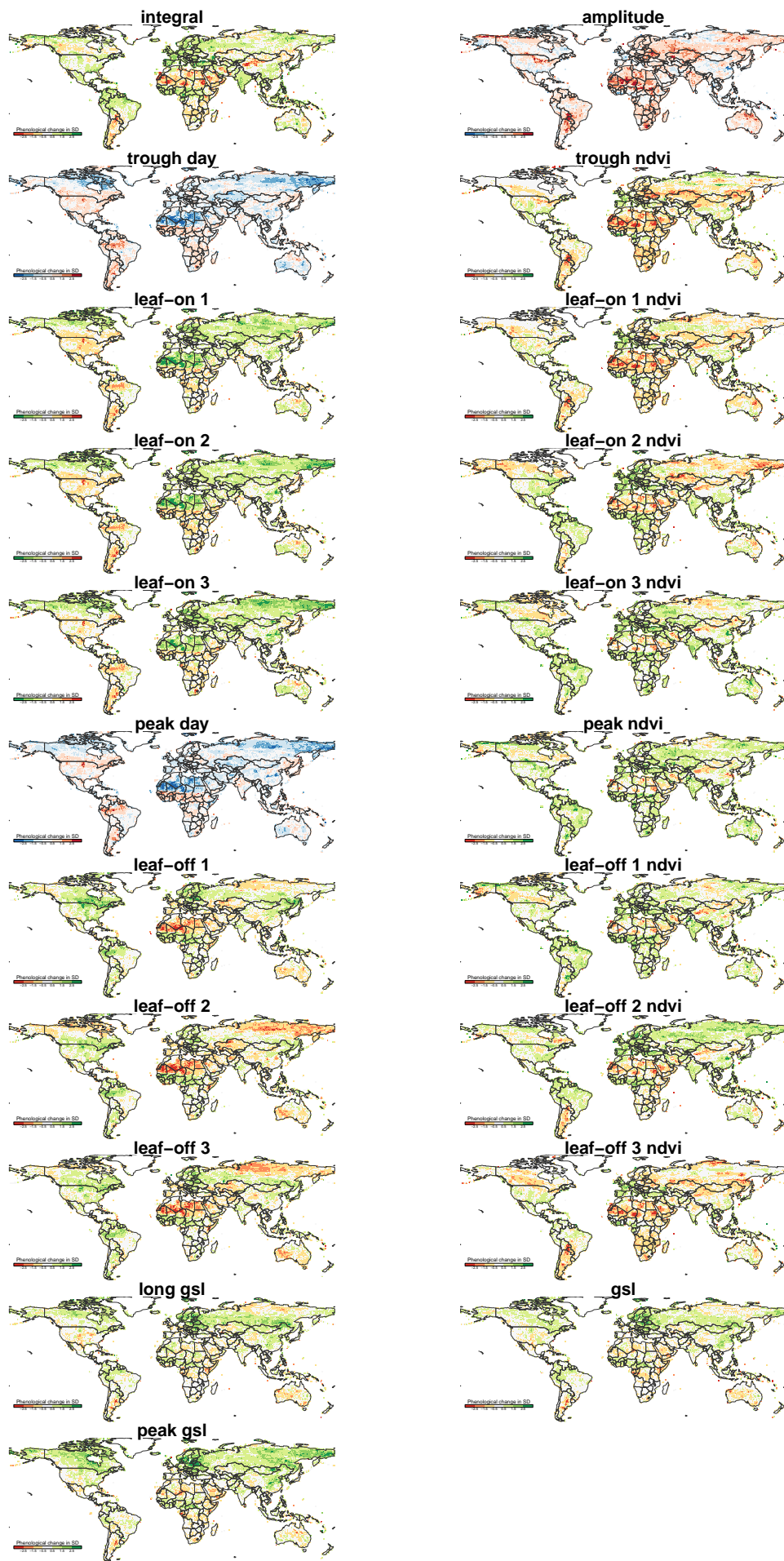


Figure A.2: Change in vegetation activity between the studied time windows (1981-1990 and 2003-2012) in SD units for 21 phenological metrics.

APPENDIX A. PHENOLOGICAL CHANGE

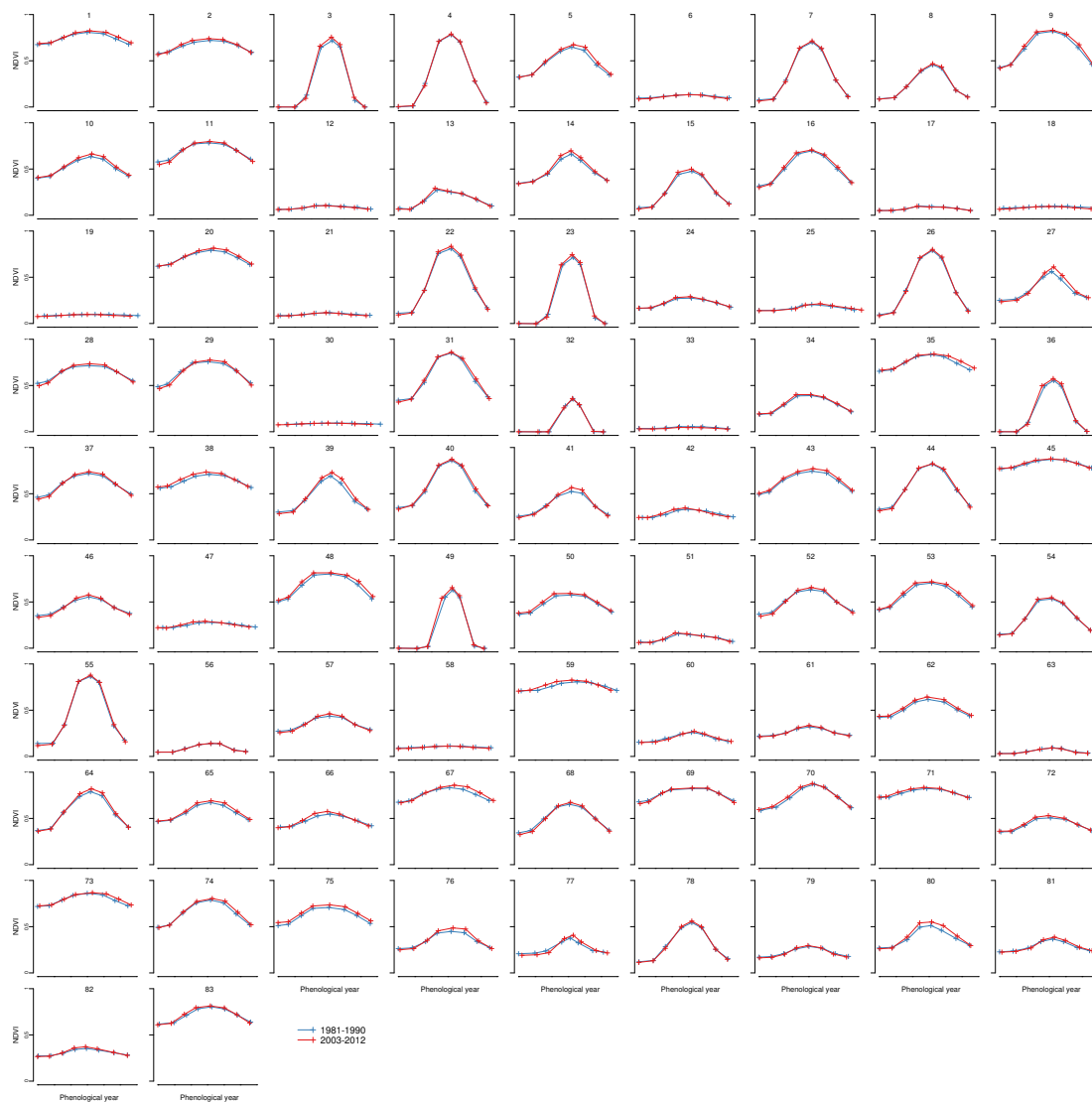


Figure A.3: Per phenome change in vegetation activity between the studied time windows (1981-1990 in black and 2003-2012 in red). The units are NDVI and day of year. Symbols indicate the metrics as described in Figure 2.1.

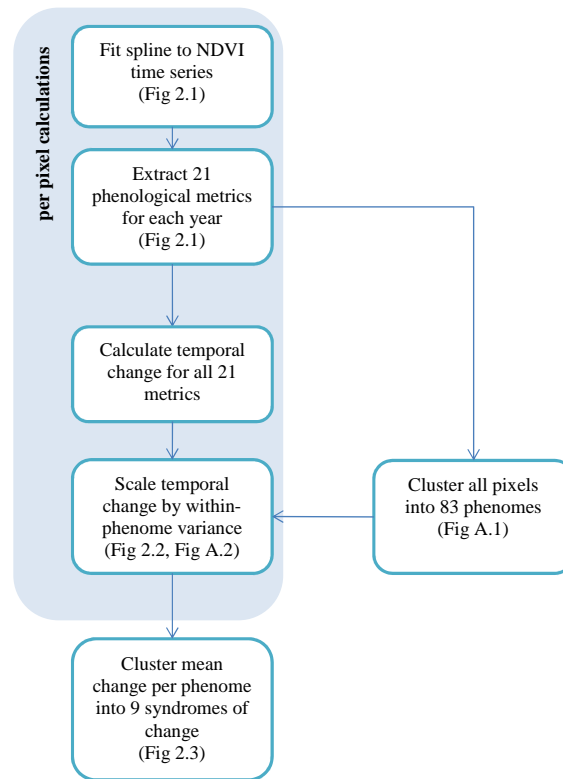


Figure A.4: A work-flow diagram summarising the steps in our analysis.

Appendix B

Convergence in the physiological niche of evergreen and deciduous vegetation

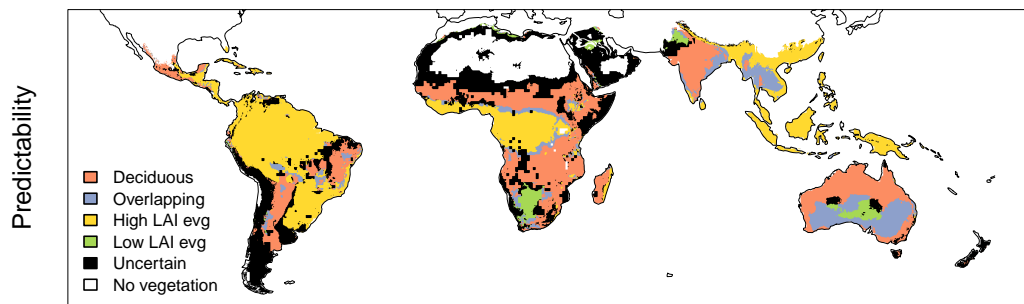


Figure B.1: Overlap in phenome projections from different realms. Unlike in Figure 3.4, the overlap excludes projections from the native realm. Colours represent areas where projections from every foreign realm agree on a particular phenome (red, yellow, green), on overlapping phenomes (blue) or on areas devoid of vegetation (white). Areas in black are where the projection from at least one foreign realm did not coincide with the projections from the other foreign realms.

Appendix C

Effects of leaf phenology and leaf habit on the carbon budget of African savanna trees

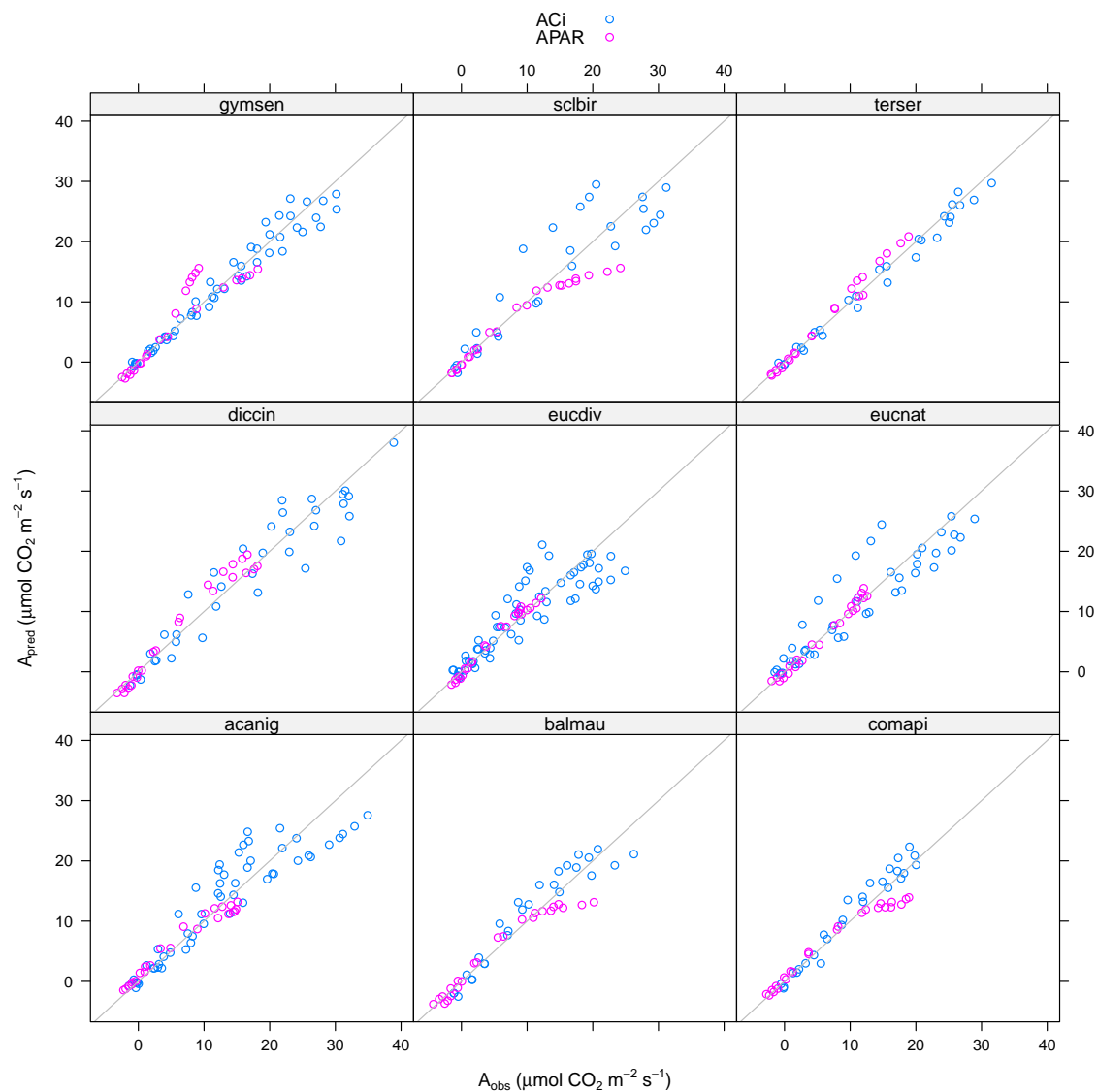


Figure C.1: Observed and predicted photosynthetic rates for nine species. ACi are measurements in which CO_2 concentration was varied and APAR are measurements in which light intensity was varied. The grey line shows the 1 to 1 line.

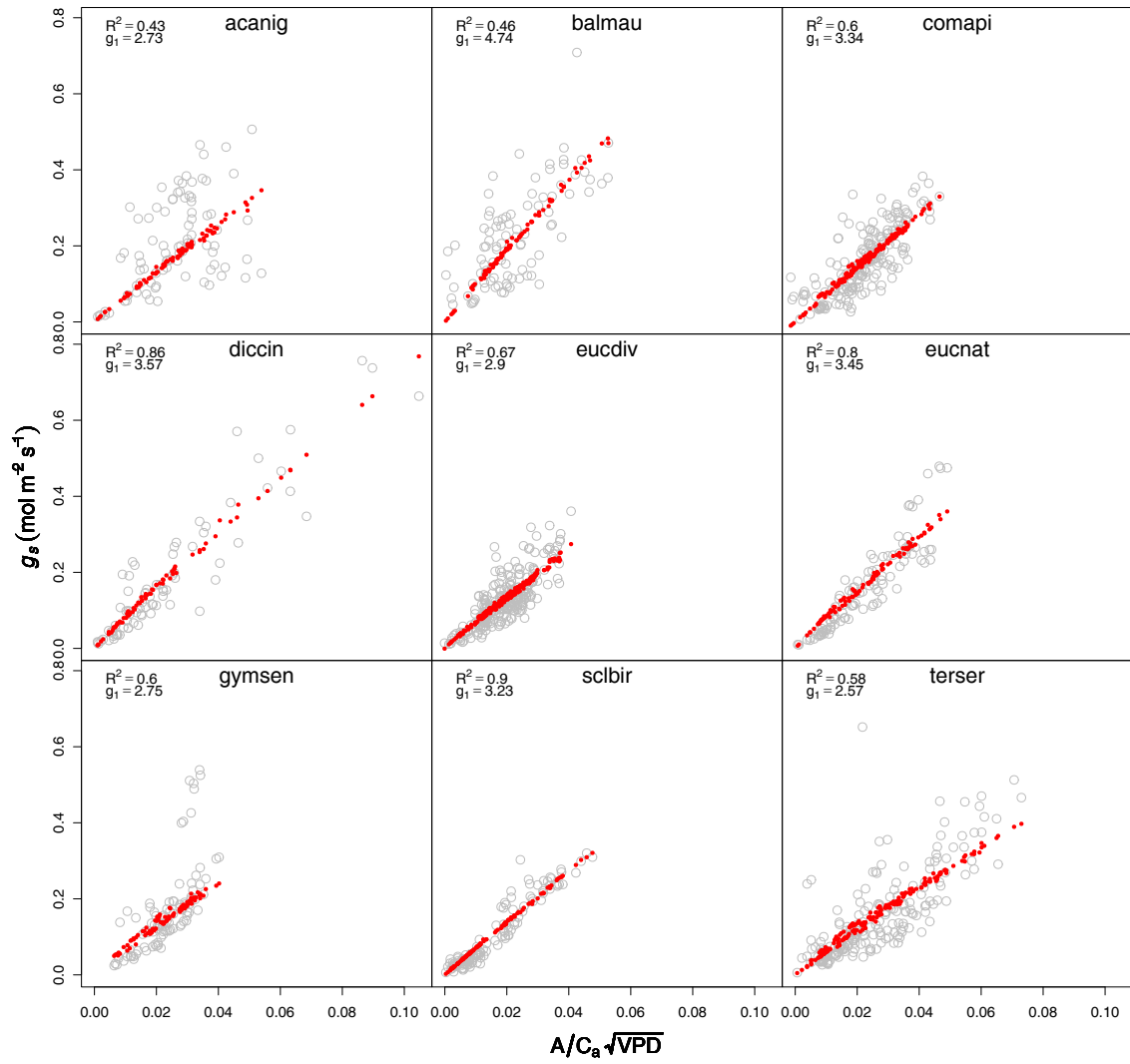


Figure C.2: Observed stomatal conductance in grey and predicted optimal stomatal conductance (Equation 4.4) in red.

Appendix D

Soil water retention curves for the major soil types of the Kruger National Park

Robert Buitenwerf, Andrew Kulmatiski and Steven I. Higgins¹²

¹Author declarations: AK and RB designed the study. RB collected the data and performed the analyses. RB wrote the paper with assistance from AK and SIH.

²The work presented in this appendix has been published in *Koedoe* **56** pg 1-9.

Abstract

Soil water potential is crucial to plant transpiration and thus to carbon cycling and biosphere-atmosphere interactions, yet it is difficult to measure in the field. Volumetric and gravimetric water contents are easy and cheap to measure in the field but can be a poor proxy of plant available water. Soil water content can be transformed to water potential using soil moisture retention curves. We provide empirically-derived soil moisture retention curves for seven soil types in Kruger National Park, South Africa. Site-specific curves produced excellent estimates of soil water potential from soil water content values. Curves from soils derived from the same geological substrate were similar, potentially allowing the use of one curve for basalt soils and one curve for granite soils. This dataset is anticipated to help hydrologists and ecophysiologicalists understand water dynamics, carbon cycling and biosphere-atmosphere interactions under current and changing climate conditions in the region.

Introduction

Soil moisture is a key driver of plant productivity in many ecosystems as water-stressed plants close their stomata to curb water loss, resulting in reduced CO₂ assimilation rates, and thus growth (Lambers *et al.*, 2008). To try to understand water availability, ecologists, agronomists and land managers often use measurements of gravimetric (g of water g⁻¹ soil) or volumetric (cm³ of water cm⁻³ soil) soil water to estimate water availability to plants. These measurements can easily be made by a wide array of sensors or simply by weighing and drying soil samples. The problem with these measurements is that they do not necessarily provide information about whether or not water is available to plants. This is because surface tension can bind large amounts of water to soils with high internal surface area (i.e., clays), at such large negative pressures that plants cannot oppose them and therefore cannot take up water (Vogel, 2012). The negative pressure with which water is bound to the soil is the soil water potential.

In non-saline soils, the relationship between soil water content and soil water potential largely depends on texture. Clay particles have a large surface area relative to their volume and therefore have the ability to bind large amounts of water. As a result, a clay soil with e.g. 10% moisture may have a highly negative water potential making water uptake impossible for most plants. Sand particles are more spherical and therefore have a lower surface to volume ratio. Consequently a sand soil with 10% moisture may have a water potential close to zero, allowing easy uptake of water by plants. Temperate crops can transpire water through their stomata, and therefore photosynthesise, down to a soil water potential of about -1.5 MPa. While this is called the permanent wilting point, some plants in arid systems are able to transpire water at soil water potentials as low as -5 MPa (Baldocchi *et al.*, 2004; Rodríguez-Iturbe & Porporato, 2004). Ecologists, vegetation modellers, and those modelling biosphere-atmosphere interactions therefore need accurate estimates of soil water potential in the range from -5 to 0 MPa to predict and explain stomatal responses, carbon dynamics, and water and energy budgets.

Pedo-transfer functions transform variables that are easy and cheap to measure into more informative variables that are too hard or expensive to measure directly (Bouma, 1989). One such function is the soil water retention curve, which transforms soil water content to soil water potential. The water retention curve is often estimated from information on soil texture, but can be determined precisely by measuring both variables simultaneously on samples under controlled conditions. Here we provide empirically-derived soil water characteristic curves for seven soils representing the major soil types of the Kruger National Park (KNP). We test whether the same curve can be used for soils with similar texture.

Methods

Study site

KNP is situated in the north-east of South Africa between 30.9–32.0 °E and 22.3–25.5 °S. KNP receives between 450 and 750 mm yr⁻¹ of rain, most of which falls between October and March. Average temperatures are around 25 °C in summer and around 20 °C in winter. Most of KNP is underlain by either basaltic rock that weathers into clay-rich soils or granitic rock that weathers into sandy soils. Both these dominant parent materials are old: basaltic rock was formed ~200 MA while the granite was formed ~2050 MA (Venter *et al.*, 2003). Seven dominant soil types from across the KNP (Venter *et al.*, 2003) were sampled (Figure D.1; Table D.1). The sampled soil types cover approximately 65% of the park.

Approach

Using a soil auger, samples were collected at three depths: at the top of the profile (0–10 cm), at the bottom (110 cm or degraded bedrock, whichever was shallower) and in the middle (see Table D.2 for details). Soils were air-dried and sieved in a 2 mm aperture sieve

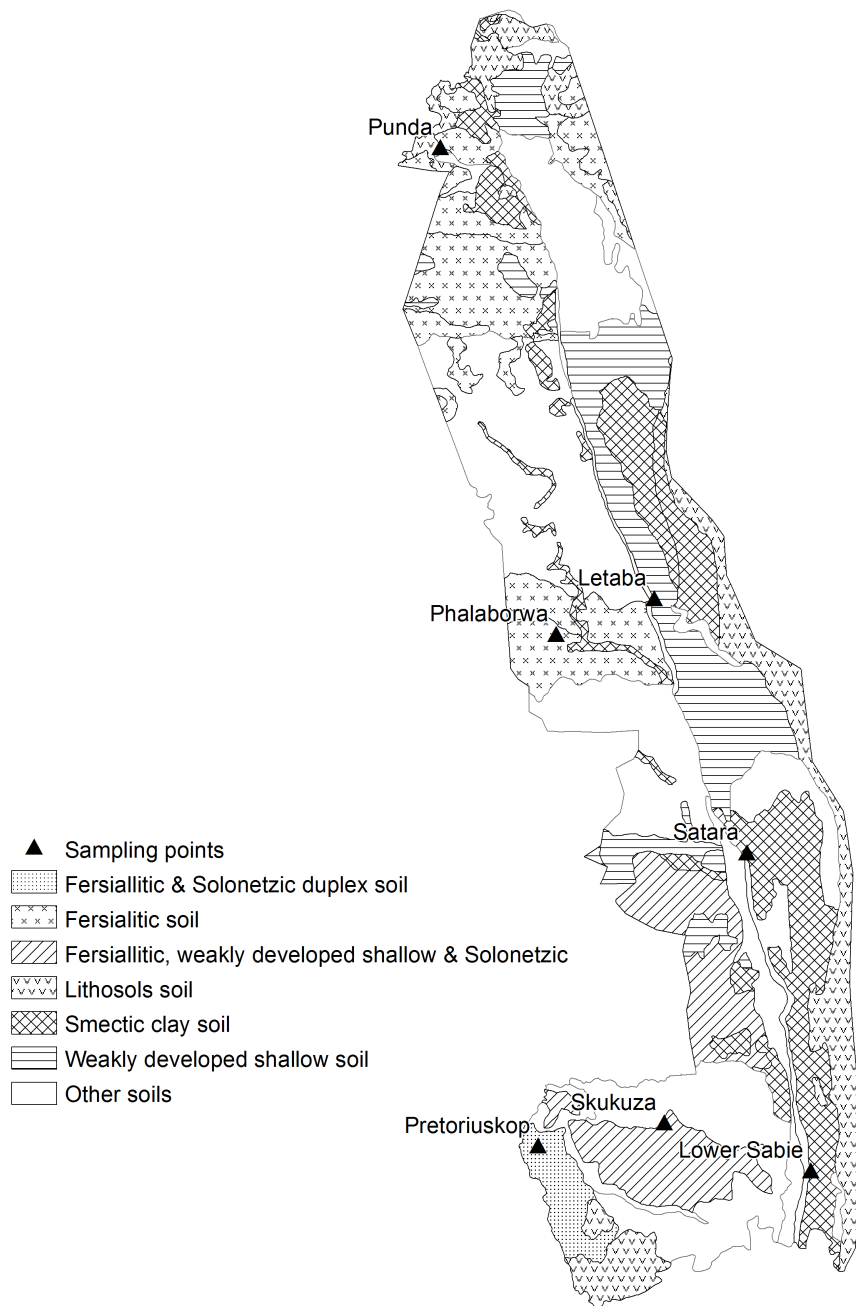


Figure D.1: Dominant soil types of the Kruger National Park that were sampled in this study following Venter *et al.* (2003).

Table D.1: Coordinates of the sampling sites and description of soils at those sites following Venter *et al.* (2003). The sand, silt, and clay fractions are the mean of all samples from a site in percentages \pm the standard error.

Site	Longitude	Latitude	Substrate	Description of dominant soil type	Sand	Silt	Clay
Letaba	31.5195	-23.7796	Basalt	Calcareous shallow clays	32 \pm 7	31 \pm 5	37 \pm 3
Lower Sabie	31.9063	-25.1916	Basalt	Pedocutanic clays, mainly brown and black	42 \pm 7	26 \pm 2	32 \pm 9
Phalaborwa	31.2779	-23.8676	Granite	Coarse fersiallitic sands and loams, mainly yellow and grey	-	-	-
Pretoriuskop	31.2336	-25.1300	Granite	Coarse fersiallitic sand, solonetzic duplex soil	85 \pm 2	10 \pm 2	5 \pm 2
Punda	30.9922	-22.6668	Sandstone	Arenaceous sediments	96 \pm 2	3 \pm 0	1 \pm 1
Satara	31.7484	-24.4065	Basalt	Pedocutanic clays, mainly brown and black	46 \pm 5	37 \pm 4	17 \pm 3
Skukuza	31.5450	-25.0730	Granite	Coarse fersiallitic sand, shallow sand, solonetzic duplex soil	82 \pm 7	10 \pm 2	8 \pm 6

to remove large roots and rocks. The proportion of rock with dimensions greater than 2 mm was generally negligible (i.e. < 3%).

Water retention curves

Soil moisture retention curves were derived empirically using an instrument that exploits the chilled-mirror technique (WP4T, Decagon Devices Inc., Pullman). A soil sample is inserted into the device and equilibrated with the headspace of a sealed chamber, so that the water potential of the air in the chamber is the same as the water potential of the sample. The point of condensation on a mirror is detected by shining a light beam onto the mirror and recording its reflectance with a light sensor. At the point of condensation the temperature of the mirror is recorded, allowing the water potential of the air, and therefore of the sample, to be calculated. The instrument measures the water potential with an accuracy of 0.05 MPa over the range of -0.1 to -0.5 MPa and with an accuracy of 0.1 MPa over the range of -0.5 to -300 MPa. Therefore, it adequately covers the range relevant to plant growth. Water content of the sample at the time of measuring water potential is determined gravimetrically (i.e. it is weighed and reweighed after oven-drying at 60 °C to a constant weight). Since the relationship between water potential and water content is often hysteretic (affected by the initial state of the system), we constructed soil moisture retention curves from both drying and wetting soils.

Soil from each sampling location and depth was subdivided into 15 samples of 5–6 g each, which were used to construct a single drying curve and a single wetting curve for each depth at each sampling location. For the drying curve, the samples were initially saturated with distilled water, sealed, and left to equilibrate overnight. Water potential and moisture content were then measured repeatedly as the samples dried out (air-dried). A typical curve was completed within a day. For the wetting curve, incremental amounts of moisture were added to initially dry samples, to achieve a range of saturation levels.

Samples were then sealed and left to equilibrate overnight, after which the water potential and the moisture content were measured.

Empirical models for the water retention curve are typically written to be solved for water content (see Assouline *et al.* (1998) for an overview). We fitted two widely used models proposed by van Genuchten (1980) and Fredlund & Xing (1994) that were rewritten to solve for water potential given a known water content using non-linear regression in R (R Core Team, 2014). We compared the performance of these models to simpler power and exponential functions, which were fitted by maximising the likelihood using iterative methods (Plummer, 2014). We fitted these functions to both the entire measured range of water potentials (0 to -100 MPa), and to a subset that is relevant to plant growth (0 to -8 MPa).

To assess the variability between soils from different sites but from the same geology, we compared predictions of water potential from site-specific curves to curves for which sites were grouped by geology. We did this for four levels of water content (0.03, 0.05, 0.1, and 0.15 g g⁻¹). For this analysis soils from Punda, which are derived from quartzite (Venter *et al.*, 2003), were included with granite derived soils as they had a very similar texture.

Soil texture

Particle size affects the total surface area for a given mass or volume of soil, and therefore the shape of the water retention curve. To quantify sand, silt, and clay fractions we used the hydrometer method (Bouyoucos, 1962). For each sample between 40 and 50 g of soil was dispersed with an electrical mixer in 100 ml of a 5% sodium hexametaphosphate ((NaPO₃)₆) solution, to break down clay aggregates. This mixture was allowed to soak overnight and mixed again the next morning before it was transferred to a 1 L cylinder that was filled up to 1 L with distilled water. Sediment was dispersed with a plunger and hydrometer readings were taken after 40 s and 6 h 52 m. Fractions were calculated as:

$$clay = \frac{H_{t=24720}}{w} \quad (D.1)$$

$$silt = \frac{H_{t=40}}{w} \quad (D.2)$$

$$sand = 1 - silt - clay \quad (D.3)$$

where H is the hydrometer reading at t seconds after inserting the hydrometer, and w is the sample weight in grams. Hydrometer readings were corrected for the added $(\text{NaPO}_3)_6$ by subtracting the hydrometer reading of a cylinder with 100 ml $(\text{NaPO}_3)_6$ solution filled up with distilled water. Temperature was measured at the time of each hydrometer reading and 0.4 g L^{-1} of solute concentration was added to the hydrometer reading for every $^\circ\text{C}$ above $20 \text{ }^\circ\text{C}$ (http://uwlab.soils.wisc.edu/files/procedures/particle_size.pdf).

Results

As expected, soils from basalt substrate have much higher clay content than soils from granitic substrate (Table D.1, Table D.2).

The Fredlund & Xing (1994) model appeared to fit the data well with R^2 values > 0.99 for most curves, however the confidence intervals on the parameter estimates could not be estimated using standard techniques, suggesting that the parameters were not identifiable. In other words, multiple combinations of parameter values can result in an identical fit. This outcome is likely to be a symptom of over-parametrisation of the model. The van Genuchten (1980) model did not converge well, also hinting at over-parametrisation. Therefore we only report results from the simpler power and exponential functions.

Table D.2: Parameter estimates (a and b), standard deviations (sd) of the parameter estimates, and goodness of fit (R^2), for the power functions fitted as water retention curves for soils in KNP.

Site	Depth (cm)	% sand	% silt	% clay	Drying				Wetting					
					a	a (sd)	b	b (sd)	R^2	a	a (sd)	b	b (sd)	R^2
Letaba	0-20	45.00	22.50	32.50	1.09e ⁻⁴	1.29e ⁻⁶	4.572	0.005	0.97	8.12e ⁻⁸	3.72e ⁻⁹	7.221	0.019	0.95
	40-60	25.00	33.75	41.25	1.29e ⁻⁴	2.14e ⁻⁶	4.889	0.008	0.96	1.78e ⁻⁶	5.08e ⁻⁸	6.543	0.012	1.00
	70-90	25.00	37.50	37.50	1.91e ⁻⁴	2.01e ⁻⁶	4.080	0.004	0.95	6.05e ⁻⁶	2.23e ⁻⁷	5.810	0.016	0.96
Lower Sabie	0-15	35.00	26.25	38.75	4.44e ⁻⁵	5.47e ⁻⁷	5.209	0.005	0.96	4.91e ⁻⁶	1.35e ⁻⁷	5.880	0.012	0.98
	30-40	35.00	22.50	42.50	2.07e ⁻⁶	4.72e ⁻⁸	6.574	0.010	0.97	1.64e ⁻⁶	1.20e ⁻⁷	6.375	0.033	0.95
	60-75	55.00	30.00	15.00	2.66e ⁻⁸	9.62e ⁻¹⁰	7.751	0.015	0.98	3.24e ⁻⁷	2.70e ⁻⁸	6.511	0.033	1.00
Phalaborwa	0-10	-	-	-	1.68e ⁻³	3.48e ⁻⁵	2.141	0.006	0.90	4.53e ⁻²	1.54e ⁻³	0.998	0.010	0.96
	30-40	-	-	-	2.18e ⁻²	4.54e ⁻⁴	1.504	0.006	0.91	1.18e ⁻⁵	5.03e ⁻⁷	3.589	0.012	0.81
	75-80	-	-	-	1.10e ⁻⁴	1.28e ⁻⁵	3.011	0.036	0.96	1.17e ⁻⁴	4.09e ⁻⁶	2.877	0.010	0.98
Pretoriuskop	0-10	91.00	9.00	0.00	3.09e ⁻³	5.52e ⁻⁵	1.874	0.004	0.98	1.36e ⁻⁵	4.11e ⁻⁷	3.159	0.007	0.98
	30-40	85.00	7.50	7.50	1.85e ⁻³	3.86e ⁻⁵	2.084	0.005	0.96	1.37e ⁻⁷	5.82e ⁻⁹	4.518	0.011	0.97
	90-100	79.00	14.50	6.50	5.40e ⁻³	3.32e ⁻⁴	1.834	0.019	0.80	1.06e ⁻⁷	1.17e ⁻⁸	4.943	0.030	0.98
Punda	0-10	97.00	3.00	0.00	7.35e ⁻³	9.00e ⁻⁵	1.647	0.003	0.96	3.33e ⁻⁵	1.18e ⁻⁶	2.877	0.009	0.86
	30-40	94.00	3.50	2.50	1.09e ⁻²	1.75e ⁻⁴	1.458	0.004	0.98	5.01e ⁻⁵	4.44e ⁻⁶	2.673	0.022	0.95
Satara	100-110	-	-	-	2.92e ⁻³	3.68e ⁻⁵	1.788	0.003	0.97	7.16e ⁻⁵	1.52e ⁻⁵	2.487	0.056	0.87
	0-10	55.00	33.75	11.25	5.31e ⁻³	1.00e ⁻⁴	2.819	0.008	0.91	2.77e ⁻⁴	9.25e ⁻⁶	3.980	0.013	0.99
	30-35	47.50	32.50	20.00	3.20e ⁻³	4.61e ⁻⁵	3.706	0.007	0.93	5.00e ⁻⁴	1.45e ⁻⁵	4.474	0.015	0.94

The best fit to individual curves in the -0.5 to -8 MPa range was provided by a power function of the form (Table D.2, Figure D.2):

$$\Psi = \frac{a}{\Theta^c} \quad (\text{D.4})$$

where Ψ is water potential in MPa, Θ is gravimetric water content in g g^{-1} , and a and c are estimated coefficients. For a given water content, water potentials from drying curves were generally lower than for wetting curves (Figure D.2).

When combining data from all sites per geological substrate, the residuals of the power function fits showed systematic bias. We therefore use an exponential model to describe the data aggregated by geology. The exponential model fits these grouped data reasonably well in the -0.5 to -8 MPa range: basalt $R^2=0.59$, granite $R^2=0.66$ (Figure D.3, see Figure D.5 for 0 to -100 MPa range). We note that R^2 values should be interpreted with caution in non-linear regression, and that the standard error of the regression (SER) is a better measure of goodness of fit: basalt SER=1.42 MPa, granite SER=1.13 MPa. The equation to convert soil water content to water potential for basaltic (clayey) soils in the -0.5 to -8 MPa range is:

$$\Psi = 0.21 + 45.51e^{-25.25\Theta} \quad (\text{D.5})$$

For granitic (sandy) soils in the -0.5 to -8 MPa range, the equation is:

$$\Phi = 0.51 + 17.35e^{-75.85\Theta} \quad (\text{D.6})$$

To assess the accuracy of these geology-specific curves, we compare the range in water potential for four water contents (0.03, 0.05, 0.10, and 0.15) as predicted by the site-specific models to the predicted water potential using the geology specific curve (Figure

APPENDIX D. SOIL WATER RETENTION CURVES

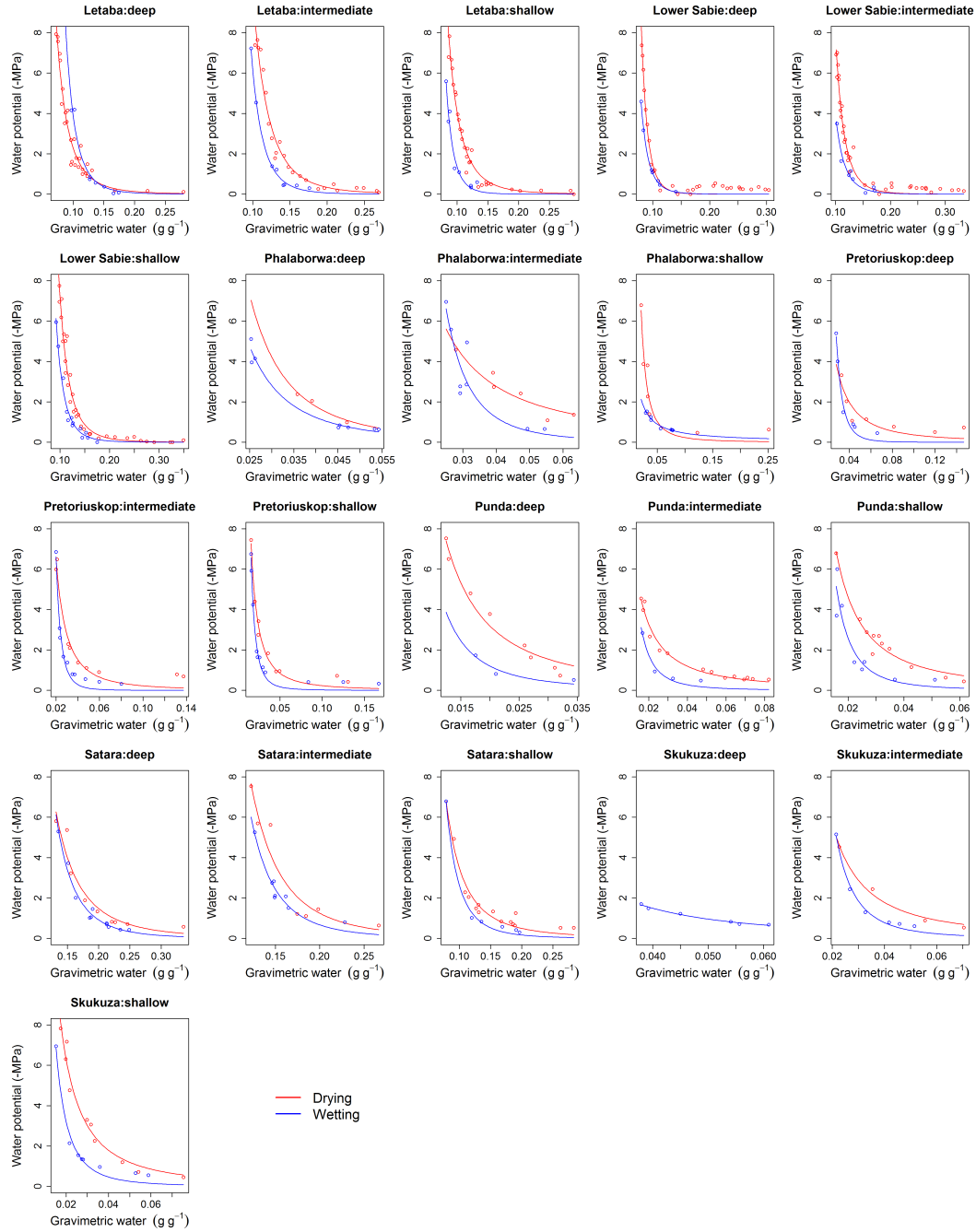


Figure D.2: The relationship between soil moisture and water potential in the range relevant to plant growth, for each of the sampled soils in KNP. Note that the pressures on the y-axis are negative pressures. The water retention curves were fitted using a power function. The parameter values for the curves are given in Table D.2.

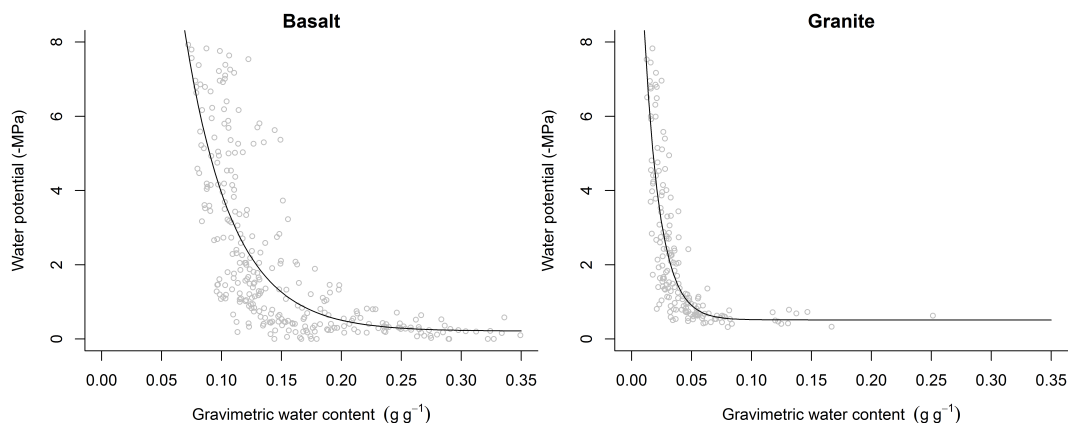


Figure D.3: The relationship between soil moisture and water potential in the range relevant to plant growth, for basalt and granite derived soils in KNP. Note that the pressures on the y-axis are negative pressures. The water retention curves were fitted using an exponential model.

D.4). The geology-specific curves predict water potentials close to the median value of site-specific curves, suggesting that they might be useful for modelling applications.

Discussion

Ecophysiological and hydrological interpretation of soil water content, an affordable measure of soil moisture, requires the use of pedo-transfer functions that transform water content to water potential. We generated such water retention curves with a WP4T instrument (Decagon Devices Inc., Pullman) using empirical data, and provide curves for common soil types in the KNP, South Africa. A power function provided a good fit for individual samples (Equation D.4, Table D.2), and depending on the required accuracy, a single exponential function per geological substrate may be used (Equations D.5 and D.6). At low water contents (i.e., ~5% for granitic and ~15% for basaltic soils) water potentials estimated from our pedo-transfer functions begin to vary widely among sites, reflecting differences in clay content (Figure D.4). Thus, researchers interested in precise

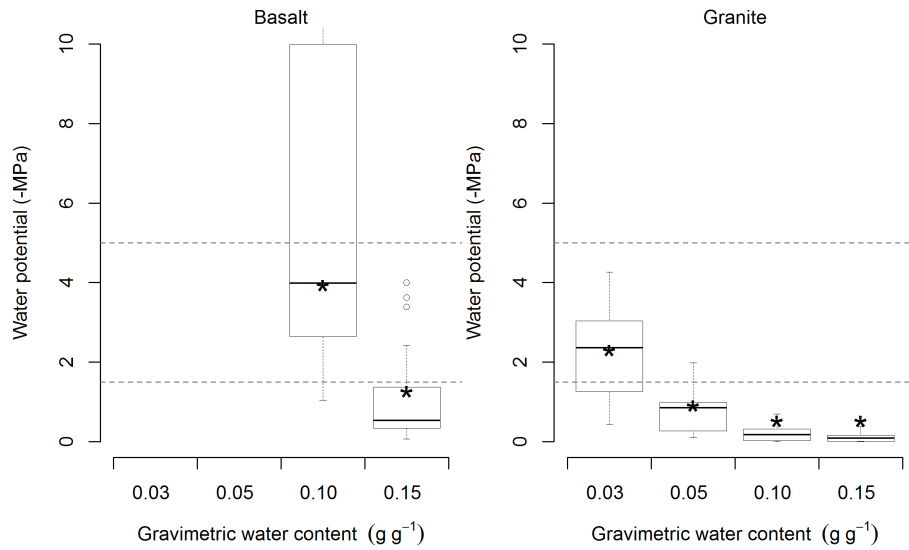


Figure D.4: Comparing site-specific and geology-specific curves. Each box shows the range of predicted water potentials from all site-specific curves per geological substrate type, for a given water content. The solid horizontal line in the box denotes the median of predicted values. The horizontal dotted lines indicate the wilting range (-1.5 to -5 MPa). The * symbols show the predicted values from the geology-specific curves. The water potentials at water contents of 0.03 g g⁻¹ and 0.05 g g⁻¹ in basaltic soils are not shown as they are < -25 MPa and not relevant for plant physiological processes.

estimates of soil water potentials in dry soils should use our site-specific functions (Table D.2). However, these water potentials are below the permanent wilting range (-1.5 to -5 MPa; Figure 3) and represent small volumes of soil water.

Researchers using the equations provided here should take care to avoid several potential problems. First, our analyses relied on the chilled-mirror technique. This method is highly accurate in the dry range (i.e. -0.5 to -300 MPa), but less accurate in the wet range of soils (i.e. -0.001 to -0.5 MPa). It should be noted that some crop species, in particular, may become water limited at -0.03 MPa (Rodríguez-Iturbe & Porporato, 2004). Second, the functions presented here are based on gravimetric soil water measurements, while some field sensors measure soil moisture volumetrically. To use the functions provided here, volumetric soil moisture should be divided by the bulk density of the soil. Bulk density in KNP varies with texture, spatially, and with soil depth (Wigley *et al.*, 2013). When converting gravimetric or volumetric contents to water potentials, researchers should be aware of the potential role of coarse rock fragments. A soil sensor that provides volumetric water content in a rocky soil will underestimate soil water potentials because the volumetric sensor reports the water content of a volume comprised of both rock and soil.

In conclusion, the presented soil water retention curves will improve estimates of plant available water from measurements of volumetric or gravimetric soil moisture in KNP and surrounding areas with similar geological substrates.

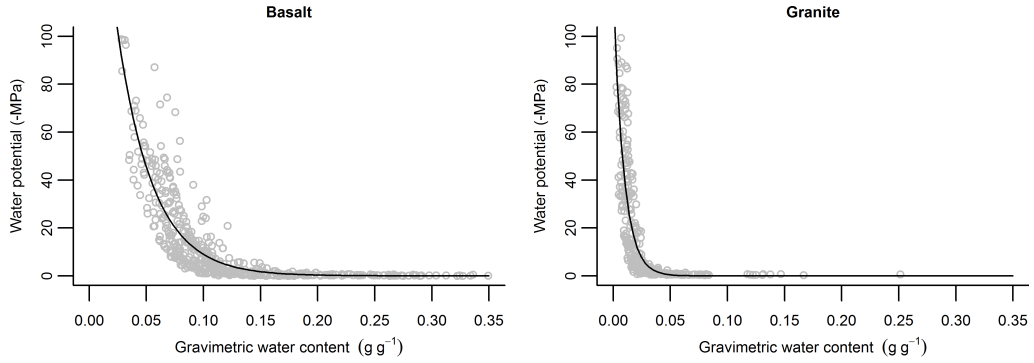


Figure D.5: The relationship between soil moisture and water potential in the 0 to -100 MPa range, for basalt and granite derived soils in KNP. Note that the pressures on the y-axis are negative pressures. The water retention curves were fitted using an exponential model. The equation for basaltic (clayey) soils in KNP is: $\Psi = 0.01 + 228.15e^{-32.30\Theta}$ and for granitic (sandy) soils in KNP: $\Psi = 0.01 + 119.40e^{-110.69\Theta}$ where Ψ is water potential in MPa, Θ is gravimetric water content in g g^{-1} . R^2 values are 0.78 and 0.70 for basaltic and granitic soils respectively. Standard errors of the regression are 8.74 MPa and 13.15 MPa for basaltic and granitic soils respectively.

Appendix E

Curriculum Vitae

Robert Buitenwerf

Curriculum Vitae

<i>Date of birth:</i>	1 August 1983	Ecosystems & Global Change
<i>Nationality:</i>	The Netherlands	Landcare Research
<i>Email:</i>	buitenwerfr@landcareresearch.co.nz	Lincoln
<i>Phone:</i>	+642040276273	New Zealand

RESEARCH AND PROFESSIONAL EXPERIENCE

2015- **Researcher**, Landcare Research, Lincoln, New Zealand

2011-2015 **PhD**, Johann Wolfgang Goethe University, Germany
Leaf-phenology: from global patterns to leaf-level processes
Supervisor: Prof. Steven I. Higgins

2011 **Researcher**, University of Cape Town, South Africa
Analysed and published long-term data sets of tree density in savannas.
with *Prof. William J. Bond*

2010-2011 **Environmental consultant**, Palabora Mining Company, South Africa
Design biodiversity action plan. Coordinate stakeholder meeting.

2010/2011 **Research assistant**, University of New South Wales, Australia
Collect botanical specimens in South Africa and Europe.

2010 **Research assistant**, University of Cape Town, South Africa
Install and monitor atmospheric N deposition collectors. Chemical analyses.

2009-2010 **Project manager**, BirdLife South Africa, South Africa
Develop eco-tourism initiatives with local communities.

2009 **Teaching assistant**, Organisation for Tropical Studies, South Africa
Supervise student research projects, lecturing, logistics.

2007-2009 **Researcher**, South African Environmental Observation Network, South Africa
Analyse and publish long-term vegetation data, educational outreach.

EDUCATION

2011- **PhD**, Goethe University, Germany (*in progress*)

2004-2006 **MSc in Ecology**, University of Groningen, The Netherlands
Thesis 1: The influence of termites on nutrient cycling in an African savanna, Hluhluwe-iMfolozi Park, South-Africa (*supervisor: Prof. H. Olff*)
Thesis 2: Barnacle goose (*Branta leucopsis*) droppings as vegetation fertilizers or parasite hotspots? (*supervisor: Prof J.P. Bakker*)
Thesis 3: Seed retention in salt marsh plants: an interplay between seed traits and environmental variables. (*supervisor: Prof J.P. Bakker*)

2001-2004 **BSc in Biology**, University of Groningen, The Netherlands

1995-2001 **Secondary Education**, Liudger College, The Netherlands

PEER-REVIEWED PUBLICATIONS

- Buitenwerf R.**, L. Rose, S.I. Higgins. 2015. Three decades of multi-dimensional change in global leaf phenology. *Nature Climate Change*, in print.
- Buitenwerf R.**, A. Kulmatiski, S.I. Higgins. Soil water retention curves for the major soil types of the Kruger National Park. *Koedoe*, 56, 1-9.
- Rollins L-A., A.T. Moles, S. Lam, **R. Buitenwerf**, J.M. Buswell, C.R. Brandenburger, H. Flores-Moreno, K.B. Nielsen, E. Couchman, G.S. Brown, F.J. Thomson, F. Hemmings, R. Frankham, W.B. Sherwin. 2013. High genetic diversity is not essential for successful introduction. *Ecology and Evolution* 3: 4501-4517.
- Buitenwerf R.**, W.J. Bond, N. Stevens, W.S.W. Trollope. 2012. Increased tree densities in South African savannas: >50 years of data suggests CO₂ as a driver. *Global Change Biology* 18: 675-684.
- Buitenwerf R.**, A.M. Swemmer, M.J.S. Peel. 2011. Long-term dynamics of herbaceous vegetation structure and composition in two African savanna reserves. *Journal of Applied Ecology* 48: 238-246.
- Buitenwerf R.**, N. Stevens, C.M. Gosling, T.M. Anderson, H. Olf. 2011. Interactions between large herbivores and litter removal by termites across a rainfall gradient in a South African savanna. *Journal of Tropical Ecology* 27: 375-382.
- Chang E.R., R.M. Veeneklaas, **R. Buitenwerf**, J.P. Bakker and T.J. Bouma. 2008. To move or not to move: determinants of seed retention in a tidal marsh. *Functional Ecology* 22(4): 720-727.
- Freymann B.P., **R. Buitenwerf**, O. DeSouza, H. Olf. 2008. The importance of termites (Isoptera) for the recycling of herbivore dung in tropical ecosystems: a review. *European Journal of Entomology* 105(2): 165-173.
- Van der Graaf A.J., **R. Buitenwerf** and J. Stahl. 2006. Forage enhancement through faecal deposition in migratory Barnacle Geese? – Experimental tests along the East Atlantic flyway. Pp. 121-132 in A.J. van der Graaf. 2006. *Geese on a green wave: flexible migrants in a changing world*. PhD dissertation. University of Groningen, Groningen, The Netherlands.

TRAINING AND DEVELOPMENT

- 2006 ArcGIS course, University of Groningen, The Netherlands
- 2005 Ecology/Conservation field course, Tropical Biology Association, Tanzania

AWARDS AND GRANTS

2008	Workshop	SAEON Graduate Student Network	2500 Rand
2006	Travel	Marco Polo	750 Euro
2006	Travel	Groninger Universiteits Fonds	250 Euro
2005	Travel	Marco Polo	800 Euro

2005	Awarded course admission	Tropical Biology Association	
2005	Travel	British Ecological Society	350 Euro
2005	Travel	Groninger Universiteits Fonds	250 Euro
2004	Travel	Groninger Universiteits Fonds	300 Euro

REVIEWER

Journal of Arid Environments	Journal of Biogeography
Journal of Environmental Management	Koedoe

SKILLS

Computing:	Linux OS, R, ArcGIS, JAGS,
Field equipment:	Licor LI6400 photosynthesis system, Licor LI8100 soil CO ₂ flux system, Licor LAI-2000 plant canopy analyser, Decagon Porometer, Campbell data loggers, Dielectric soil moisture probes

CONFERENCES AND WORKSHOPS

- 2013 **EcoTas 2013**, Auckland, New Zealand: *Global leaf phenology: 1982-2006*
- 2012 **Workshop** on CO₂, climate and human effects on land cover change in South Africa, Boxburg, South Africa
- 2011 **10th Annual Savanna Science Network Meeting**, Skukuza, South Africa: *Increased tree densities in South African savannas: >50 years of data suggests CO₂ as a driver*
- 2010 **Workshop** on CO₂, climate and human effects on land cover change in South Africa, Cape Town, South Africa
- 2010 **SAEON Summit**, Cape Town, South Africa: *Long-term dynamics of herbaceous vegetation structure and composition in two African savanna reserves*
- 2009 **7th Annual Savanna Science Network Meeting**, Skukuza, South Africa: *Vegetation structure and composition in a Lowveld savanna are affected by climatic variables*
- 2008 **Annual SAEON Graduate Student Network meeting**, de Hoop Nature Reserve, South Africa: *Long term changes in the herbaceous layer of two private reserves in the Lowveld*
- 2008 **Annual meeting Grassland Society of Southern Africa**, Badplaas, South Africa: *Long term changes in the herbaceous layer of two private reserves in the Lowveld and a discussion of monitoring techniques*
- 2008 **6th Kruger Science Networking meeting**, Skukuza, South Africa: *Long term changes in the herbaceous layer of two private reserves in the Lowveld*
- 2004 **Coastal Ecology Workshop 2004**, Saint Malo, France: *Seed retention: Interplay between seed traits and environmental variables* (poster)
- 2004 **Biodiversity: adaptation versus change**, Haren, The Netherlands: *Vegetation patterns related to clay thickness on a European salt marsh* (poster)